RING-OPENING METATHESIS OF BULKY NORBORNENE MONOMERS

AND

RADICAL-MEDIATED HYDROPHOSPHONATION OF OLEFINS

Thesis by

Christopher S. Daeffler

In Partial Fulfillment of the Requirements

For the Degree of

Doctor of Philosophy

California Institute of Technology

Pasadena, California

2013

(Defended July 27, 2012)

<u>Acknowledgements</u>

<u>Friends:</u> Dr. Ian Tonks, Justin Chartron, Dave Montgomery, Jacob Bitterman, Tanya Ellerbrock, Catrina Pheeney, Casey Deyle, Kaycie Deyle

<u>Abstract</u>

This thesis discusses two major topics: the ring-opening metathesis polymerization (ROMP) of bulky monomers and the radical-mediated hydrophosphonation of olefins. The research into the ROMP of bulky monomers is further divided into three chapters: wedge-shaped monomers, the alternating copolymerization of 1-methyloxanorbornene derivatives with cyclooctene, and the kinetic resolution polymerization of 1-methyloxanorbornene derivatives. The wedge-shaped monomers can be polymerized into diblock copolymers that possess photonic crystal properties. The alternating copolymerization of 1-methyloxanorbornene derivatives with cyclooctene is performed with > 90% alternation *via* two different routes: typical alternating copolymerization and a sequence editing approach. The kinetic resolution polymerization of these same 1-methyloxanorbornene monomers achieves only modest selectivity (S=4), but there is evidence that the growing polymer chain forms a helix that influences the selectivity of the resolution. The last topic is the radical-mediated hydrophosphonation of olefins. This synthetic method provides access to Wittig reagents that are capable of highly *cis*-selective olefinations of aldehydes.

Table of Contents

Introduction

This thesis is presented in a modified journal format.[1] Each chapter could be considered an article on its own. The first three chapters are unified by a single reaction, ring-opening metathesis polymerization (ROMP). The introduction will serve as a background for these chapters, providing a brief history of the field with synthetic and mechanistic insights into the reaction. The last chapter stands separately from the first three, and it contains its own introductory section in the body of the chapter.

Olefin metathesis is an incredibly versatile reaction, applied to bulk chemical synthesis, fine chemicals, and polymerizations, and thus has been reviewed extensively.[2] The basic steps are the same for all catalyst and olefins, with a few additional steps depending on the ligands and metal center (Figure I.1). Most modern olefin metathesis catalysts are isolable metal complexes, while the earliest reports of early- and late-transition metal-mediated olefin metathesis involved metal carbenes generated *in situ* from a mixture of reagents. The first step is the coordination of an olefin to a metal carbene complex. The coordinated olefin then undergoes a [2+2] cycloaddition with the metal carbene double bond to form a metallocyclobutane. If the metallocyclobutane cycloreverts in the opposite sense, it performs a productive olefin metathesis step, swapping the partners on the olefin with the carbene that was carried on the metal center. The new, coordinated olefin dissociates from the metal center to yield the desired product and new metal carbene, which can re-enter the catalytic cycle.
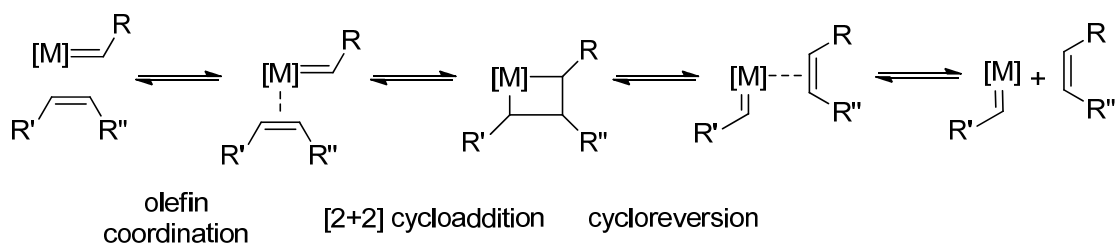
**Figure I.1.** The current understanding of the olefin metathesis mechanism

As mentioned, olefin metathesis can lead to a wide variety of products, depending on the type of the olefin that is employed (Figure I.2). Examples of small molecule application of olefin metathesis are ring-closing metathesis (RCM), cross metathesis (CM), and ring-opening cross metathesis (ROCM). In RCM, an α,ω-diolefin closes to form a ring, usually with the extrusion of a small molecule such as ethylene. CM is similar, but involves two acyclic olefins, also with the extrusion of ethylene. ROCM can be considered the reverse of RCM and CM, where a strained cyclic olefin undergoes ring cleavage by a small linear olefin.

Along with small molecule reactions, olefin metathesis can be used to perform polymerizations. Acyclic diene metathesis polymerization (ADMET) is the repeated cross metathesis of dienes to polymers under conditions of high concentration and often active removal of ethylene. Ring-opening metathesis polymerization (ROMP) is similar to ROCM, where a strained cyclic olefin is opened. In the case of ROMP, as opposed to ROCM, a small linear olefin is not incorporated into the opened cyclic olefin. Rather, another equivalent of strained cyclic olefin is reacted to grow the polymer chain. ROMP, ADMET, and RCM are all part of continuum of cyclic olefin reactivity. Most of the
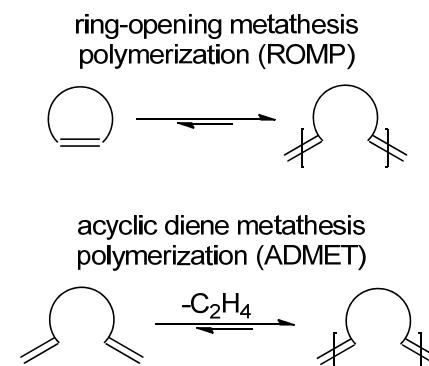
work in this thesis focuses on ROMP, so there will be greater attention to this later in the

Introduction.

Small Molecule Olefin Metathesis

ring-closing metathesis (RCM)

cross metathesis (CM)

ring-opening cross metathesis (ROCM)

Olefin Metathesis Polymerization

ring-opening metathesis
polymerization (ROMP)

acyclic diene metathesis
polymerization (ADMET)
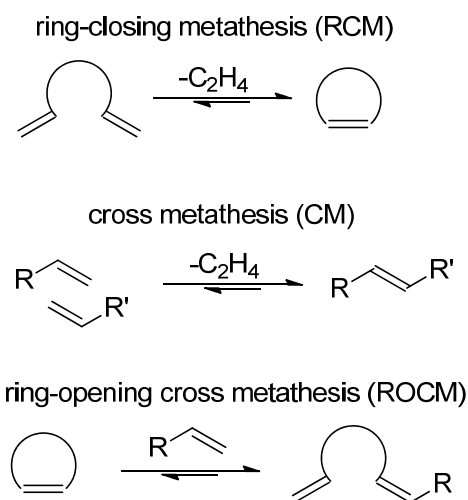
Figure I.2. Olefin metathesis reactions

The characteristics of the metal center are critical to the course of the olefin

metathesis reaction. Like most catalysts, olefin metathesis catalysts are designed to

balance the 'devil's triangle' of catalysis: stability, selectivity, and activity (Figure I.3).

During the development of olefin metathesis, researchers improved each of these factors,

and this can be directly related to the metal center used in the catalyst. The earliest

catalysts were titanium compounds, which are highly reactive with many other functional

groups *except* olefins (Figure I.4). As catalyst development has progressed, molybdenum

catalysts, which possess high activity but moderate stability to other functional groups,

and ruthenium catalysts with good selectivity and high functional group tolerance have

become the state of the art. As far as regioselectivity and enantioselectivity are

concerned, it is challenging to draw comparisons between molybdenum and ruthenium olefin metathesis catalysts because the results are highly dependent on ligand structure and substrate selection.
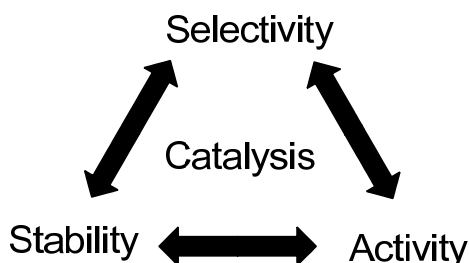

Figure I.3. The 'devil's triangle' of catalysis

Titanium	Tungsten	Molybdenum	Ruthenium	
Acids	Acids	Acids	**Olefins**	
Alcohols and H_2O	Alcohols and H_2O	Alcohols and H_2O	Acids	▲
Aldehydes	Aldehydes	Aldehydes	Alcohols and H_2O	Increasing
Ketones	Ketones	**Olefins**	Aldehydes	Reactivity
Esters and Amides	**Olefins**	Ketones	Ketones	▲
Olefins	Esters and Amides	Esters and Amides	Esters and Amides	

Figure I.4. Functional group tolerance (stability) of transition olefin metathesis catalysts
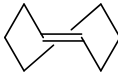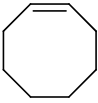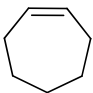
In our group, we have sought to develop a series of the ruthenium-based olefin metathesis catalysts (Figure I.5). The first widely used ruthenium olefin metathesis catalyst was **A**, introduced in 1995.[3] It was known that electron-rich phosphines provided more active ruthenium complexes in olefin metathesis[4], so it was hypothesized that strongly donating N-heterocyclic carbene (NHC) ligands would also form effective catalysts when ligated to ruthenium. This led to the development of catalysts **C** (1999)[5], **D** (2002)[6], and **B** (2007)[7], which all bear NHC ligands of comparable donating ability,

but with a range of steric bulk. All four ruthenium catalysts (**A**, **B**, **C**, and **D**) are commercially available.
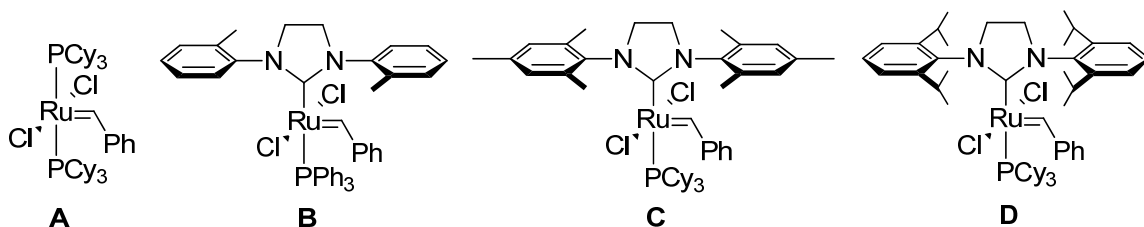
Figure I.5. Commercially available ruthenium olefin metathesis catalysts

As mentioned, one of the most important facets of olefin metathesis is its applicability to many fields of synthetic chemistry. In this thesis, I will focus on the application of known olefin metathesis catalysts in the area of polymer chemistry, specifically ROMP. ROMP can be performed with a variety of strained cyclic monomers. Norbornenes, because of their ease of modification and high ring strain, are the most common. Under most conditions, the ROMP of norbornenes is considered 'living': it possesses a chain-growth mechanism, the rate of initiation is much higher than the rate of propagation ($k_i >>> k_p$), there are very few chain termination reactions and chain transfer is extremely slow to the extent that it does not compete with propagation. *Cis*-cyclooctene, on the other hand, still undergoes ROMP in a chain-growth manner, but chain transfer is very prevalent and leads to the high polydispersity of polycyclooctenes compared to polynorbornenes.

Cyclic olefins ▽ ▭ ⬡ ⬡=⬡ ⯃ ⬠ ⬠

Strain (kcal/mol)   54.5   30.6   27.2   16.7   7.4   6.7   6.8

Figure I.6. Strained cyclic olefin commonly employed in ROMP

In the research covered here, norbornene-based monomers are the choice, and they have been designed to have steric bulk that will affect their properties (Figure I.7). For Chapter 1, this means adding a large wedge-shaped group at the end of the monomer as a way to mimic polymeric macromonomers. These wedge monomers can be used to synthesize diblock polymers that form photonic crystals. Chapters 2 and 3 deal with the polymerization of 1-methyloxanorbornene derivatives, which are shown to perform alternating copolymerizations with cyclooctene and kinetic resolution polymerizations, respectively.

Wedge Polymers

ROMP → photonic crystal

1-Methyloxanorbornenes

→ alternating copolymerization with cyclooctene

→ kinetic resolution polymerization and helical polymer
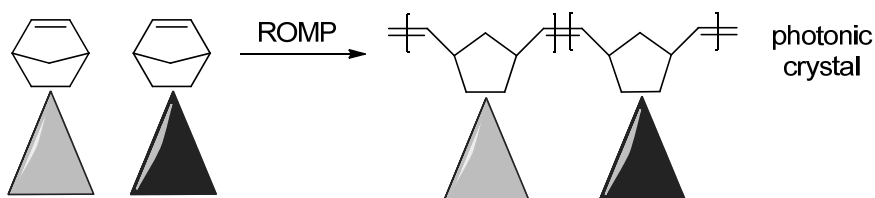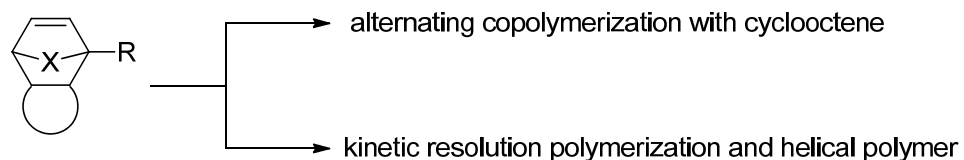
Figure I.7. Graphical outline for Chapters 1, 2, and 3

[1] Figures, tables and schemes will be labeled as 'X.Y', where X is the chapter number and Y is the figure, table, or scheme number. Compound labels are internal to each chapter. Endnotes are labeled sequentially *within* each chapter.

[2] Trnka, T. M.; Grubbs, R. H. *Acc. Chem. Res.* **2001**, *34*, 18–20.

[3] Schwab, P.; France, M. B.; Ziller, J. W.; Grubbs, R. H. *Angew. Chem. Int. Ed. Engl.* **1995**, *34*, 2039–2041.

[4] Dias, E. L.; Nguyen, S. T.; Grubbs, R. H. *J. Am. Chem. Soc.* **1997**, *119*, 3887–3897.

[5] Scholl, M.; Ding, S.; Lee, C. W.; Grubbs, R. H. *Org. Lett.* **1999**, *1*, 953–956.

[6] Dinger, M. B.; Mol, J. C. *Adv. Synth. Catal.* **2002**, *344*, 671–677.

[7] Stewart, I. C.; Ung, T.; Pletnev, A. A.; Berlin, J. M.; Grubbs, R. H.; Schrodi, Y. *Org. Lett.* **2007**, *9*, 1589–1592.

Chapter 1

Ring-Opening Metathesis Polymerization of Wedge-Shaped Norbornene Monomers

Abstract

This chapter presents the synthesis and polymerization of two wedge-shaped norbornene monomers, one bearing long alkyl chains, the other with pendant aromatic groups. Both homopolymers and a diblock copolymer were prepared. The diblock copolymer was allowed to deposit a thin film from solution which demonstrated photonic crystal properties.

Introduction

Among polymeric materials, the linear topology is the most easily synthesized, and it is this class that comprises nearly all of the polymers that we encounter in our everyday life. Many other topologies exist, including cyclic,[1] dendritic,[2] and brush[3] (Figure 1.1). The topology of the polymer can be used to control the materials properties. In the case of brush polymers, the polymeric brush 'bristles' impart a rigidity to the main chain backbone that reduces chain entanglement and enables rapid self-assembly into lamellar structures with photonic crystal properties.
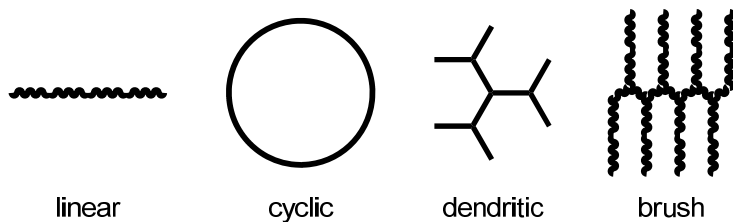
Figure 1.1. Representative polymer topologies

As an alternative to the polymer side chains in brush polymers, it was thought that bulky side groups could serve the same purpose. Such side groups would be monodisperse and have a wider range of shapes and functional groups available compared to all-polymer brushes. For this purpose, we chose two derivatives of the generic norbornene 'wedge' monomer (**W**) with dodecyl groups (**AW**) and benzyl groups (**BnW**). Monomers **AW** and **BnW** are like G1 dendrimers, with their bulk confined to a specific shape. Ring-opening metathesis polymerization (ROMP) allows for the homopolymerization of one wedge monomer or the block copolymerization of both monomers (Figure 1.2).

Homopolymerization

Block Copolymerization

poly-(**AW**-*block*-**BnW**)
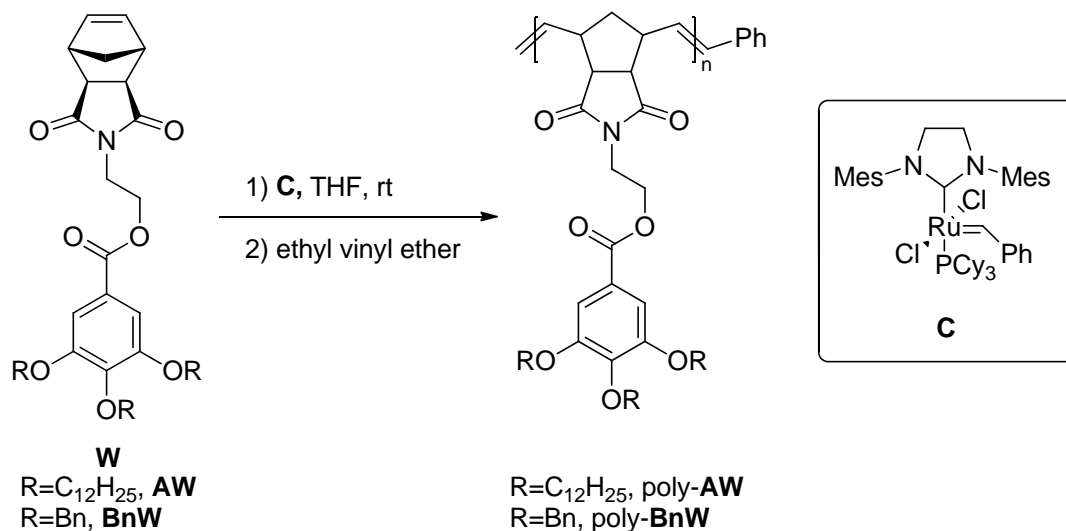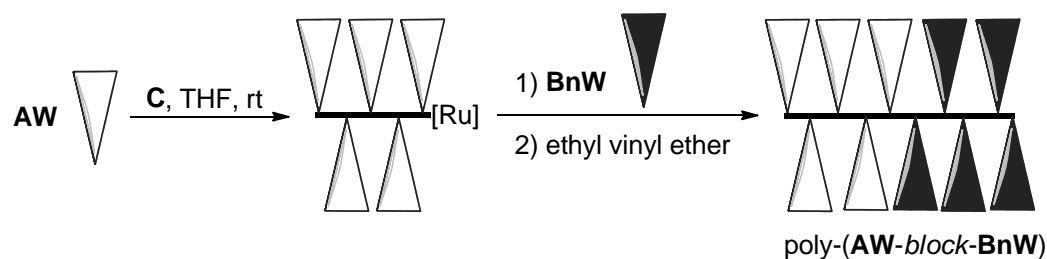
Figure 1.2. The homopolymerization and block copolymerization of wedge monomers **AW** and **BnW**

A block polymerization was carried out with **BnW** and **AW** ([**BnW**]$_0$:[**AW**]$_0$:[**C**]=300:300:1) with the resulting polymer possessing M_n=1.5*10^6 Da, M_w=3.52*10^6 Da, and a polydispersity index (PDI) of 2.351. The molecular weight data for this sample of poly-(**BnW**-*block*-**AW**) indicate that there was likely a large amount of initiator decomposition, resulting in a broad PDI and a degree of polymerization (DP) of about 1100 for each monomer. Thin film deposition of the white poly-(**BnW**-*block*-**AW**)

by solvent evaporation from methylene chloride (room temperature, one day), THF (40 °C, one day), or benzene (40 °C, two days) yield bright blue films, indicating the formation of photonic crystals. Transmittance spectra of two films cast from methylene chloride show that the films weakly reflect visible light in the purple and blue regions (Figure 1.3). The high polydispersity of the block polymer leads to a very broad reflectance band, where there is significant reflectance above 400 nm even though the peak lies somewhere in the ultraviolet region.
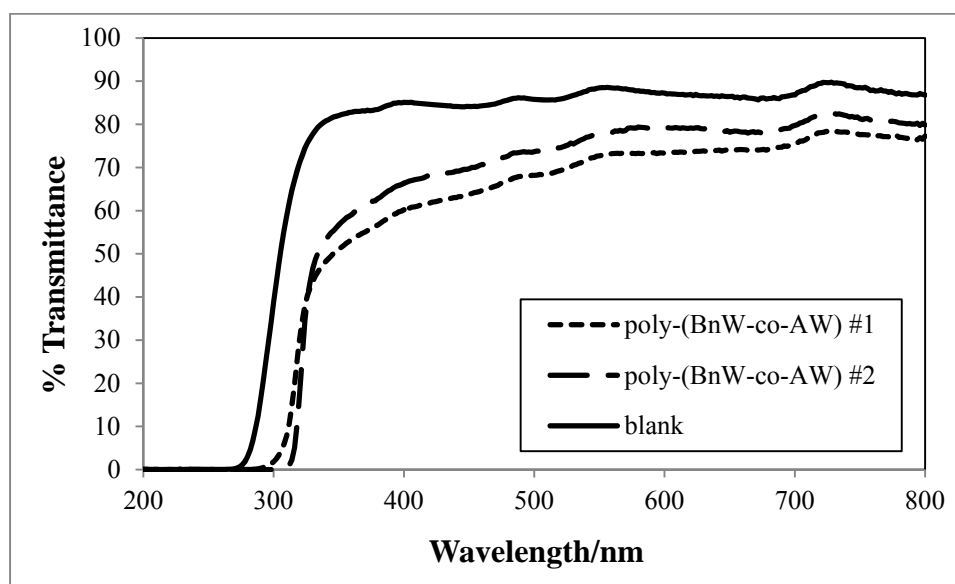
Figure 1.3. Transmittance spectra of poly-(**BnW**-*co*-**AW**) in a glass vial

Conclusions

The initial results for the wedge diblock copolymers are promising and merit further studies. The next phase of this project will be to prepare a good quality diblock

copolymer, that is, one with high molecular weight and low polydispersity. Further modifications to the wedge structure are possible, as well. Many different types of functional groups can be appended to the wedge to change its properties and the first-generation dendrimer could be expanded to more generations should a larger wedge be desired.

Supporting Information

Materials

THF and CH_2Cl_2 were purified by passage through a solvent purification system.[4] Initiator **4** was prepared from $(H_2IMes)(PCy_3)Cl_2RuCHPh$ according to the literature procedure.[5] Norbornene derivative **3** was prepared according to the literature procedure.[6] Complex $(H_2IMes)(PCy_3)Cl_2RuCHPh$ (**4**) was a gift from Materia, Inc. $CDCl_3$ was obtained from Cambridge Isotopes. All other chemicals were obtained from Sigma-Aldrich Corporation and used as received.

General Methods

NMR spectra were recorded in $CDCl_3$ or acetone-d_6 on a Varian INOVA 500 MHz spectrometer with the VNMRJ software package in the High-Resolution Nuclear Magnetic Resonance Facility at the California Institute of Technology (Caltech). ^1H and ^{13}C chemical shifts are referenced relative to the residual solvent peak ($CDCl_3$: δ=7.26 for ^1H and δ=77.23 for ^{13}C; acetone-d_6: 2.05 for ^1H and 206.7 and 29.9 for ^{13}C). Spectral

analysis was performed on MestReNova software. High-resolution mass spectra were provided by Caltech's Mass Spectrometry Facility. Gel permeation chromatography (GPC) was performed in tetrahydrofuran (THF) on two MZ-Gel 10 μm columns composed of styrene-divinylbenzene copolymer (Analysentechnik) and connected in series, with a miniDAWN TREOS multiangle laser light scattering (MALLS) detector, ViscoStar viscometer and Optilab rEX differential refractometer (all three from Wyatt Technologies). No calibration standards were used, as light scattering is considered an accurate measurement of molecular weight. Assuming 100% mass elution from the column, the dn/dc of **poly(AW)** was 0.087 (average of 3 samples) and the dn/dc of **poly(BnW)** was 0.152 (average of 5 samples). GPC data analysis was performed with ASTRA software.

Alkyl Wedge (AW) Synthesis

Methyl 3,4,5-tris(dodecyloxy)benzoate (1a).
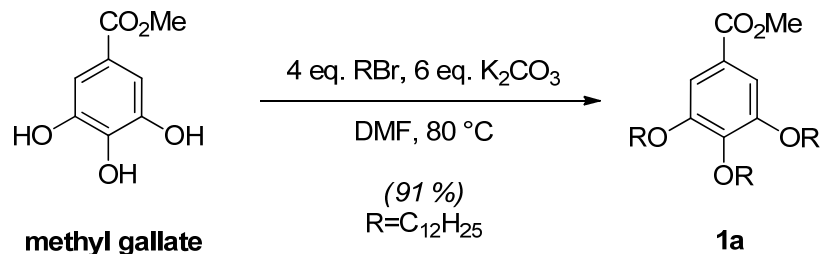
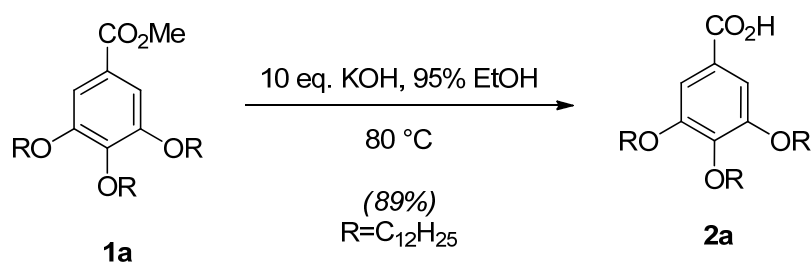A 250 ml round bottomed flask equipped with a stirbar was charged DMF (50 ml). The solution was sparged for 30 minutes with argon. After sparging, flask was sequentially charged with methyl gallate (1.9 g, 10 mmol, 1 eq), bromodecane (10 ml, 40 mmol, 4 eq), and potassium carbonate (8.5 g, 60 mmol, 6 eq). The flask was then equipped with a

Vigreux column and heated to 80 °C for 12 hours. Upon cooling to room temperature, the reaction mixture was diluted with water (100 ml) and extracted with diethyl ether (2x100 ml). The combined organic phases were washed with water (100 ml) then 50% brine (100 ml) and dried over magnesium sulfate. The combined organic phases were filtered through a plug of basic alumina. The solvent was removed by rotary evaporation to yield an oil, which became white solid **1a** (6.2 g, 9.1 mmol, 91%) *in vacuo*. ^{1}H NMR (500 MHz, CDCl$_3$): δ 7.25 (2H, s), 4.00 (2H, t, J=6.5 Hz), 3.99 (4H, t, J=6.5 Hz), 3.87 (3H, s), 1.80 (4H, quintet, J=7 Hz), 1.73 (2H, quintet, J=7 Hz), 1.46 (6H, quintet, J=7 Hz), 1.38–1.19 (48H, bs), 0.87 (9H, t, 7 Hz). ^{13}C{^{1}H} NMR (126 MHz, CDCl$_3$): δ 166.93, 152.81, 142.36, 124.64, 107.97, 104.99, 73.48, 69.16, 52.09, 31.95, 31.93, 30.33, 29.75, 29.74, 29.73, 29.70, 29.67, 29.64, 29.57, 29.40, 29.37, 29.31, 26.08, 26.06, 22.70, 22.68, 14.14, 14.12. HRMS (FAB+): calculated 689.6084, found 689.6095.

3,4,5-tris(dodecyloxy)benzoic acid (2a).

A 250 ml round bottomed flask equipped with a stirbar was charged with **1** (4.1 g, 6 mmol, 1 eq), potassium hydroxide (3.4 g, 60 mmol, 10 eq) and 95% EtOH (30 ml). The round bottom flask was equipped with a water-cooled condenser. The suspension was refluxed (~ 80 °C) for 4 hours. Upon cooling, the reaction mixture thickened

substantially. The solid was filtered with a Büchner funnel and washed with cold (-20

°C) 95% EtOH to give a white solid. The white solid was suspended in Et_2O (100 ml).

Concentrated HCl (6 ml) was added to the ethereal suspension, followed by the

precipitation of potassium chloride. Water (50 ml) was added then separated from the

organic phase. The organic phase was washed with water (2x50ml) and brine (1x50ml)

and dried over sodium sulfate. The solution was filtered and the solvent was removed by

rotary evaporation to yield **2a** as a white solid (3.6 g, 5.3 mmol, 89 %). ^1H NMR (500

MHz, $CDCl_3$): δ 7.32 (2H, s), 4.04 (2H, t, J=7 Hz), 4.02 (4H, t, J=7 Hz), 1.82 (4H,

quintet, J=7 Hz), 1.75 (2H, quintet, J=7 Hz), 1.48 (6H, quintet, J=7 Hz), 1.39–1.22 (48H,

bs), 0.88 (9H, t, J=7 Hz). $^{13}C\{^1H\}$ NMR (126 MHz, $CDCl_3$): δ 171.02, 152.85, 143.16,

123.47, 108.56, 104.99, 73.55, 69.20, 31.95, 31.93, 30.34, 29.76, 29.74, 29.73, 29.70,

29.67, 29.64, 29.57, 29.40, 29.37, 29.28, 26.08, 26.05, 22.70, 14.12. HRMS (ES):

calculated 673.5771, found 673.5771.


Alkyl Wedge Monomer (AW).
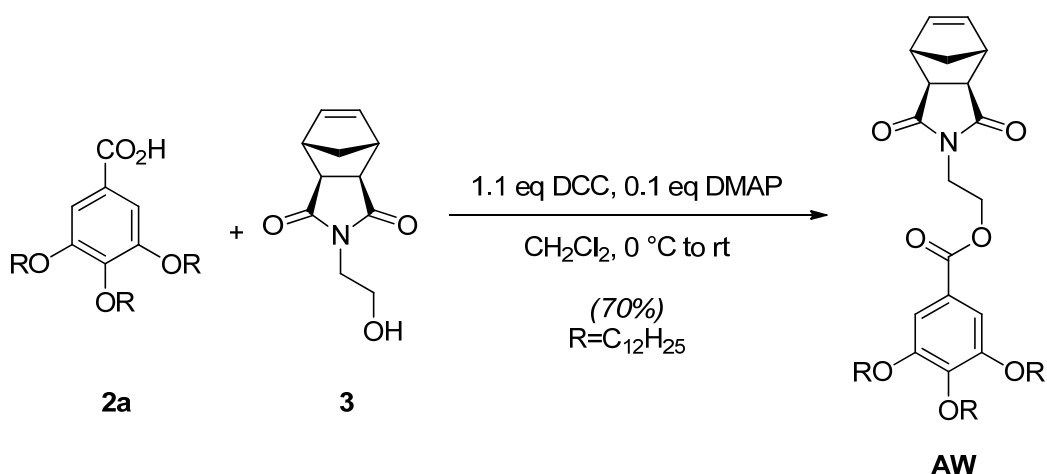
A 100 ml Schlenk flask equipped with a stirbar was flame-dried under vacuum. The cooled flask was backfilled with argon and charged with **2** (3.8 g, 5.6 mmol, 1 eq), alcohol **3** (1.3 g, 6.2 mmol, 1.1 eq), 4-dimethylaminopyridine (66 mg, 0.56 mmol, 0.1 eq), and CH_2Cl_2 (25 ml). The solution was cooled to 0 °C in an ice bath, with precipitation of some reagents. Dicyclohexylcarbodiimide (1.3 g, 6.2 mmol, 1.1 eq) was added to the cooled solution, and the reaction was stirred at 0 °C for 30 minutes. The reaction was warmed to room temperature and stirred for 18 hours. The resulting suspension was filtered and the solid was washed with CH_2Cl_2 (25 ml). Solvent was removed from the filtrate by rotary evaporation to yield very viscous oil. Ethanol (95%, 100 ml) was added to the oil and stirred for 3 hours. The resulting white solid was filtered and residual solvent was removed *in vacuo* to yield the alkyl wedge monomer **AW** (3.4 g, 3.9 mmol, 70%). ^{1}H NMR (500 MHz, CDCl$_3$): δ 7.20 (2H, s), 6.27 (2H, t, J=2 Hz), 4.40 (2H, t, J=5 Hz), 4.01 (6H, t, J=1 Hz), 3.90 (2H, t, J=5 Hz), 3.23 (2H, m), 2.69 (1H, d, J=2 Hz), 1.82 (4H, quintet, J=7 Hz), 1.73 (2H, quintet, J=7Hz), 1.55 (1H, s), 1.48 (6H, m), 1.43–1.21 (50H, br), 0.88 (9H, t, J=7 Hz). ^{13}C{^{1}H} NMR (126 MHz, CDCl$_3$): δ 177.69, 166.06, 152.81, 142.46, 137.77, 124.01, 107.98, 73.47, 69.12, 61.63, 47.85, 45.25, 42.69, 37.53, 31.95, 31.93, 30.34, 29.76, 29.74, 29.73, 29.71, 29.70, 29.67, 29.66, 29.58, 29.41, 29.40, 29.37, 29.33, 26.11, 22.70, 14.12. HRMS (ES+): calculated 864.6717, found 864.6716.

Benzyl Wedge Monomer (BnW) Synthesis.

Methyl 3,4,5-tribenzylbenzoate (1b).
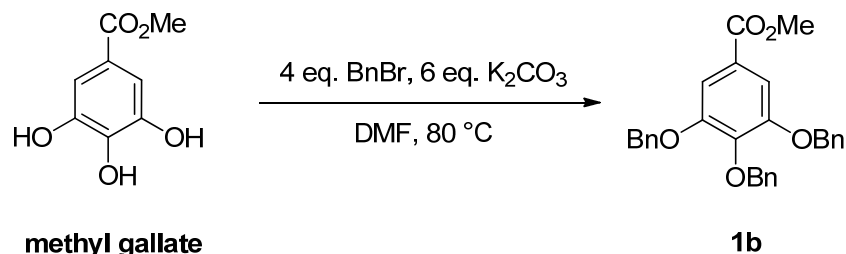
A 250 ml round bottomed flask equipped with a stirbar was charged DMF (50 ml). The solution was sparged for 30 minutes with argon. After sparging, flask was sequentially charged with methyl gallate (1.9 g, 10 mmol, 1 eq), benzyl bromide (4.8 ml, 40 mmol, 4 eq), and potassium carbonate (8.5 g, 60 mmol, 6 eq). The flask was then equipped with a Vigreux column and heated to 80 °C for 12 hours. Upon cooling to room temperature, the reaction mixture was diluted with water (100 ml) and extracted with diethyl ether (2x100 ml). The combined organic phases were washed with water (100 ml) then 50% brine (100 ml) and dried over magnesium sulfate. The combined organic phases were filtered through a plug of basic alumina. The solvent was removed by rotary evaporation to yield an oil, which became white solid **1b** (3.9 g, 98.5 mmol, 85%) *in vacuo*. ^{1}H NMR (500 MHz, CDCl$_3$): δ 7.48–7.44 (4H, m), 7.43–7.38 (8H, m), 7.37–7.33 (2H, m), 7.30–7.26 (3H, m), 5.16 (4H, s), 5.14 (2H, s), 3.91 (3H, s). ^{13}C{^{1}H} NMR (126 MHz, CDCl$_3$): δ 166.62, 152.55, 142.41, 137.43, 136.65, 128.53, 128.51, 128.17, 128.01, 127.93, 127.53, 125.21, 109.99, 109.07, 75.12, 71.23, 52.22. HRMS (FAB) calculated 454.17.80, found 454.1782.

3,4,5-tribenzylbenzoic acid (2b).
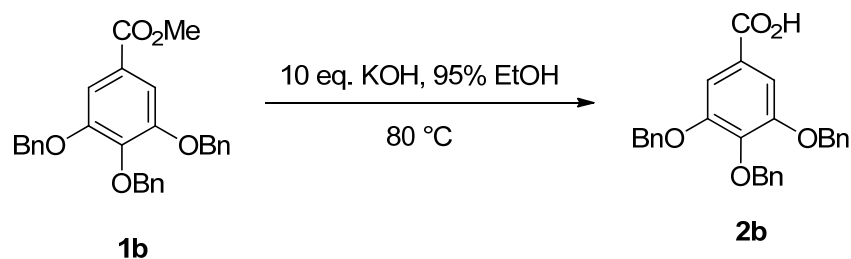
A 250 ml round bottomed flask equipped with a stirbar was charged with **2a** (3.9 g, 8.5 mmol, 1 eq), potassium hydroxide (4.8 g, 85 mmol, 10 eq), and 95% EtOH (43 ml). The round bottom flask was equipped with a water-cooled condenser. The suspension was refluxed (~ 80 °C) for 4 hours. Upon cooling, the reaction mixture thickened substantially. The solid was filtered with a Büchner funnel and washed with cold (-20 °C) 95% EtOH to give a yellow solid. The solid was suspended in Et$_2$O (100 ml). Concentrated HCl (6 ml) was added to the ethereal suspension, followed by the precipitation of potassium chloride. The suspension was filtered, and washed with water. The filtrate was dissolved in acetone and dried over MgSO$_4$. Filtration and solvent removal by rotary evaporation yielded **2b** (1.85 g, 4.2 mmol, 49%). ^{1}H NMR (500 MHz, acetone-d_6): δ 7.55 (4H, d, *J*=7 Hz), 7.48–7.44 (4H, m), 7.41 (4H, tt, *J*=7 Hz, 1.5 Hz), 7.35 (2H, tt, *J*=7 Hz, 1.5 Hz), 7.30–7.25 (3H, m), 5.23 (4H, s), 5.14 (2H, s). ^{13}C{^{1}H} NMR (126 MHz, acetone-d_6): δ 166.23, 152.62, 142.17, 137.95, 137.20, 128.41, 128.28, 128.04, 127.86, 127.73, 127.64, 125.70, 108.87, 74.59, 70.76. HRMS (FAB) calculated 441.1702, found 441.1682.

Benzyl Wedge Monomer (BnW).
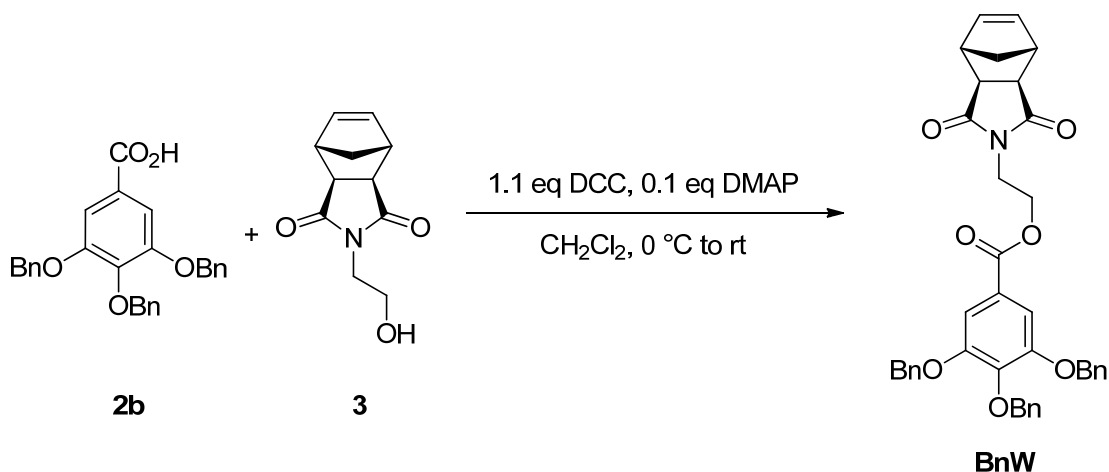
A 100 ml Schlenk flask equipped with a stirbar was flame-dried under vacuum. The cooled flask was backfilled with argon and charged with **2b** (1.7 g, 3.8 mmol, 1 eq), alcohol **3** (865 mg, 4.2 mmol, 1.1 eq), 4-dimethylaminopyridine (46 mg, 0.38 mmol, 0.1 eq), and CH_2Cl_2 (20 ml). The solution was cooled to 0 °C in an ice bath, with precipitation of some reagents. Dicyclohexylcarbodiimide (862 mg, 4.2 mmol, 1.1 eq) was added to the cooled solution, and the reaction was stirred at 0 °C for 30 minutes. The reaction was warmed to room temperature and stirred for 18 hours. The resulting suspension was filtered and the solid was washed with CH_2Cl_2 (25 ml). Solvent was removed from the filtrate by rotary evaporation to yield an off-white solid. Ethanol (95%, 100 ml) was added to the oil and stirred for 3 hours. The resulting white solid was filtered and residual solvent was removed *in vacuo* to yield **BnW** (1.9 g, 3.1 mmol, 82%).

^{1}H NMR (500 MHz, CDCl3): 7.49 (4H, d, *J*=8 Hz), 7.42–7.34 (10H, m), 7.29–7.26 (3H, m), 6.28 (2H, t, *J*=1.6 Hz), 5.18 (4H, s), 5.14 (2H, s), 4.43 (2H, t, *J*=5 Hz), 3.94 (2H, t, *J*=5 Hz), 3.24 (2H, s), 2.70 (2H, s), 1.42 (1H, d, *J*=10 Hz), 1.25 (1H, d, *J*=10 Hz).

^{13}C{^{1}H} NMR (126 MHz, CDCl3) δ 177.76, 165.76, 152.55, 142.50, 137.77, 137.45,

136.71, 128.52, 128.49, 128.16, 127.98, 127.92, 127.56, 124.60, 109.03, 75.08, 71.11, 61.86, 47.85, 45.26, 42.67, 37.50. HRMS (FAB) calculated 629.2413, found 629.2392.

Polymerization of Alkyl Wedge Monomer to P(AW).
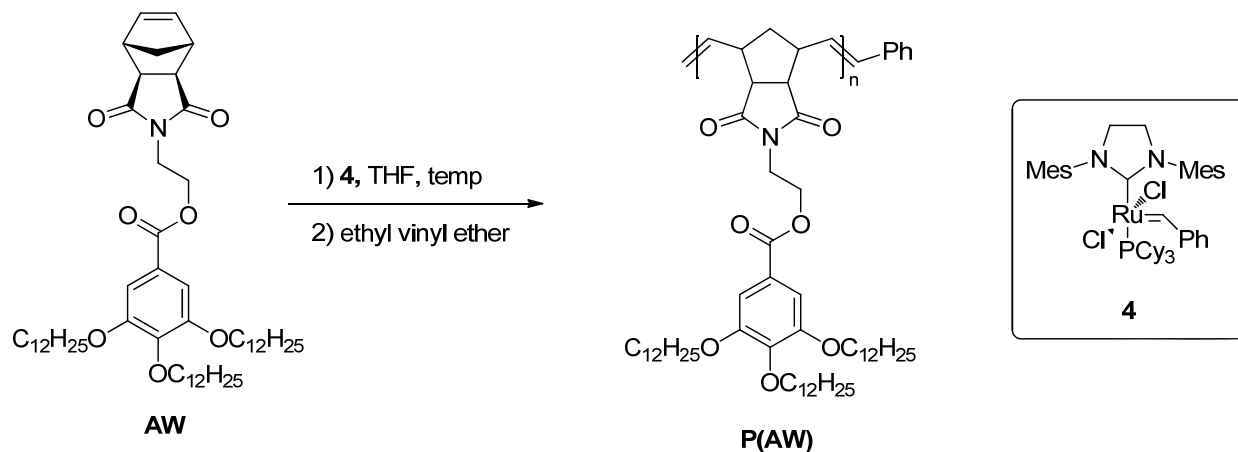
In a nitrogen-filled glovebox, a scintillation vial was charged with monomer **AW** (1.7 g, 2 mmol) and THF (10 ml). In a separate vial, a stock solution (0.01M) of initiator **4** was prepared in THF. The appropriate amount of initiator solution was added to the monomer solution. The reaction vial was sealed and removed from the glovebox. At the appropriate time, the polymerization was quenched with ethyl vinyl ether (1 ml). The wedge polymer **P(AW)** was precipitated into acetone directly from the quenched reaction mixture. The remaining solvent was removed *in vacuo* to yield an amorphous white solid (Table 1.1).

Table 1.1. Reaction Conditions for **AW** Polymerization

| Sample	$[M]_0/[I]$	reaction time (min)	yield	temp. (°C)
CSD-V-051A	200	30	70%	20
CSD-V-051B	400	60	76%	20
CSD-V-061A	1000	30	63%	50
CSD-V-061B	2000	45	60%	50

Polymerization of Benzyl Wedge Monomer to P(BnW).

BnW **P(BnW)**
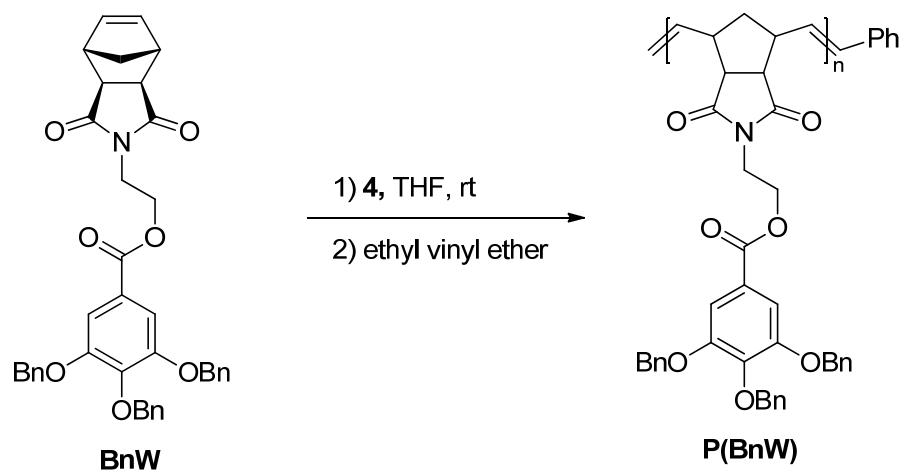
In a nitrogen-filled glovebox, a scintillation vial was charged with monomer **BnW** (470 mg, 0.75 mmol) and THF (3 ml). In a separate vial, a stock solution (0.01M) of initiator **4** was prepared in THF. The appropriate amount of initiator solution was added to the monomer solution. The reaction vial was sealed and removed from the glovebox. At the appropriate time, the polymerization was quenched with ethyl vinyl ether (1 ml). The wedge polymer **P(BnW)** was precipitated into methanol directly from the quenched reaction mixture. The polymer was collected by filtration, redissolved in dichloromethane then precipitated into methanol again. The polymer was again collected by filtration. The remaining solvent was removed *in vacuo* to yield a white solid (Table 1.2).
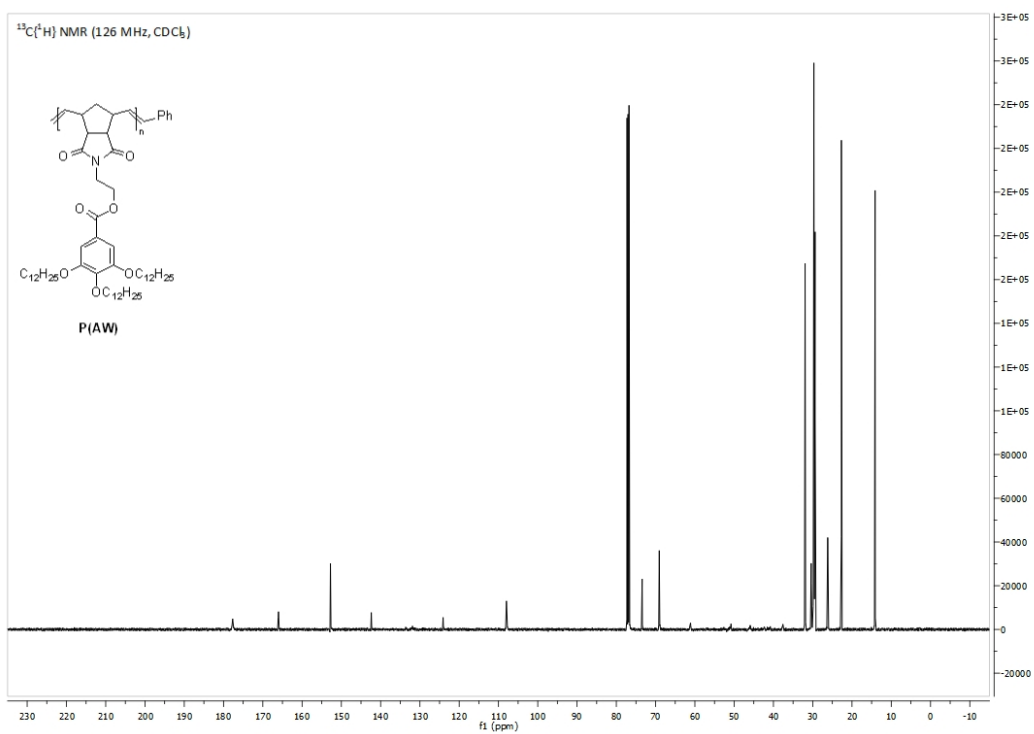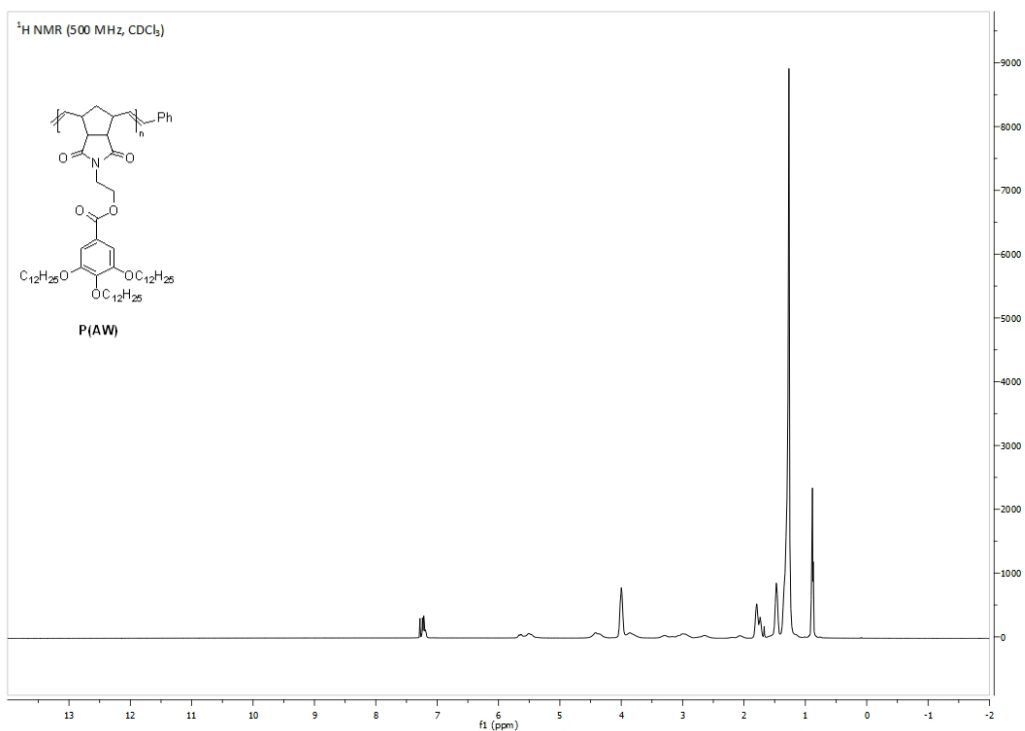
Table 1.2. Reaction Conditions for **BnW** Polymerization

Sample	$[M]/[I]_0$	Reaction time (min)	Yield (%)
CSD-V-118A	200	15	94
CSD-V-118B	400	30	93
CSD-V-118C	800	60	93

Block Copolymerization of **AW** and **BnW**
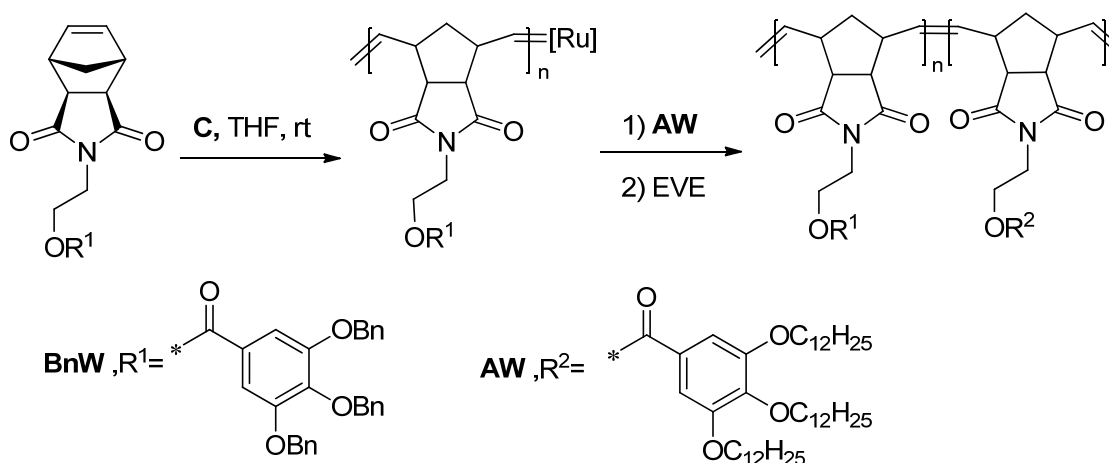
In a nitrogen-filled glovebox, **BnW** (125 mg, 0.2 mmol, $[BnW]_0$:$[AW]_0$:$[C]$=300:300:1) was dissolved in THF (1 ml) in a scintillation vial. A catalyst stock solution was prepared from **C** (2.3 mg, 2.7 µmol) in THF (1 ml). A portion of the catalyst stock solution (0.25 ml) was added to the **BnW** solution in one portion. The solution rapidly thickens. After 1 hour, a solution of **AW** (173 mg, 0.2 mmol) in THF (1 ml) was added to the living poly-**BnW** solution. The second block was allowed to polymerize for 1 hour. The vial was removed from the glovebox and the reaction was quenched with ethyl vinyl ether (1 ml) for 5 minutes, which caused some polymer to precipitate. The cloudy suspension was redissolved with methylene chloride, then precipitated into acetone (100 ml). The white solid was collected and dried *in vacuo* to

yield poly-(**BnW**-*block*-**AW**) (260 mg, 87%).   Molecular weight: M_n=1.5*10^6 Da, M_w=3.52*10^6 Da, PDI=2.35.

¹H NMR (500 MHz, CDCl₃)

P(AW)

¹³C{¹H} NMR (126 MHz, CDCl₃)

P(AW)

¹H NMR (500 MHz, CDCl₃)

P(BnW)

¹³C{¹H} NMR (126 MHz, CDCl₃)

P(BnW)
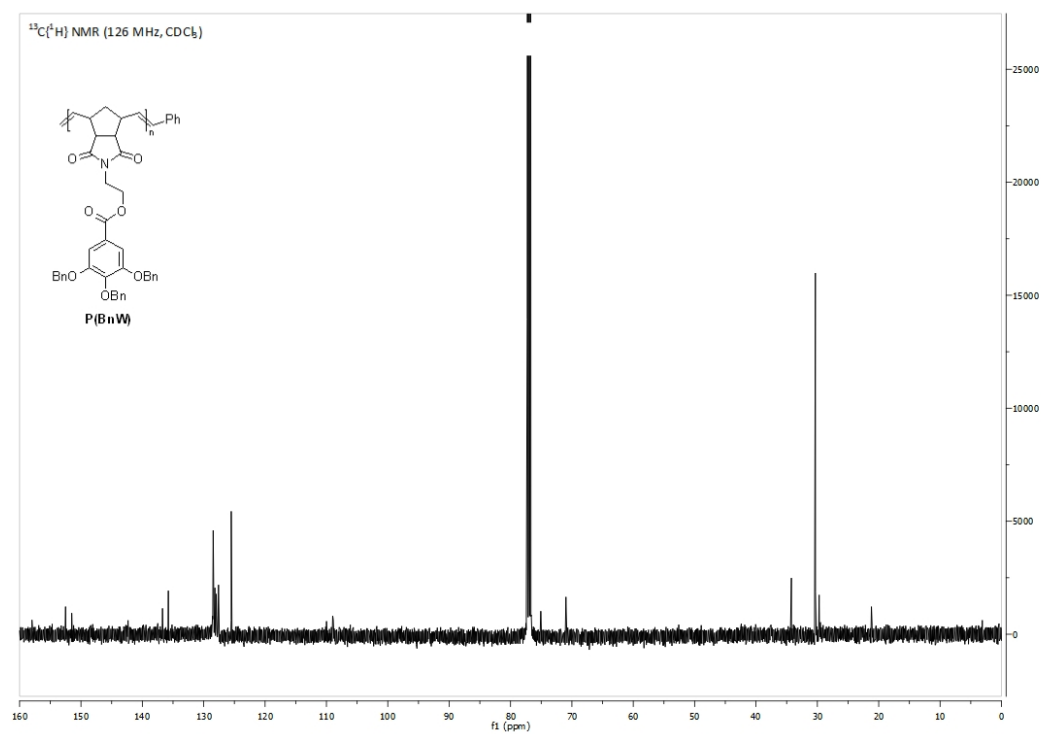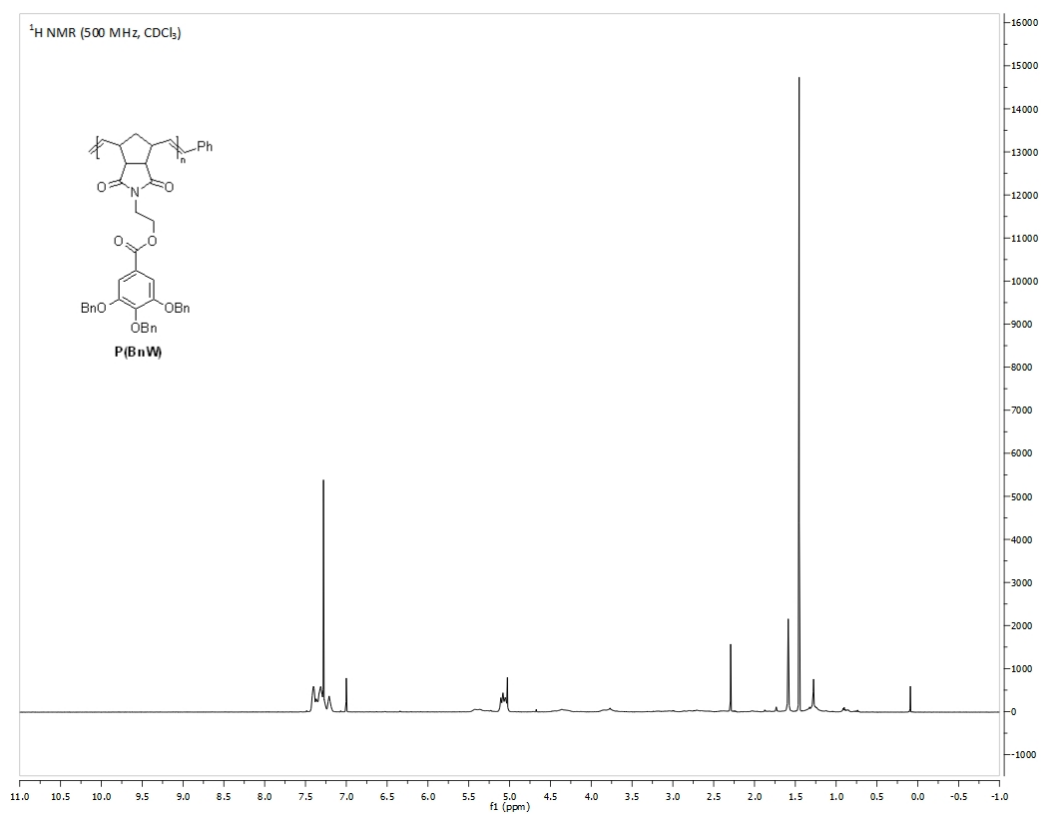
[1] (a) Bielawski, C. W.; Benitez, D.; Grubbs, R. H. *Science*, **2002**, *297*, 2041–2044. (b) Culkin, D. A.; Jeong, W.; Csihony, S.; Gomez, E. D.; Balsara, N. P.; Hedrick, J. L.; Waymouth, R. M. *Angew. Chem.* **2007**, *119*, 2681–2684.

[2] (a) Newkome, G. R.; Yao, Z; Baker, G. R.; Gupta, V. K. *J. Org. Chem.* **1985**, *50*, 2003–2004. (b) Hawker, C. J.; Fréchet, J. M. J. *J. Am. Chem. Soc*. **1990**, *112*, 7638–7647.

[3] (a) Xia, Y.; Olsen, B. D.; Kornfield, J. A.; Grubbs, R. H. *J. Am. Chem. Soc.* **2009**, *131*, 18525–18532. (b) Xia, Y.; Kornfield, J. A.; Grubbs, R. H. *Macromolecules* **2009**, *42*, 3761–3766.

[4] Pangborn, A. B.; Giardello, M. A.; Grubbs, R. H.; Rosen, R. K.; Timmers, F. J. *Organometallics* **1996**, *15*, 1518–1520.

[5] Love, J. A.; Morgan, J. P.; Trnka, T. M.; Grubbs, R. H. *Angew. Chem., Int. Ed. Engl.* **2002**, *41*, 4035–4037.

[6] Matson, J. B.; Grubbs, R. H. *J. Am. Chem. Soc.* **2008**, *130*, 6731–6733.

Chapter 2

Catalyst-Dependent Routes to Alternating Copolymers of a 1- Substituted

Oxanorbornene and Cyclooctene

Abstract

The alternating copolymerization of *cis*-cyclooctene and 1-substituted oxanorbornenes with commercially available ruthenium-based olefin metathesis catalysts was investigated. We discovered that $RuCl_2(CHPh)(PCy_3)_2$ performs a standard alternating copolymerization, but that there is another route to the desired A-B alternating copolymers. The 'sequence editing' route involves the initial polymerization of *cis*-cyclooctene, followed by a ring-opening cross metathesis step that introduces the 1-substituted oxanorbornene monomer in the polycyclooctene chain and largely avoids oxanorbornene homopolymerization. Selectivity for the alternating diads in the polymer exceeds 90%. Polymer molecular weight can be controlled by linear olefin chain-transfer reagents during sequence editing.

Introduction

Polymer sequence control is a critical component across the broad spectrum of science, from biology to materials engineering. Biological systems produce nucleotide polymers whose sequence fidelity underpins both the maintenance and evolution of life. While synthetic chemistry will always be challenged to reach the incredible specificity of enzymatic catalysis, some technologies have achieved commendable control over alternating copolymerizations. For example, many step-growth polymers are obligate

alternating copolymers.[1]   Common examples of chain-growth systems with high alternating sequence regularity include epoxide-CO_2[2] and ethylene-CO materials[3].

One of the most ubiquitous polymerization reactions is ring-opening metathesis polymerization (ROMP), owing to its operational simplicity and high functional group tolerance. ROMP is not well known for the synthesis of alternating copolymers, but some reports exist for the copolymerization of norbornene derivatives and *cis*-cyclooctene. These include examples utilizing ruthenium catalysts design by Chen[4] and Buchmeiser[5], along with monomer control by our group[6] and that of Coughlin[7]. Ruthenium, osmium, and iridium catalysts can be prepared *in situ* to perform the alternating copolymerization of norbornene and cyclopentene.[8]   In many cases, the reaction conditions that produce polymer with the most alternating structure require an excess of COE over norbornene.

Results and Discussion

We sought to expand the ease and scope of alternating copolymerizations with ROMP. To meet this goal, we decided to pursue a method controlled by monomer sterics (Figure 2.1). Such a scheme would involve the incorporation of a bulky 1-substituted norbornene **1** followed by cis-cyclooctene (**2**) in an alternating fashion. The substitution in the 1-position on **1** should discourage homopolymerization of this monomer, while the high ring strain inherent to norbornenes would promote its incorporation with relatively unencumbered **2** as the ultimate unit.
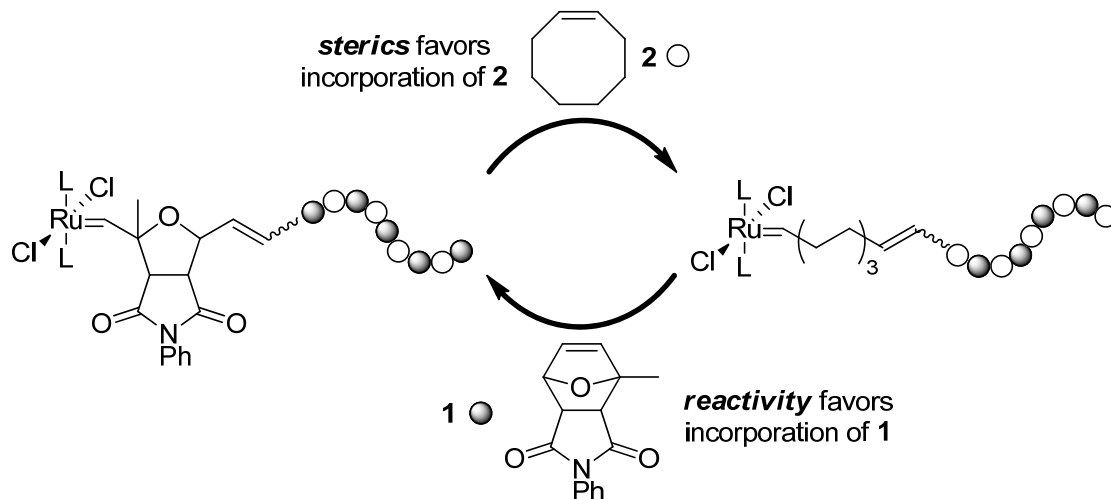
Figure 2.1. Monomer-controlled alternating copolymerization of *cis*-cyclooctene and a 1-substituted norbornene

We screened a panel of commercially available ruthenium-based olefin metathesis catalysts. Catalysts **A**, **B**, **C**, and **D** offer a range of electronic and steric variations that will help us map the parameters in this study (Figure 2.2).[9] Furthermore, ruthenium-based alkylidene complexes tend to tolerate oxygen, water, and more classes of functional groups than their early transition metal counterparts.[10] Using an equimolar mixture of **1** and **2**, we performed a statistical copolymerization with each of the catalysts to synthesize poly(**1**-*alt*-**2**) (Table 2.1). We evaluated the catalysts by measuring the percentage of alternating diads with ¹H NMR, where the olefinic signals for each type of diad are readily distinguishable (see Supporting Information for the complete analysis). The sequence composition of each polymer is catalyst dependent. The N-heterocyclic carbene (NHC) ligated series of catalysts (**B**, **C**, and **D**) showed an expected increase in selectivity from 44% to 50% to 73% for alternating diads with an increase in steric bulk, supporting our initial hypothesis.
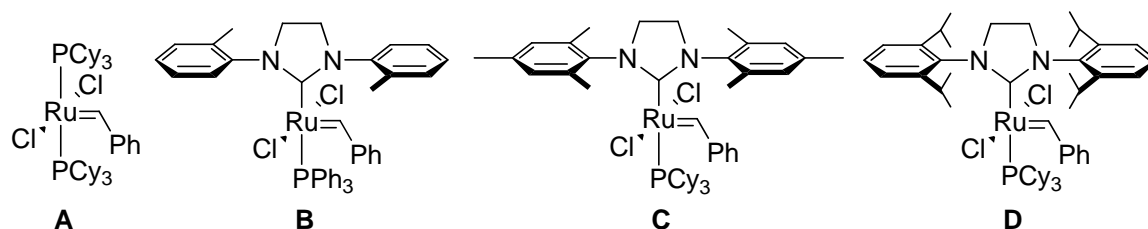
Figure 2.2. Ruthenium-based olefin metathesis catalysts in this study

With the success of our initial screen, we decided to delve deeper into the kinetic parameters of the alternating copolymerization of **1** and **2**. We employed the initial rates[11] method to obtain reactivity ratios for the catalysts, where r_1 is the reactivity ratio for **1** and r_2 is the reactivity ratio for **2**. The data were analyzed with the Kelen-Tüdös (KT) linear method and the Kuo-Chen (KC) exponential method, which closely agreed. Unfortunately, rapid and complete homopolymerization of COE to polycyclooctene (**P2**) prevented the calculation of reactivity ratios for **B** and **D**.

Table 2.1. Diad Analysis of poly(1-*alt*-2)
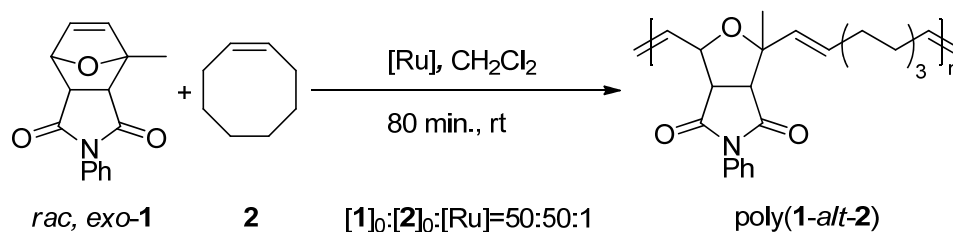
[Ru]	yield/%	alternation/%[a]	M_n/kDa	M_w/kDa	PDI
A	56	56	22.6	25.7	1.140
B		44			
C	75	50	55.0	79.2	1.440
D	82	73	16.9	26.5	1.573

(a) Alternation was calculated as the percentage of total diads that are alternating diads measured by ^{1}H NMR.

The reactivity ratios were revealing as to the efficacy of alternating copolymerization of **1** and **2** by catalysts **A** and **C** (Table 2.2). Ratio r_1 for **A** is 0.004 (KT) and 0.007 (KC), confirming the initial observation that **1** undergoes very sluggish homopolymerization in the presence of **A**. Homopolymerization of **2** by **A** is much more competitive, but still not the dominant polymerization sequence, with r_2=0.666 (KT) and 0.562 (KC). The products r_1r_2(KT) and r_1r_2(KC) are 0.003 and 0.004, respectively, indicating that the copolymerization of **1** and **2** by **A** has strongly alternating character.

Table 2.2. Reactivity Ratios

| [Ru]	method	r_1	r_2	r_1r_2
A	KT	0.004	0.666	0.003
A	KC	0.007	0.562	0.004
C	KT	0.091	3.290	0.299
C	KC	0.199	3.730	0.742
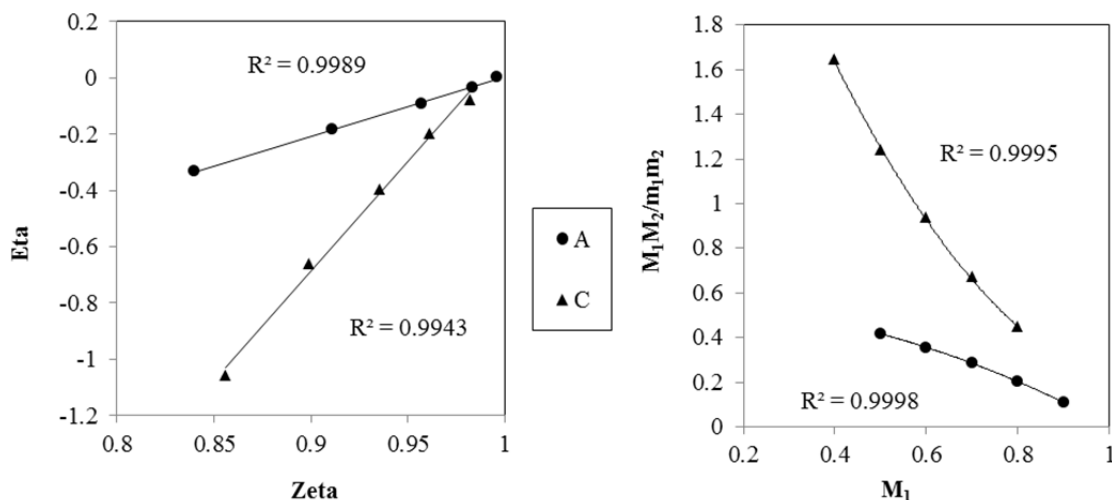
Details for the Kelen-Tüdös (left) and Kuo-Chen (right) fits are provided in the Supporting Information.

For catalyst **C**, selectivity degrades for all processes. Incorporation of **2** after **1** is still preferred, but less favorably (r_1(**C**, KT)=0.91 and r_1(**C**, KC)=0.199). The selectivity for **2** actually reverses, demonstrating at least a threefold preference for **2** homopolymerization over **1** incorporation after **2**. The products r_1r_2(C, KT)=0.300 and r_1r_2(C, KC)=0.742 indicate that the polymerization of **1** and **2** with **C** has little alternating character. Taken together, these data show that **A** is the only screened catalyst that performs a standard alternating polymerization.

The reactivity ratio study also revealed an apparent contradiction with the first screen. We originally stated that **D** was the most effective catalyst for alternating

copolymerization, providing poly(**1**-*alt*-**2**) with 73% alternating diads. When examined for a reactivity ratio, though, **D** only polymerized **2**. Our hypothesis to explain the discrepancy follows: catalyst **D** first homopolymerizes **2**, then performs ring-opening cross metathesis (ROCM) between **1** and the still-active olefins of P**2**. The olefins of PCOE are passivated to further metathesis when included in an alternating diad, due to the unfavorable steric repulsion that accompanies catalyst ligation to those sites. This 'sequence editing' scenario is also likely for **B**, which also only produced P**2** from the reactivity ratio study (Figure 2.3).
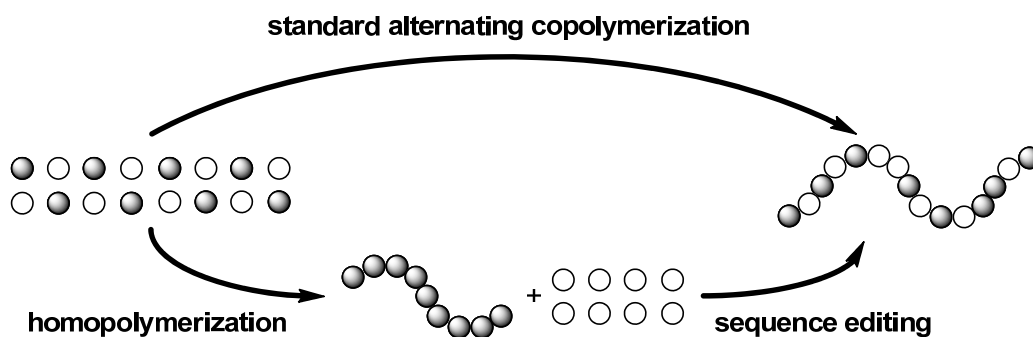
Figure 2.3. Sequence editing compared to standard alternating copolymerization

To test our hypothesis, we prepared and isolated a sample of poly-**2** (M_n=3632, M_w=5770, PDI=1.588), then subjected it to **1** and the panel of ruthenium-based olefin metathesis catalysts. At a 2 mol% catalyst loading, **D** was the fastest catalyst, with **C** only slightly less active, and each surpassed 90% conversion after 25 minutes. Catalyst **B** only performs sequence editing to approximately 50% conversion and likely decomposes under the reaction conditions. While it is the least active of the catalysts, **A** does not appear to decompose (Figure 2.4).
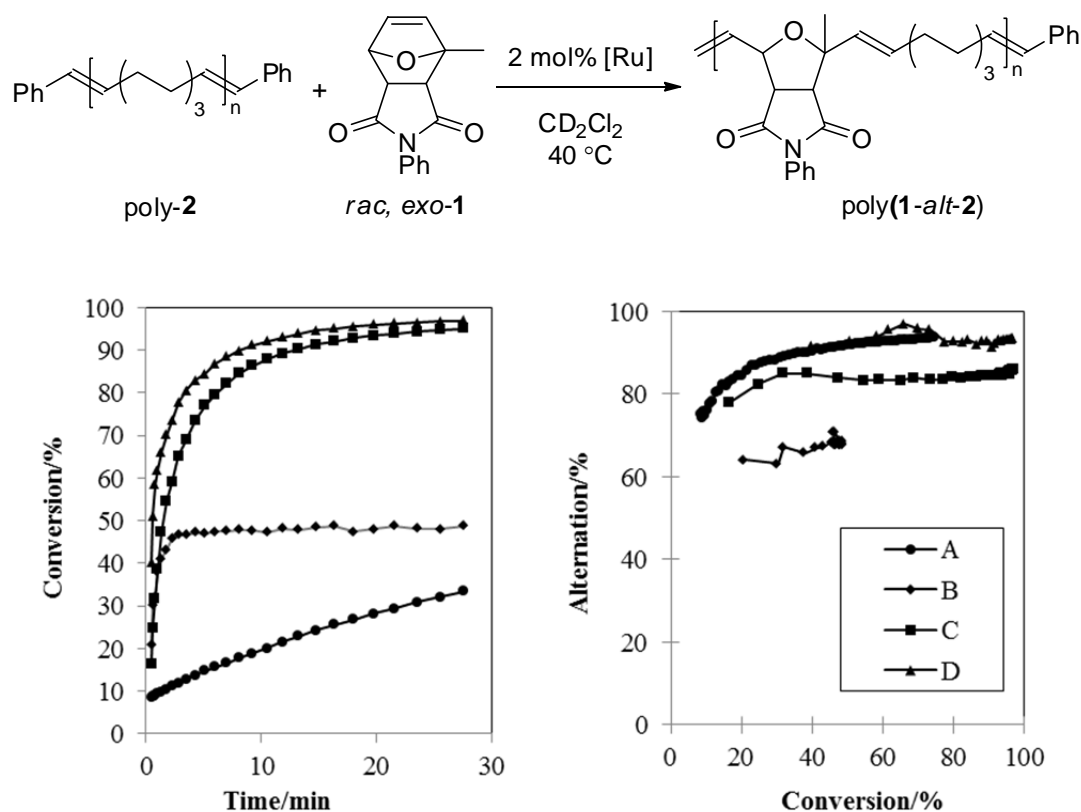
Figure 2.4. Catalyst evaluation for reaction rate and selectivity. The reactions were monitored by ^{1}H NMR

For the most part, the sequence editing experiments agree with our initial analysis. Catalysts **A** and **D** are the most selective (> 90% alternation), again due to steric reasons. As the size of the NHC ligand decreases from **D** to **C** to **B**, so does the quantity of alternating diads (Figure 2.4). Combined with the reaction rate data, **D** has a unique combination of activity and selectivity for sequence editing.

With a good understanding of the relationships between catalyst structure, activity, and selectivity, we sought to deduce the factors behind molecular weight control. Sequence editing with ROMP is based on a poly-**2** backbone, whose molecular weight is

known to be controlled by linear olefin chain-transfer reagents (CTA). Furthermore, chain transfer is required to introduce each unit of **1** into poly-**2** during the sequence-editing step. To probe the effects of chain transfer, we preformed poly-**2** with ratios of [**2**]/[CTA] from 10 to 150 (CTA=*trans*-stilbene) and catalyst **D**, then introduced an equimolar amount of **1** to the reaction vessel (Figure 2.5).
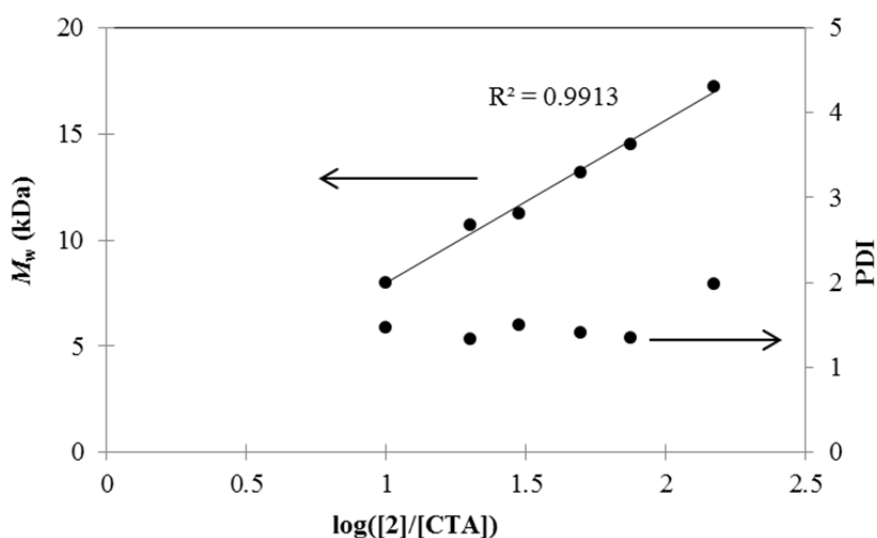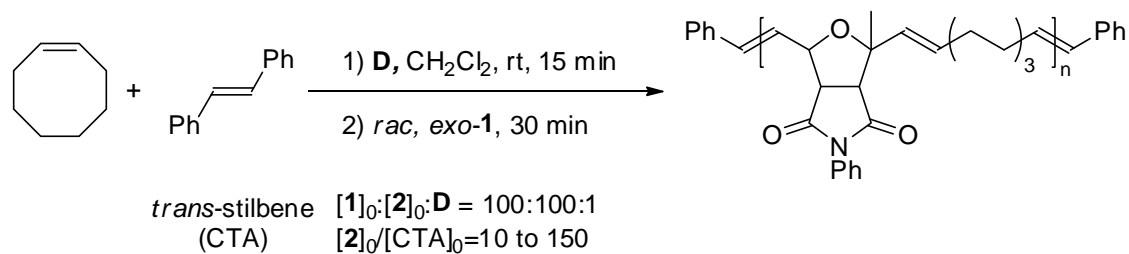
Figure 2.5. Molecular weight control of sequence editing by chain transfer

The molecular weight control experiments revealed three interesting points. First, the M_w has a linear relationship with the $\log([\mathbf{2}]_0/[CTA]_0)$ with *tran*-stilbene as the CTA. Second, polydispersity is moderate, hovering between 1.3 and 1.5 for the most part. This

is expected for a polymer formed from many chain transfer steps. Lastly, sequence editing is possible and well- controlled even without the isolation of poly-**2**.

Conclusions

The ring-opening metathesis alternating copolymerization of **1** and **2** with ruthenium catalysts showed that there exist two catalyst-dependent pathways to poly(**1**-*alt*-**2**). Catalyst **A** is the only catalyst that performed a 'standard' alternating copolymerization, We further discovered that there is another route to poly(**1**-*alt*-**2**): the initial production of poly-**2** followed by a sequence-editing step that introduces **1** at each active olefin. All examined catalysts could perform sequence editing to varying extents, with **D** being both the most active and most selective catalyst, likely due to the steric bulk of its NHC ligand. The molecular weight of the sequence-edited polymer can be controlled by the ratio of monomer-to-chain transfer reagent. Further work in this area will seek to expand the monomer scope, both to increase selectivity for alternation and to include functional monomers.

Supporting Information

General Information

NMR spectra were recorded in $CDCl_3$ or CD_2Cl_2 on Varian Mercury 300 MHz or INOVA 500 MHz spectrometers in the High-Resolution Nuclear Magnetic Resonance Facility at the California Institute of Technology (Caltech), unless otherwise noted. ^{1}H and ^{13}C chemical shifts are referenced relative to the residual solvent peak ($CDCl_3$ δ=7.27 for ^{1}H and δ=77.23 for ^{13}C; CD_2Cl_2 δ=5.32 for ^{1}H and δ=54.00 for ^{13}C). Spectral

analysis was performed on MestReNova software. High-resolution mass spectra were provided by Caltech's Mass Spectrometry Facility. Gel permeation chromatography (GPC) was performed in tetrahydrofuran (THF) on two MZ-Gel 10-µm columns composed of styrene-divinylbenzene copolymer (Analysentechnik) and connected in series, with a miniDAWN TREOS multiangle laser light scattering (MALLS) detector, ViscoStar viscometer, and Optilab rEX differential refractometer (all three from Wyatt Technologies). No calibration standards were used, as light scattering is considered an accurate measurement of molecular weight. Each sample was weighed and the dn/dc was calculated assuming 100% mass elution from the column. GPC data analysis was performed with ASTRA software.

Materials

CH_2Cl_2 was purified by passage through a solvent purification system.[12] $CDCl_3$ and CD_2Cl_2 were obtained from Cambridge Isotopes. CD_2Cl_2 was purified by vacuum transfer from P_2O_5. Catalysts **A**, **B**, **C**, and **D** were gifts from Materia, Inc. All other solvents and chemicals were obtained from Sigma-Aldrich Corporation and used as received.

Synthesis of **1**.

rac, exo-**1**
60%
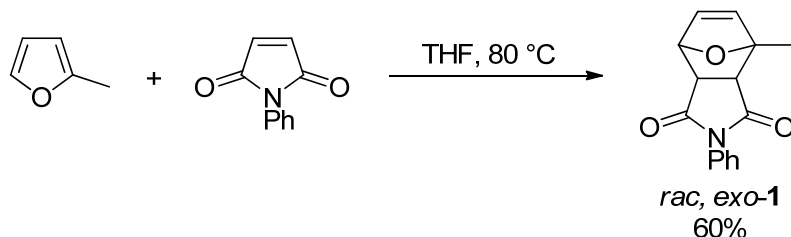
A 500 ml roundbottom flask equipped with a magnetic stirbar was charged with N-phenylmaleimide (34.6 g, 0.2 mol, 1 equiv), 2-methylfuran (35 ml, 0.4 mol, 2 equiv), and THF (200 ml). The mixture was heated to 80 °C and refluxed for 6 hours. The yellow solution was then cooled to room temperature. A white microcrystalline solid precipitates upon standing. After further cooling to -20 °C in a freezer overnight, the solid was filtered and washed with a small amount of cold THF to give **1** (30.9 g, 0.12 mol, 60%). HRMS (EI+): calculated = 255.0895, found = 255.0894.

Initial Experiments
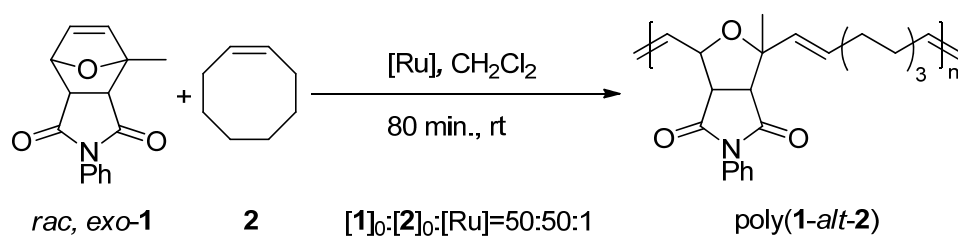
In a nitrogen-filled glovebox, **1** (516 mg, 2 mmol) was dissolved in CH_2Cl_2 (3.2 ml) in a scintillation vial equipped with a PTFE-coated magnetic stirbar. *Cis*-cyclooctene (**2**, 260 µl, 2 mmol) was added to the solution. The monomer solution (0.8 ml apiece) was aliquotted into four magnetic stirbar-equipped vials. Catalysts **A–D** (0.01 mmol each) were dissolved in CH_2Cl_2 (0.2 ml each). The separate catalyst solutions were then added in their entirety to the monomer solutions and the vials were sealed. The final monomer and catalyst ratios are $[\mathbf{1}]_0$:$[\mathbf{2}]_0$:[Ru]=50:50:1. The polymerizations were allowed to proceed for 80 minutes total. During the reaction, the vials were removed from the glovebox. After the allotted time, the polymerizations were quenched with ethyl vinyl ether (200 µl) and stirred for 15 minutes. The crude reaction mixtures were precipitated into Et_2O (35 ml). The polymer suspension was separated by centrifugation.

The pellets were dissolved in CH_2Cl_2 (5 ml) and precipitated into Et_2O (35 ml). The polymer suspension was again separated by centrifugation. The reprecipitation and centrifugation were repeated with MeOH. The final pellet was dried *in vacuo* overnight. The resulting poly(**1**-*alt*-**2**) samples were analyzed by NMR for diad composition and GPC for molecular weight data.

Reactivity Ratios

rac, exo-**1**   **2**   ([**1**]$_0$+[**2**]$_0$)/[Ru] = 1000   poly(**1**-*alt*-**2**)

                                           <5% conversion
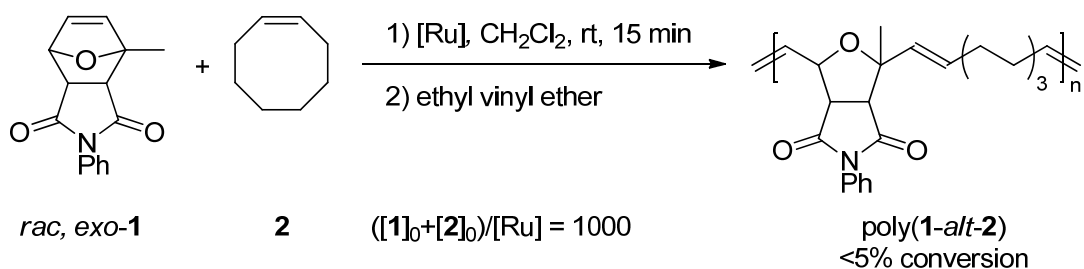
All reactivity ratio experiments were set up in a nitrogen-filled glovebox. For each catalyst, there were five monomer ratios. The monomer solutions were prepared from the designated amount of **1** in CH_2Cl_2 (14 ml) and the designated amount of **2** in scintillation vials with magnetic stirbars. Total amount of monomer for each polymerization is 10 mmol. Catalyst stock solutions were prepared from **A**–**D** with the catalyst (0.05 mmol) dissolved in CH_2Cl_2. For each different monomer solution, 1 ml of catalyst stock solution was added to initiate the polymerization. The initial ratios were ([**1**]$_0$+[**2**]$_0$)/[Ru]=1000 for all reactions. The scintillation vials were sealed and removed from the box during the 15 minute reaction time. The polymerization was terminated by the addition of ethyl vinyl ether (1 ml) and stirring for 15 minutes. The white, stringy, polymeric products were isolated by precipitation into MeOH (200 ml). Volatiles were

removed *in vacuo* overnight. The monomer incorporation ratios were measured by [1]H

NMR.

Reactivity Ratio Monomer Feeds

1 (mmol)	**1** (g)	**2** (mmol)	**2** (ul)	Molar feed ratio **1/2**	Catalysts A	B	C	D
3	0.77	7	912	0.43				X
4	1.02	6	782	0.67		X	X	X
5	1.28	5	651	1.00	X	X	X	X
6	1.53	4	521	1.50	X	X	X	X
7	1.79	3	391	2.33	X	X	X	X
8	2.04	2	261	4.00	X	X	X	
9	2.30	1	130	9.00	X			

The symbols for the Kelen-Tüdös and Kuo-Chen models are defined below.

M_1=mole fraction of **1** in the monomer feed

M_2=mole fraction of **2** in the monomer feed

m_1=mole fraction of **1** in the polymer

m_2=mole fraction of **2** in the polymer

$F=(m_2/m_1)(M_1/M_2)^2$

$G=(M_1/M_2)(1-(m_2/m_1))$

alpha=$\alpha=(F_{min}F_{max})^{1/2}$, where F_{min} and F_{max} are the lowest and highest values for a set of

experimental points, respectively

eta=$\eta=G/(\alpha+F)$

zeta=$\zeta=F(\alpha+F)$

The Fineman-Ross (FR) linear method is the simplest way to determine r_1 and r_2.

The FR method plots G against F, where r_1 is the slope and r_2 is the intercept. The Kelen-

Tüdös linear method adds the correction factor α to utilize the characteristics of the

experiment and lessen the effect of the extreme points. The KT linear method plots ζ against η, and gives $-r_2/\alpha$ as the intercept and r_1+r_2/α as the slope.

The Kuo-Chen exponential method plots $(M_1M_2)/(m_1m_2)$ against M_1. The exact exponential is subjective, but is commonly second-order for M_1. This is the case for our experiments. The reactivity ratios r_1 and r_2 are calculated from the extrapolation of the equation to $M_1=1$ and $M_1=0$, respectively.

Polycyclooctene (poly-**2**) Synthesis for Sequence Editing
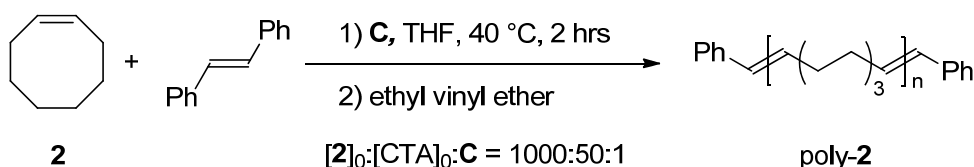
In a nitrogen-filled glovebox, *cis*-cyclooctene (2.6 ml, 20 mmol, 1000 equiv.), *trans*-stilbene (180 mg, 1 mmol, 50 equiv.) and catalyst **C** (17 mg, 0.02 mmol, 1 equiv) were dissolved in THF (10 ml) in a scintillation vial. The vial was sealed, removed from the glovebox and heated at 40 °C in an oil bath for 2 hours. Once the reaction was complete, the vial was cooled and the reaction was quenched with ethyl vinyl ether (~1 ml). The polymer (1.19 g) was recovered by precipitation into MeOH. $M_n=3632$ Da, $M_w=5770$ Da, PDI=1.588. ^{1}H and ^{13}C NMR spectra correspond with reported data.[13]

Homopolymerization of Compound **1**

rac, exo-**1** → poly-**1**

1) **C**, CH₂Cl₂, rt, 1 hr

2) ethyl vinyl ether
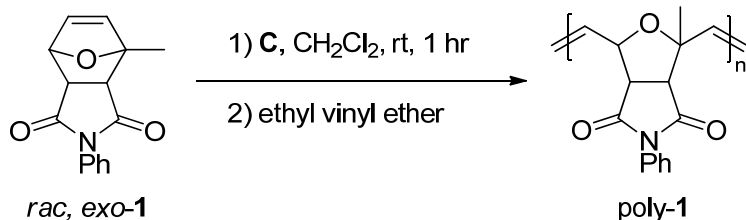
In a nitrogen-filled glovebox, **1** (290 mg, 1.1 mmol) was dissolved in methylene chloride (3 ml) in a scintillation vial with a stirbar. Catalyst **C** (10 mg, 0.012 mmol, [**1**]/[**C**]=92) was added to the monomer solution. The scintillation vial was sealed, removed from the glovebox, and allowed to stir at room temperature for 1 hour. The polymerization was quenched with ethyl vinyl ether (0.5 ml). The polymer solution was precipitated into diethyl ether (30 ml) and centrifuged to collect the solid. The supernatant was decanted. The polymer was washed with diethyl ether (30 ml), collected by centrifugation, and dried *in vacuo*. Poly(**1**) was recovered as a white solid (48 mg, 17 % isolated yield). The NMR spectra for poly(**1**) are given below.

Sequence-Editing Catalyst Evaluation

poly-**2** + *rac, exo*-**1** → poly(**1**-*alt*-**2**)

2 mol% [Ru]
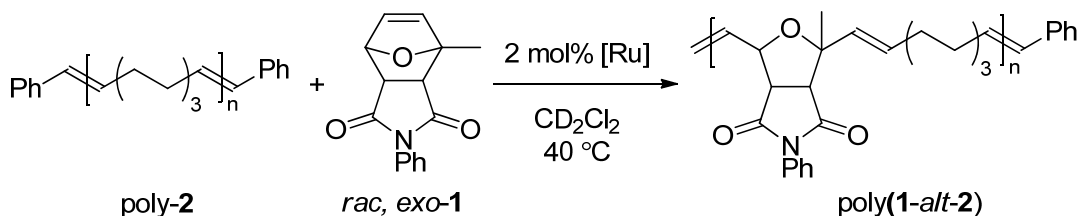
CD₂Cl₂
40 °C

In a nitrogen-filled glove-box, poly-**2** (140 mg, 1.3 mmol) and **1** (330 mg, 1.3 mmol) were dissolved in CD₂Cl₂ (6.3 ml) in a scintillation vial. This monomer stock solution was aliquotted into 4 septum screw-cap NMR tubes, with 1 ml of the stock solution in each tube. A stock solution of each catalyst was prepared (~ 0.4 ml, 0.02M)

with CD$_2$Cl$_2$ in septum screw-cap vials. All solutions were removed from the glovebox.

For each NMR rate experiment, the catalyst solution (0.2 ml) was injected into the

monomer stock solution in the NMR tube. The course of the reaction was monitored,
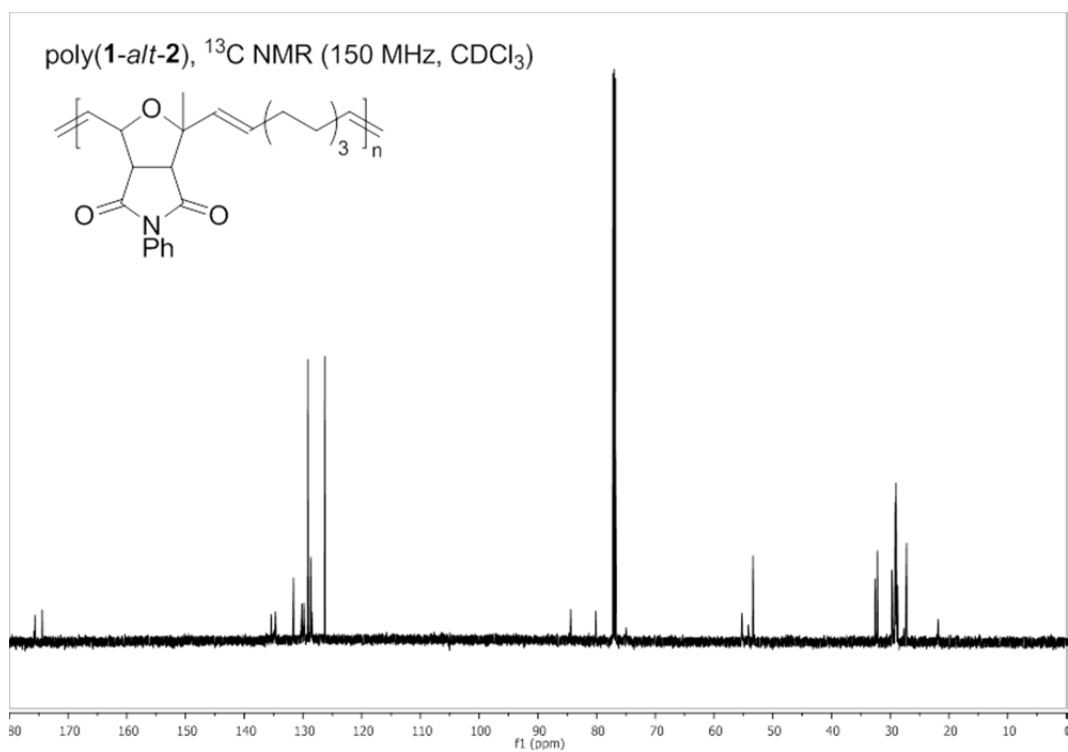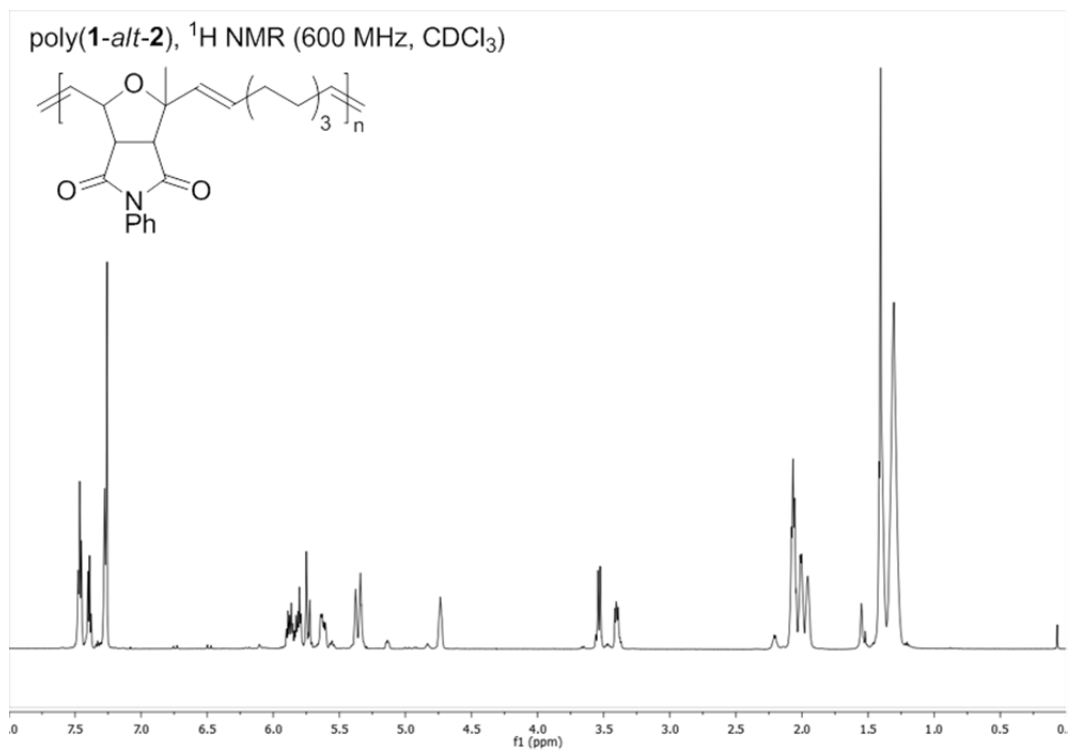
with 5 s intervals between each 8-transient experiment.
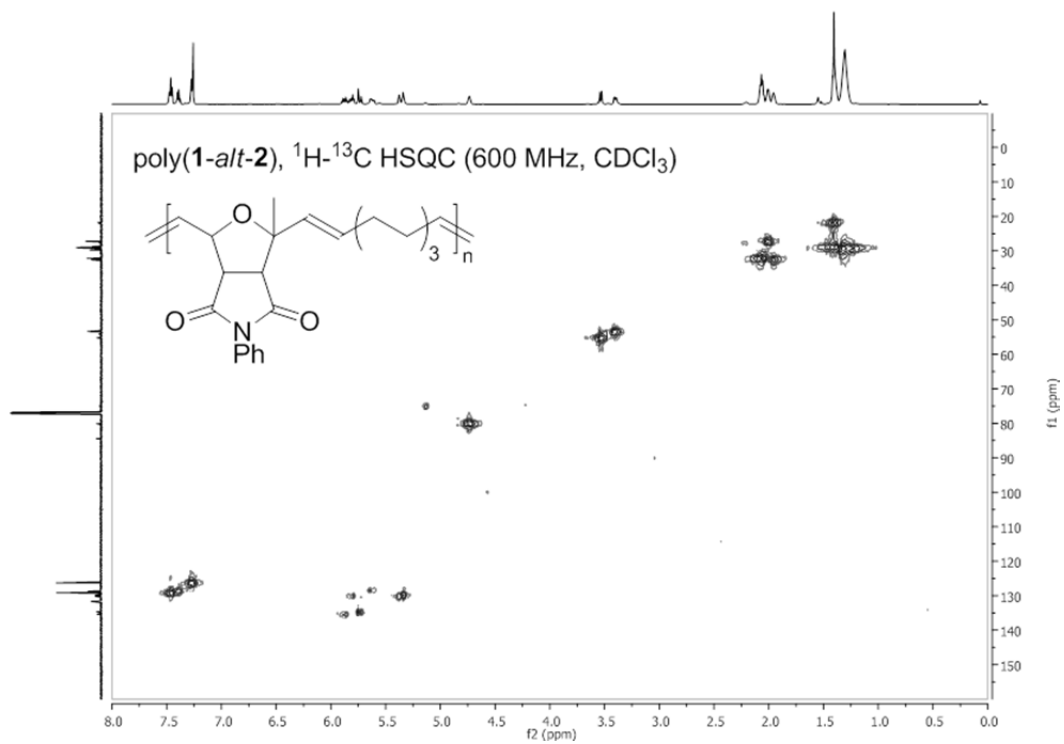
Sequence-Editing Molecular Weight Control
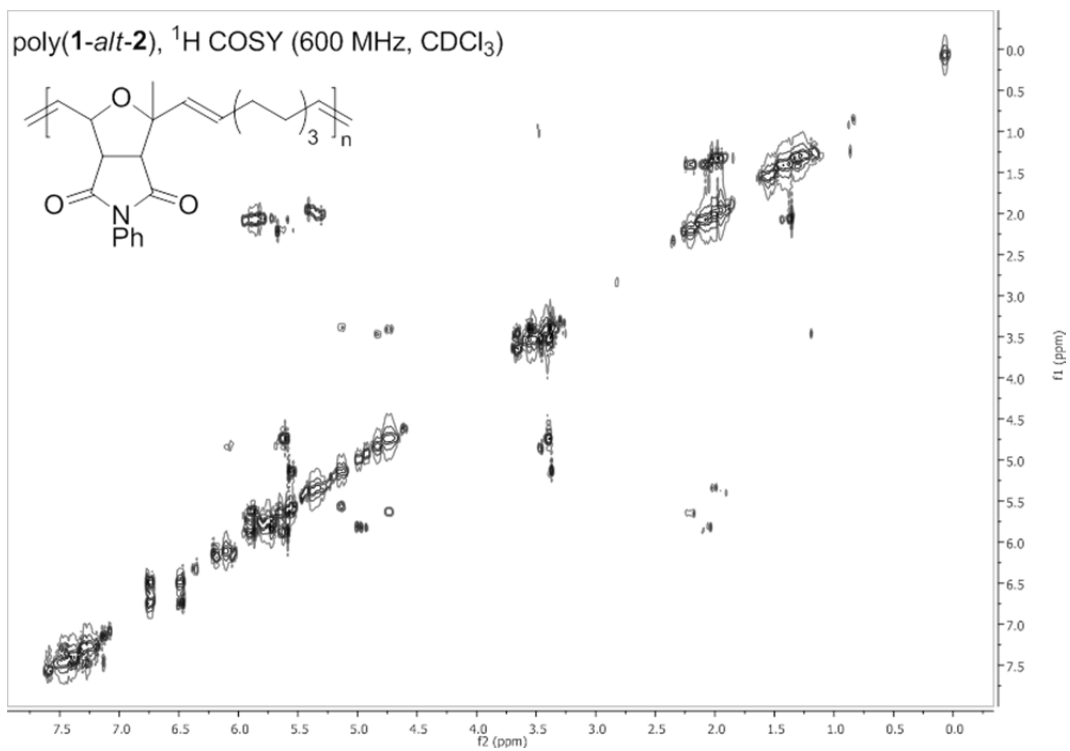

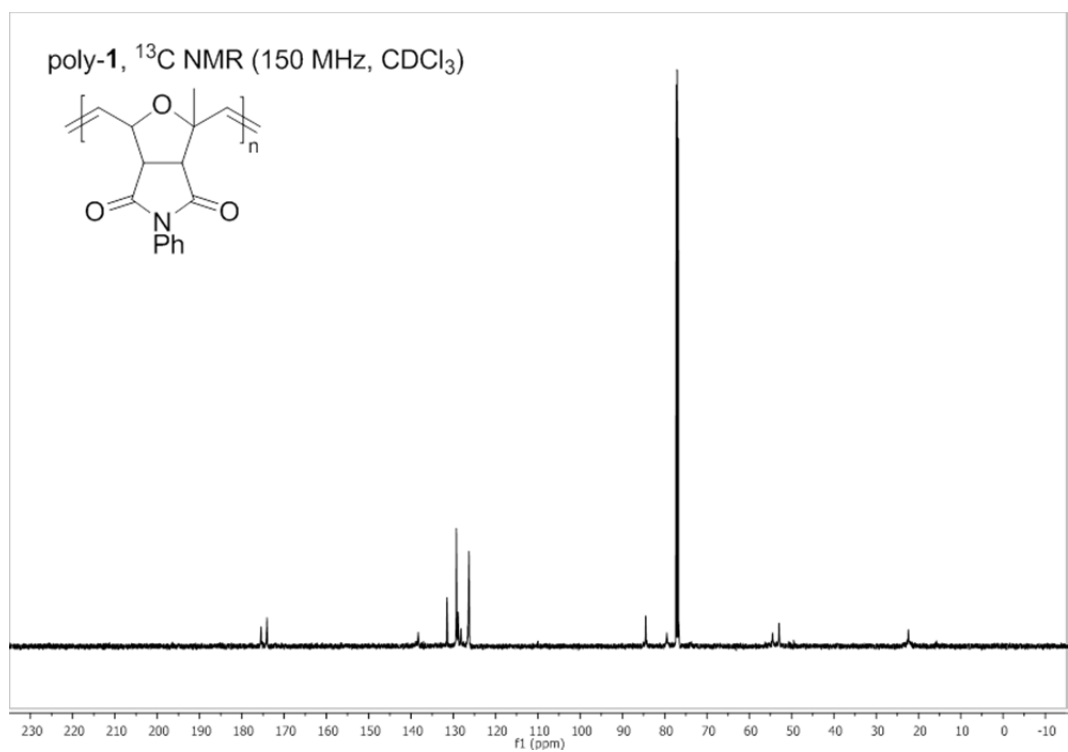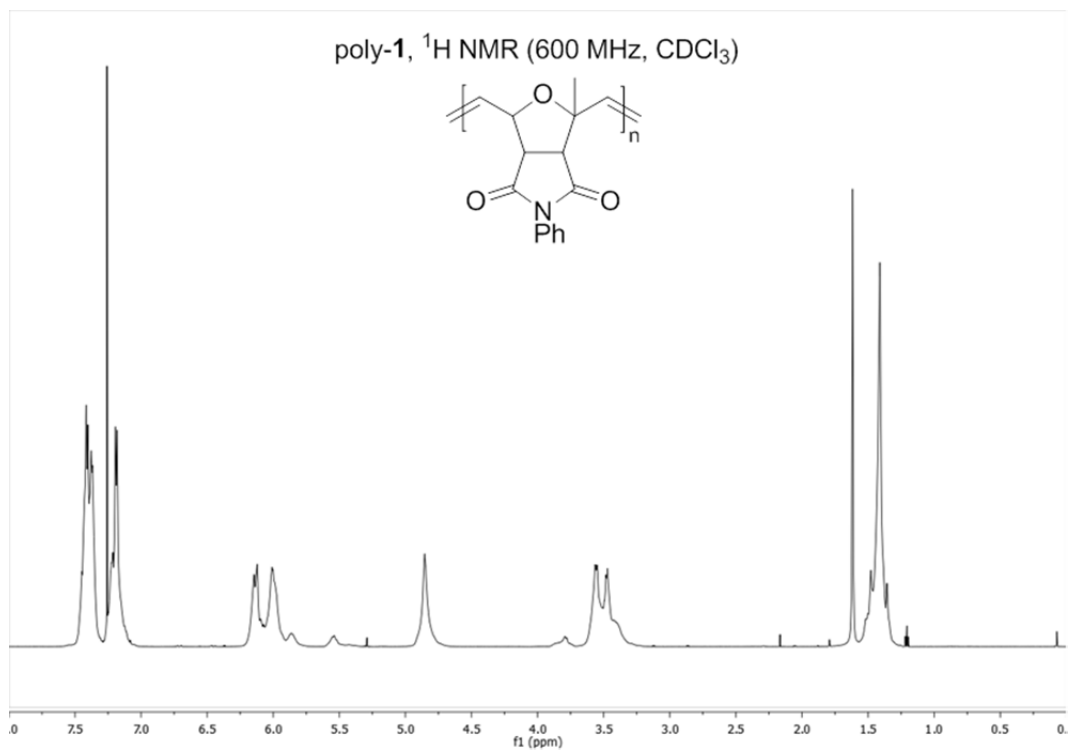trans-stilbene $[1]_0$:$[2]_0$:**D** = 100:100:1
(CTA) $[2]_0$/$[CTA]_0$=10 to 150
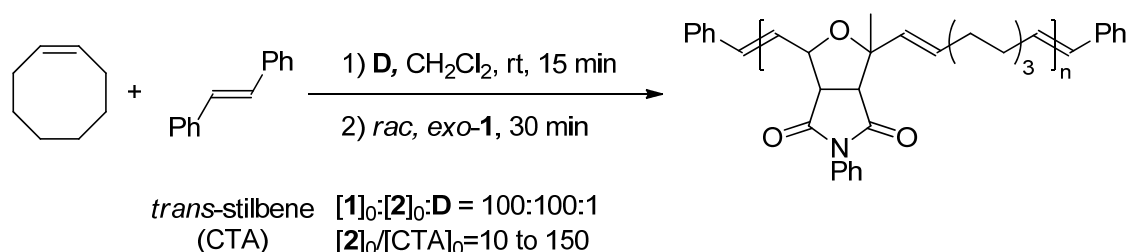
In a nitrogen-filled glovebox, four stock solutions were prepared. A stock

solution of **2** (130 μl, 1 mmol) was made in CH$_2$Cl$_2$ (2 ml). Aliquots (200 μl) were

placed in 6 vials, each equipped with a stirbar. A chain-transfer agent (CTA) stock

solution of trans-stilbene (18 mg, 0.1 mmol) in CH$_2$Cl$_2$ (1 ml) was made. The

appropriate amount of CTA stock solution was added to each vial to have the correct

2/CTA ratio. A catalyst stock solution of **D** (9.3 mg, 0.01 mmol) was prepared in CH$_2$Cl$_2$

(1 ml). To each **2**+CTA solution, 100 μl of catalyst stock solution was added to initiate

polymerization. The polymerization and chain transfer of **2** was allowed to proceed for

30 minutes. While this step proceeded, the sequence editing stock solution was prepared

from **1** (255 mg, 1 mmol) and CH$_2$Cl$_2$ (2 ml). After the polymerization of **2** was

complete, 200 μl of the sequence-editing stock solution was added to the reaction mixture

in each vial. All of the vials were sealed and removed from the glovebox. After stirring

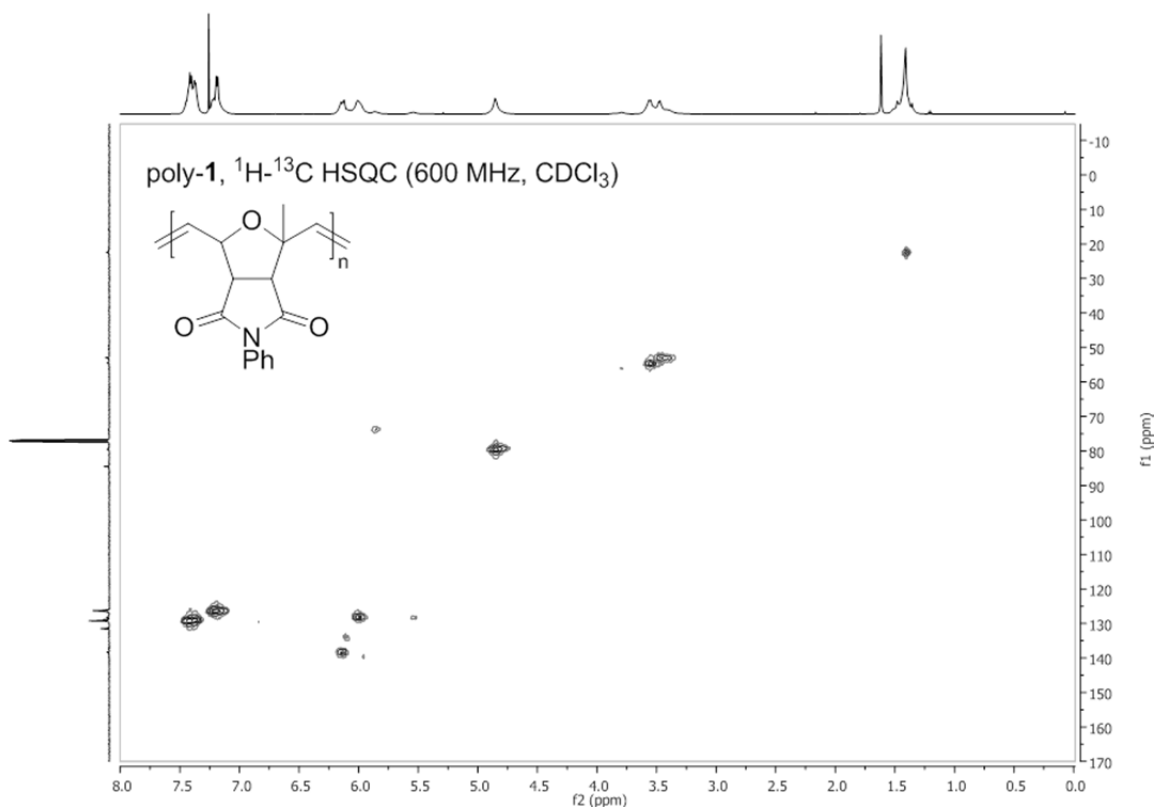for 15 minutes to complete the sequence-editing step, the reactions were quenched with
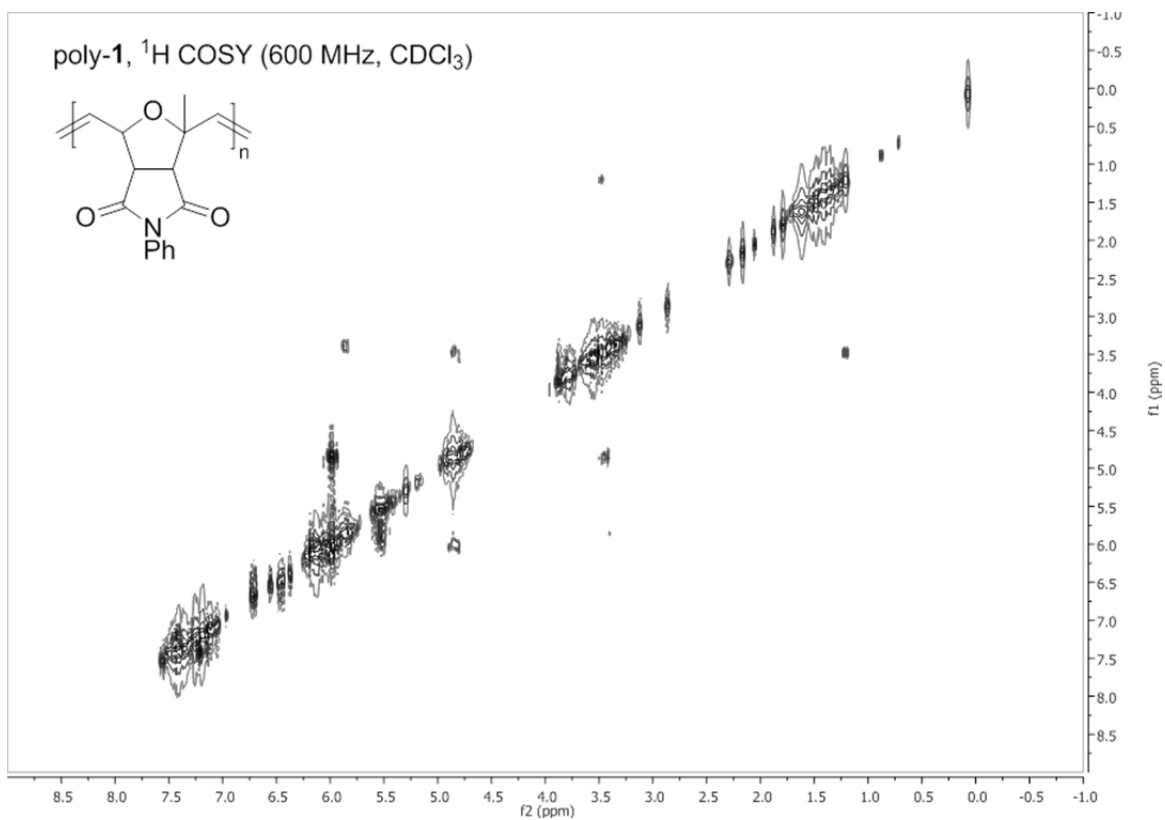
ethyl vinyl ether (200 µl). The volatiles were removed *in vacuo* to yield crude polymer, which was analyzed by GPC to obtain the molecular weight data.

$[2]_0/[CTA]_0$	mmol CTA	mg CTA	µl CTA solution
10	0.0100	1.80	100
20	0.0050	0.90	50
30	0.0033	0.60	33
50	0.0020	0.36	20
75	0.0013	0.24	13
150	0.0007	0.12	7

poly(**1**-*alt*-**2**), ¹H NMR (600 MHz, CDCl₃)

poly(**1**-*alt*-**2**), ¹³C NMR (150 MHz, CDCl₃)

poly(**1**-*alt*-**2**), ^{1}H COSY (600 MHz, CDCl$_3$)

poly(**1**-*alt*-**2**), ^{1}H-^{13}C HSQC (600 MHz, CDCl$_3$)

poly-**1**, ¹H NMR (600 MHz, CDCl₃)

poly-**1**, ¹³C NMR (150 MHz, CDCl₃)

poly-**1**, ¹H COSY (600 MHz, CDCl₃)

poly-**1**, ¹H-¹³C HSQC (600 MHz, CDCl₃)

(^{1}) Carothers, W. M. *Chem. Rev.* **1931**, *8*, 353–426.

(^{2}) (a) Darensbourg, D. J.; Holtcamp, M. W. *Macromolecules* **1995**, *28*, 7577–7579. (b) Super, M.; Berluche, E.; Costello, C.; Beckman, E. *Macromolecules* **1997**, *30*, 368–372. (c) Cheng, M.; Lobkovsky, E. B.; Coates, G. W. *J. Am. Chem. Soc.* **1998**, *120*, 11018–11019.

(^{3}) (a) Rix, F. C.; Brookhart, M.; White, P. S. *J. Am. Chem. Soc.* **1996**, *118*, 4746–4764. (b) Shultz, C. S.; Ledford, J.; DeSimone, J. M.; Brookhart, M. *J. Am. Chem. Soc.* **2000**, *122*, 6351–6356. (c) Bianchini, C.; Meli, A. *Coordin. Chem. Rev.* **2002**, *225*, 35–66.

(^{4}) (a) Bornand, M.; Chen P. *Angew. Chem. Int. Ed.* **2005**, *44*, 7909–7911. (b) Torker, S.; Müller, A.; Chen, P. *Angew. Chem. Int. Ed.* **2010**, *49*, 3762–3766. (c) Torker, S.; Müller, A.; Sigrist, R.; Chen, P. *Organometallics*, **2010**, *29*, 2735–2751.

(^{5}) Buchmeiser. M. R.; Ahmad, I.; Gurram, V.; Kumar, P. S. *Macromolecules* **2011**, *44*, 4098–4106.

(^{6}) Choi, T.; Rutenberg, I. M.; Grubbs, R. H. *Angew. Chem. Int. Ed.* **2002**, *41*, 3839–3841.

(^{7}) Ilker, M. F.; Coughlin, E. B. *Macromolecules*, **2002**, *35*, 54–58.

(^{8}) (a) Al Samak, B.; Carvill, A. G.; Hamilton, J. G.; Rooney, J. J.; Thompson, J. M. *Chem. Commun.* **1997**, 2057–2058. (b) Al Samak, B.; Amir-Ebrahimi, V.; Corry, D. G.; Hamilton, J. G; Rigby, S.; Rooney, J. J.; Thompson, J. M. *J. Mol. Cat. A* **2000**, *160*, 13–21.

(^{9}) (a) Schwab, P.; Grubbs, R. H.; Ziller, J. W. *J. Am. Chem. Soc.* **1996**, *118*, 100–110. (b) Stewart, I. C.; Ung, T.; Pletnev, A. A.; Berlin, J. M.; Grubbs, R. H.; Schrodi, Y. *Org.*

Lett. **2007**, *9*, 1589–1592. (c) Scholl, M.; Ding, S.; Woo, C. W.; Grubbs, R. H. *Org. Lett.* **1999**, *1*, 953–956. (d) Dinger, M. B.; Mol, J. C. *Adv. Synth Catal.* **2002**, *344*, 671–677.

([10]) Trnka, T. M.; Grubbs, R. H. *Acc. Chem. Res.* **2001**, *34*, 18–29.

([11]) (a) Allcock, H. R.; Lampe, F. W.; Mark, J. E. *Contemporary Polymer Chemistry*, 3rd ed.; Pearson Prentice Hall: Upper Saddle River, NJ, 2003; pp 360-368. (b) Odian, G. *Principles of Polymerization*, 4th ed.; John Wiley & Sons: Hoboken, NJ, 2004; Chapter 6. (c) Hagiopol, C. *Copolymerization: Toward a Systematic Approach*, Kluwer Academic: New York, NY, 1999.

[12] Pangborn, A. B.; Giardello, M. A.; Grubbs, R. H.; Rosen, R. K.; Timmers, F. J. *Organometallics* **1996**, *15*, 1518–1520.

[13] Alonso-Villanueva, J.; Cuevas, J. M.; Laza, J. M.; Vilas, J. L.; León, L. M. *J. App. Poly. Sci.* **2010**, *115*, 2440–2447.

Chapter 3

Kinetic Resolution of 1-Methyloxanorbornenes with a Chiral Ruthenium Initiator

Abstract

We report the first kinetic resolution polymerization by ring-opening metathesis polymerization (KR-ROMP). The polymerization profile showed a solvent-dependent variation of selectivity (S) over the course of the reaction. In THF and DCM, the resolution selectivity slowing increased over the course of the reaction, while in benzene, the selectivity was much higher in the beginning of the reaction and decreased throughout. The change in selectivity has been attributed to the helical nature of the growing polymer chain.

Introduction

The enantioselective synthesis of chiral small molecules and macromolecules is critical to both fundamental, academic studies and directed, industrial applications. Rarely do the spheres of small molecule total synthesis and polymers overlap, but this is the case for kinetic resolution polymerizations. This high-impact class of reactions simultaneously produces enantioenriched small-molecule monomers and chiral polymers for a variety of important monomers, including epoxides[1], lactide[2], methacrylamides[3], and α-olefins[4]. While kinetic resolution has been applied to many common polymerizations, there are no examples of kinetic resolution by ring-opening metathesis polymerization (KR-ROMP) to our knowledge. Since the first report of kinetic resolution by ring-closing metathesis (RCM) by chiral molybdenum alkylidene catalysts

from our group[5], there have been subsequent reports by the groups of Schrock and Hoveyda[6] and Ogasawara, Takahashi, and Kamikawa.[7] In this report, we disclose the first the example of kinetic resolution by ROMP and an unusual ligand effect on the selectivity of the polymerization.

Results and Discussion

Our model system is based on known initiator **I**, a member of a successful class of the ruthenium olefin metathesis catalysts that bear chiral monodentate N-heterocyclic carbenes (Scheme 3.1).[8] These catalysts are easily synthesized and have demonstrated selectivities up to 92% ee in asymmetric RCM at low catalyst loading (< 1 mol%). The enantioselectivity of the catalyst is derived from the chiral centers at positions 4 and 5 on NHC that impart the asymmetry to the N-aryl substituents and further to the metal center. Monomer **1** is a 1-methyloxanorbornene derivative that contains structural homology to a number of pharmaceutically active compounds.[9]
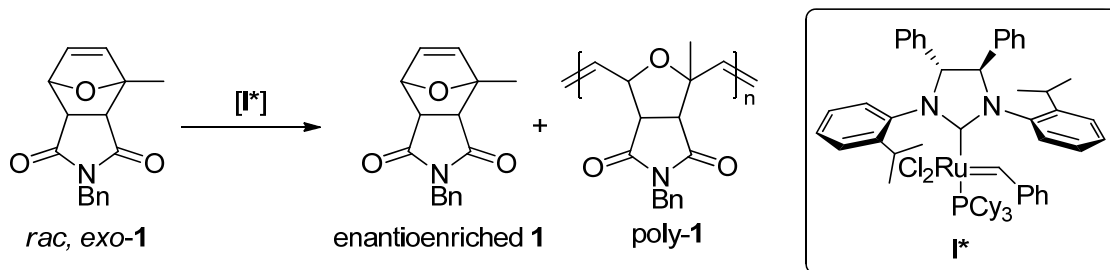

Scheme 3.1. Kinetic resolution by ring-opening metathesis polymerization (KR-ROMP)

The model KR-ROMP system was analyzed in a variety of solvents where the conversion, molecular weight, and selectivity (S) were determined over the course of the

reaction. The polymerization kinetics profiles indicate that a chain-growth mechanism still holds. The observed molecular weight is roughly fourfold higher than the theoretical molecular weight by conversion, likely caused by slow initiation. Further evidence for slow initiation comes from the broadened polydispersity of the isolated polymer (PDI_{THF}=1.1–1.2; PDI_{DCM}=1.2–1.3; PDI_{PhH}=1.3–1.4) compared to the polymers derived from norbornenes with just a proton at the 1 position. The methylated 1-position on the monomer prevents easy ligation and reaction with the initiator (Figure 3.1).

The resolution selectivity was examined next. In the cases where the reaction was performed in THF and DCM, the selectivity of the resolution increased over the course of the reaction from S=1.9 to S=3.8 for THF and S=1.4 to S=3.0 for DCM. Conversely, the resolution in toluene saw a *decrease* in the selectivity from S=15.7 to S=2.7. In most cases of kinetic resolution polymerizations, the S indicates relative rates of polymerization and stays the same throughout the reaction.
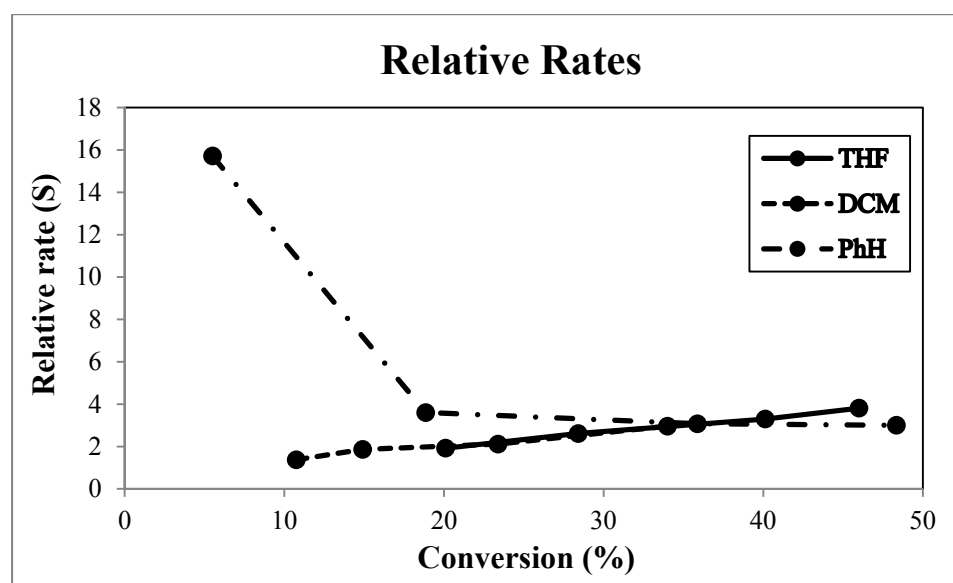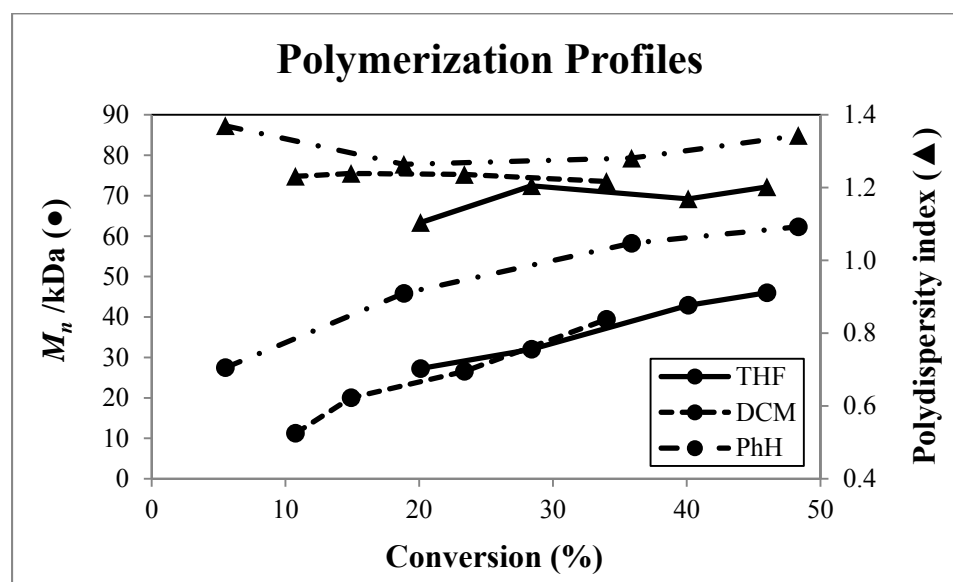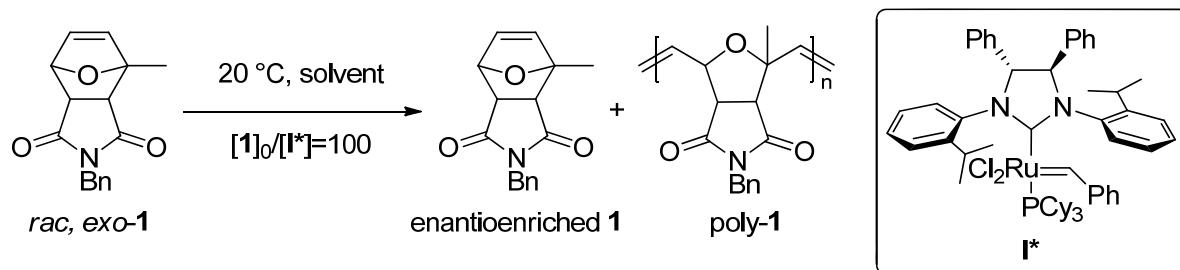
Figure 3.1. Solvent dependence for polymerization characteristics

To explain the change in selectivity over the course of the reaction, we postulated that the rigid polyoxanorbornene backbone with chiral centers may form a helix whose handedness could influence the selectivity of monomer incorporation. Polymers with excess one-handed helicity are known to have solvent-dependent handedness.[10] We synthesized monomer **2**, bearing an azobenzene moiety, to probe the effects of solvent on polymer secondary structure. Monomer **2** (λ_{max}=329 nm) was then polymerized by **I*** to poly-**2** (λ_{max}=324 nm) , where the remaining monomer possessed 17% ee (Figure 3.2).
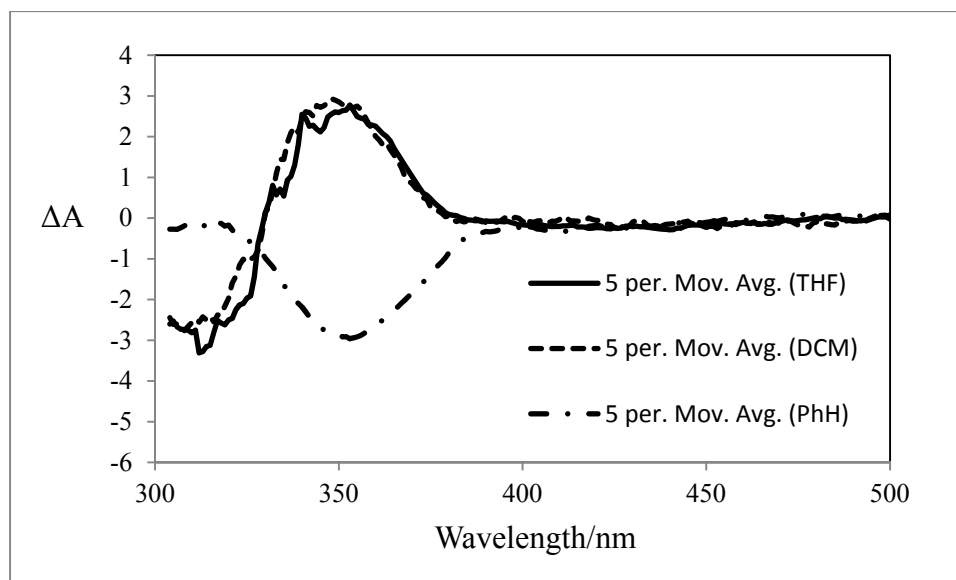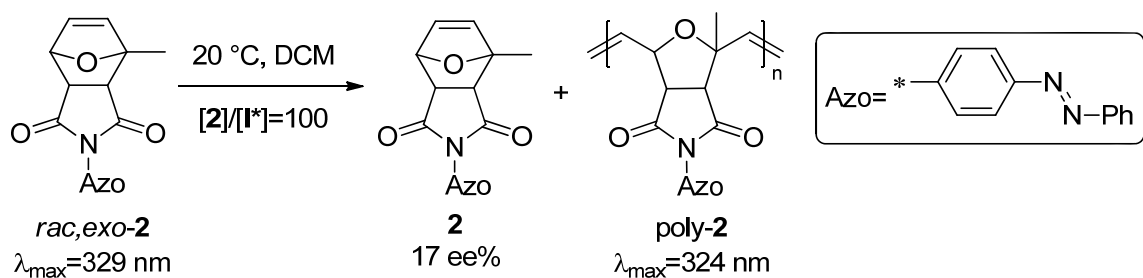
Figure 2. Solvent-dependent circular dichroism of poly-**2**

The isolated polymer was analyzed by circular dichroism and demonstrated a solvent-dependent response where samples in THF and DCM had positive ellipticity and a sample in benzene had negative ellipticity. The differences in helical sense correspond with change in selectivity differences in each reaction solvent. We believe that the stereochemical model that best explains this is one where the initiator adopts different diastereomeric conformations in THF and DCM or benzene. The growing polymer chain-end has three chiral control elements: the NHC ligand, the last incorporated monomer, and the helicity of the polymer chain. The NHC ligand is enantiopure and the same monomer is always enriched in the polymer, meaning that these factors are relatively constant. The polymer is constantly changing, though, as it grows and forms a helical structure which can influence the interaction of the ultimate incorporated monomer with the incoming monomer (Figure 3.3). Given the solvent-dependent nature of the helical sense, this is reflected in the mercurial selectivity of the resolution. The selectivity increases in THF and DCM as the polymer chain grows, which contrasts to the degradation of selectivity as the polymer chain grows in benzene.
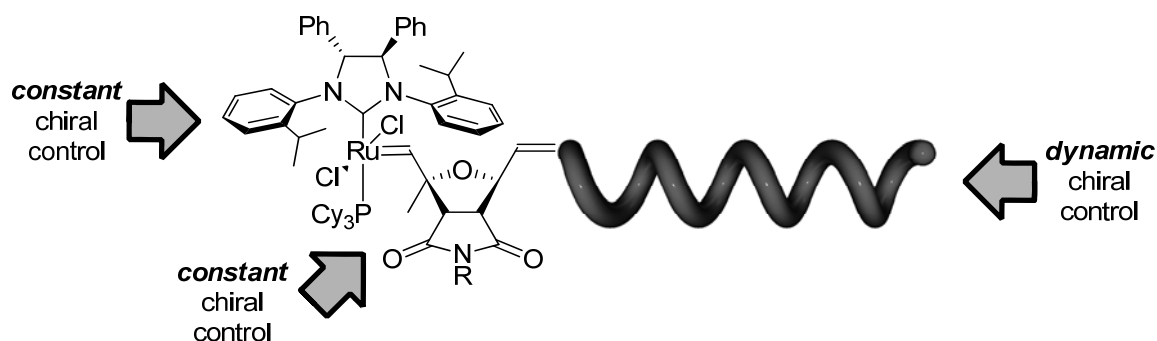
Figure 3.3. Chiral control elements for KR-ROMP.

**Supporting Information**

General Information

NMR spectra were recorded in $CDCl_3$ on Varian Mercury 300 MHz or INOVA 500 MHz spectrometers in the High-Resolution Nuclear Magnetic Resonance Facility at the California Institute of Technology (Caltech) operating VnmrJ software, unless otherwise noted. ^1H and ^{13}C chemical shifts are referenced relative to the residual solvent peak ($CDCl_3$ $\delta=7.27$ for ^1H and $\delta=77.23$ for ^{13}C). Spectral analysis was performed on MestReNova software. High-resolution mass spectra were provided by Caltech's Mass Spectrometry Facility. Gel permeation chromatography (GPC) was performed in tetrahydrofuran (THF) on two MZ-Gel 10 μm columns composed of styrene-divinylbenzene copolymer (Analysentechnik) and connected in series, with a miniDAWN TREOS multiangle laser light scattering (MALLS) detector, ViscoStar viscometer, and Optilab rEX differential refractometer (all three from Wyatt Technologies). No calibration standards were used, as light scattering is considered an accurate measurement of molecular weight. Each sample was weighed and the dn/dc was calculated assuming 100% mass elution from the column. GPC data analysis was performed with ASTRA software. Circular dichroism spectra were acquired with an AVIV circular dichroism spectrometer model 62A DS.

Enantiomeric excess (ee) was determined by supercritical fluid chromatography on a Chiralpak AD column from Chiral Technologies, Inc. (Daicel). The supercritical fluid is CO_2 at 100 bar. Specifics for both monomers are given below.

<u>Materials</u>

CH$_2$Cl$_2$ was purified by passage through a solvent purification system.[11] CDCl$_3$ was obtained from Cambridge Isotopes. Initiator **I*** was prepared as reported in reference 8a. All other solvents and chemicals were obtained from Sigma-Aldrich Corporation and used as received.

<u>Synthesis of monomer *rac, exo*-**1**</u>
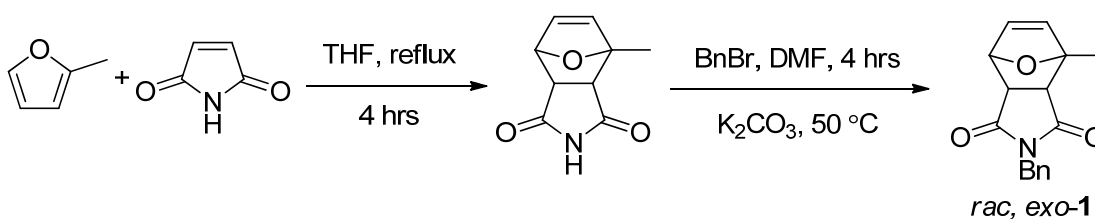
A 100 ml roundbottom flask equipped with a PTFE-coated stirbar was charged maleimide (1.9 g, 20 mmol, 1 equiv), 2-methylfuran (3.6 ml, 40 mmol, 2 equiv), and THF (20 ml). The flask was capped with a water-cooled reflux condenser, placed under an argon atmosphere, and refluxed for 4 hours. The reaction was then cooled to room temperature. The volatiles were removed by rotary evaporation to yield a beige solid (3.39 g, 94%). The spectral characteristics of the 1-methyloxanorbornene succinimide compound match those that have been reported.[12] The compound was carried on to the next step without further purification.

In the second step, a 100 ml roundbottom flask equipped with a PTFE-coated stirbar was charged with the 1-methyloxanorbornene (1.8 g, 10 mmol, 1 equiv), K$_2$CO$_3$ (2.9, 21 mmol, 2.1 equiv), and DMF (20 ml, not dry or degassed). To this suspension was added benzyl bromide (1.3 ml, 11 mmol, 1.1 equiv.) The roundbottom flask was topped with a Vigreux column and put under argon atmosphere. The suspension was

heated to 50 °C for 4 hours. The color of the solution becomes dark pink over the course

of the reaction. At the end of the reaction , the solution is cooled and diluted in distilled

water (100 ml). The aqueous solution was extracted with ether (3x 100ml). The

combined organic layers were washed with 50% saturated aqueous NaCl (2x 100 ml)

then dried over the MgSO$_4$. The drying agent was filtered away and the volatiles were

removed by rotary evaporation. The crude solid product was purified by silica gel

chromatography (hexanes/ethyl acetate v/v=3) to yield *rac, exo*-**1** (1.44 g, 6.3 mmol, 63%

yield). ^{1}H NMR (500 MHz, CDCl$_3$): δ 7.36–7.24 (5H, m), 6.51 (1H, dd, J = 6 Hz, 2 Hz),

6.33 (1H, d, J = 6 Hz), 5.22 (1H, d, J = 2 Hz), 4.66 (2H, s), 2.99 (1H, d, J = 6 Hz), 2.73

(1H, d, J = 6 Hz), 1.72 (3H, s). ^{13}C{^{1}H} NMR (125 MHz, CDCl$_3$): δ 175.87, 174.66,

140.61, 136.92, 135.54, 128.61, 128.03, 127.71, 127.69, 88.23, 80.67, 76.80, 50.68,
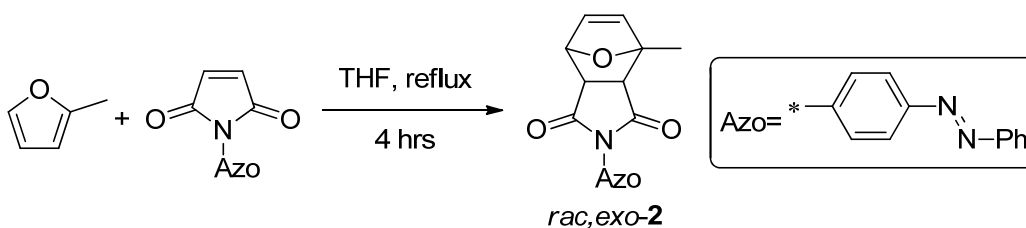
49.49, 42.38, 15.66.

Polymerization of **1**
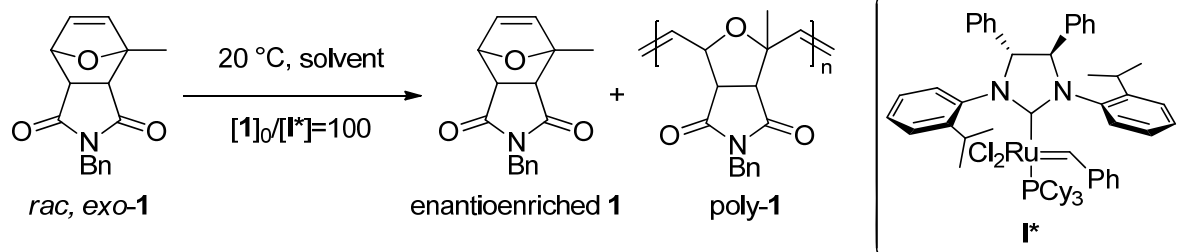
The polymerization of *rac, exo*-**1** was conducted in a nitrogen-filled glovebox. A

scintillation vial was charged with monomer **1** (269 mg, 1 mmol, 1 equiv), *p*-

methoxyanisole (27 mg, 0.2 mmol, 0.2 equiv) as an internal standard, and the appropriate

solvent (1 ml). In another vial, chiral initiator **I*** (10 mg, 0.01 mmol, [**1**]$_0$/[**I***]=100) was

dissolved in the same solvent (1 ml). The initiator solution was injected rapidly into the

monomer solution. Aliquots were taken at the designated time points and the polymerization was quenched with butyl vinyl ether (0.1 ml). The series of quenched aliquots was removed from the glovebox. Each quenched aliquot was precipitated into methanol (10 ml) in a scintillation vial. The polymer suspensions were carefully filtered through folded filter paper in a funnel into a second scintillation vial. The filtered methanol solution contained enantioenriched **1**, the internal standard, and ruthenium residue. The ratio of enantiomers and conversion were determined by analysis of this solution by SFC (10% isopropanol; depleted enantiomer=5.27 minutes and enriched enantiomer=5.66 minutes). The polymer was recovered by elution with dichloromethane from the filter paper into a third, pre-weighed scintillation vial. The volatiles were removed first by rotary evaporation then *in vacuo* overnight to yield a polymer film in most cases. The polymers were then redissolved in HPLC-grade THF and their molecular weight data was determined by GPC.

The response factor for the *p*-methoxyanisole internal standard compared to *rac,exo*-**1** at 210 nm in the ratio of the slopes of their concentration curves was 712500/356600=2.

Response Factor at 210 nm

	Monomer
	$y = 712500x + 449.7$
	$R^2 = 0.9999$
	Standard
	$y = 356600x + 236.6$
	$R^2 = 0.9995$

◆ Standard
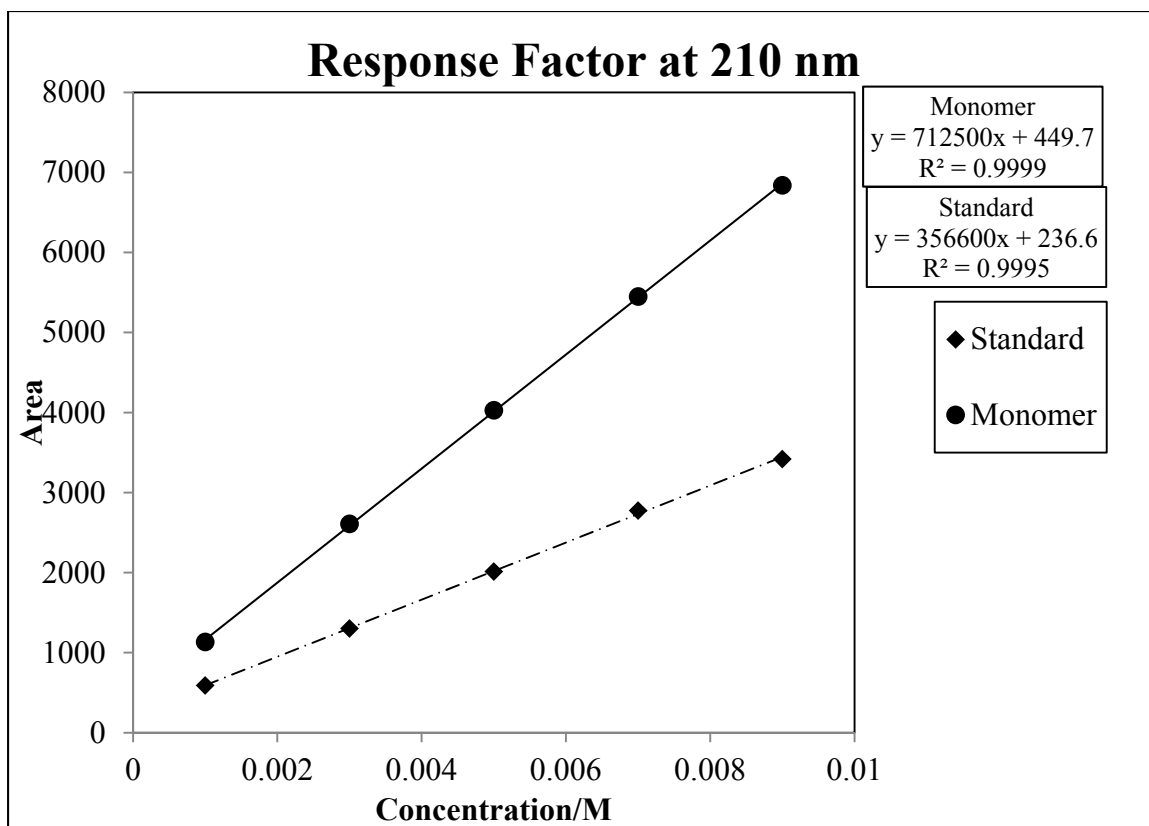
● Monomer

Synthesis of monomer *rac, exo*-**2**

A 2-dram vial equipped with a PTFE-coated stirbar was charged with 4-phenylazomaleinanil (277 mg, 1 mmol, 1 equiv), THF (1 ml), and 2-methylfuran (180 μl, 2 mmol, 2 equiv). The 4-phenylazomaleinanil was insoluble at room temperature, but dissolved upon heating. The reaction mixture was heated to 65 °C for 4 hours, then allowed to slowly cool to room temperature. The product precipitated from solution as an orange powder. The orange solid was filtered then dried overnight *in vacuo* to yield

*rac, exo-*2 (288 mg, 64% yield). ^{1}H NMR (500 MHz, CDCl$_3$): δ 8.02 (2H, m), 7.93 (2H, dd, J = 8 Hz, 2 Hz), 7.57–7.45 (5H, m), 6.58 (1H, dd, J = 6 Hz, 2 Hz), 6.39 (1H, d, J = 6 Hz), 5.34 (1H, d, J = 2 Hz), 3.17 (1H, d, J = 6 Hz), 2.90 (1H, d, J = 6 Hz), 1.82 (3H, s). ^{13}C{^{1}H} NMR (125 MHz, CDCl$_3$): δ 175.07, 173.81, 152.54, 151.96, 140.80, 137.12, 131.33, 129.12, 127.12, 123.45, 123.01, 88.73, 81.21, 76.76, 50.73, 49.59, 15.78.
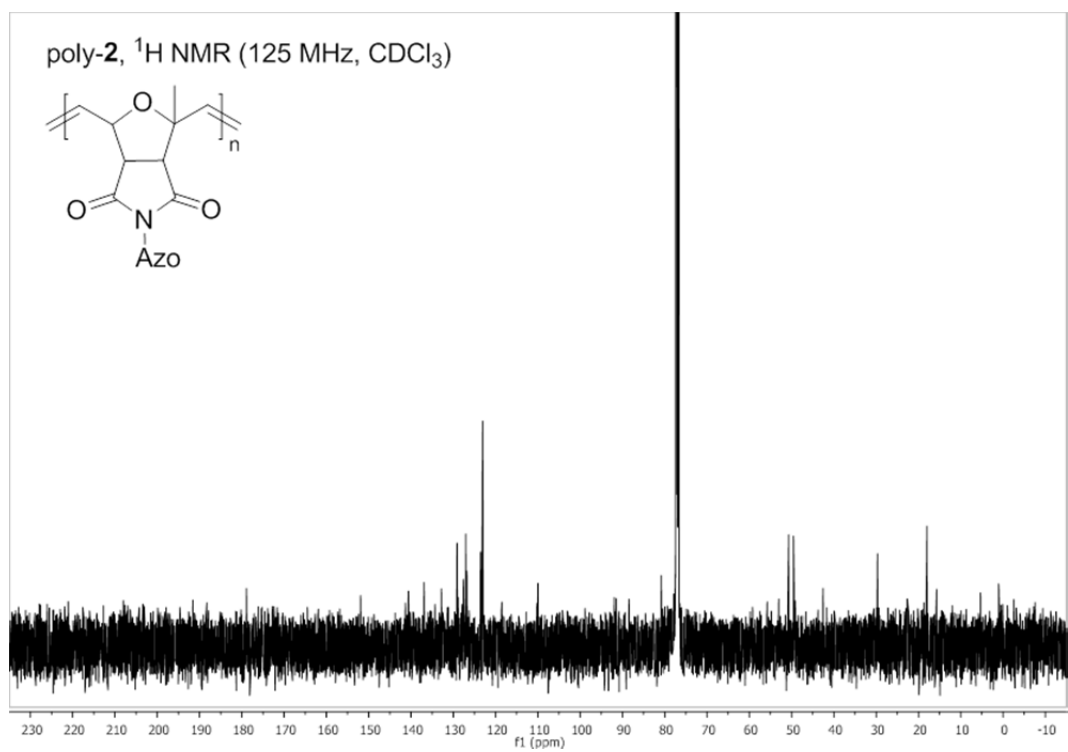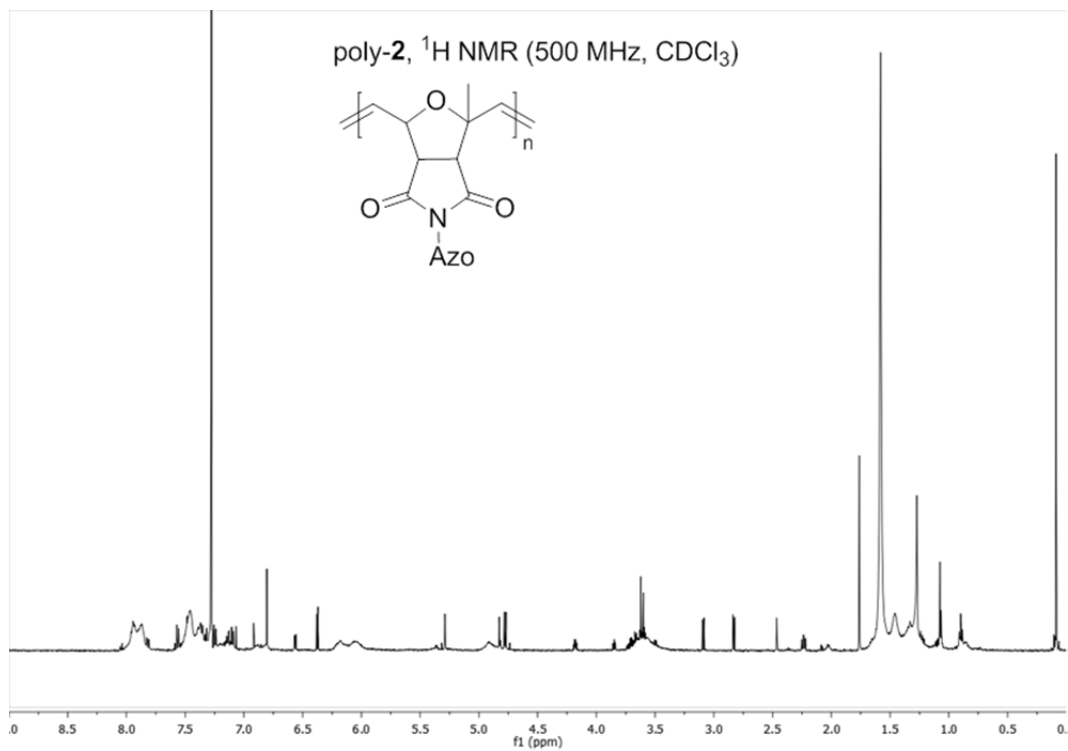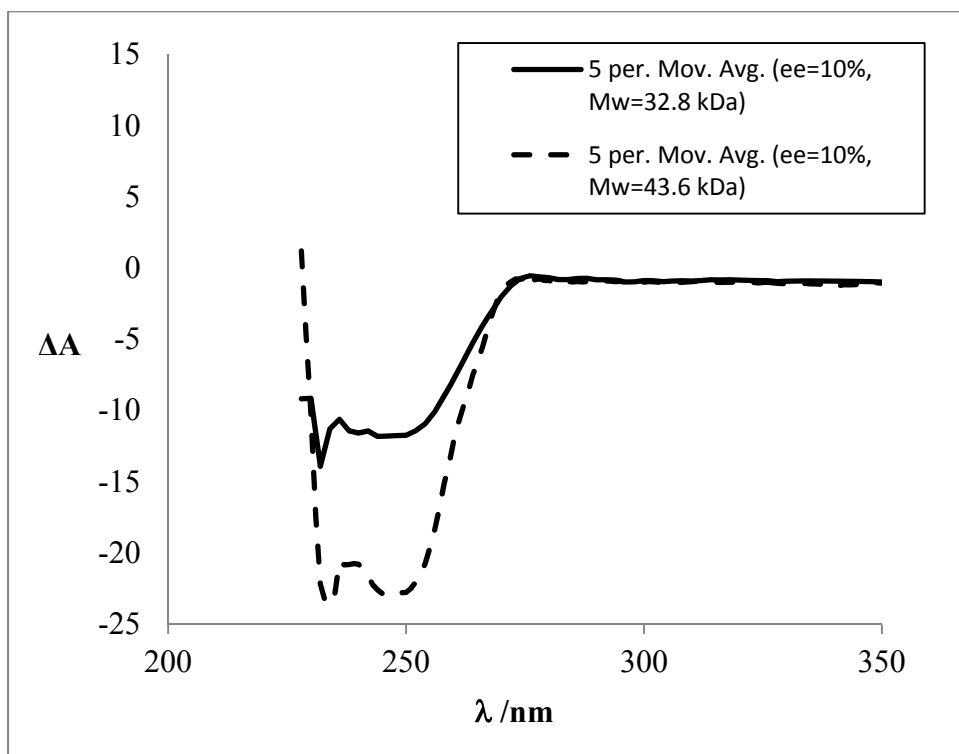
Polymerization of *rac, exo-*2
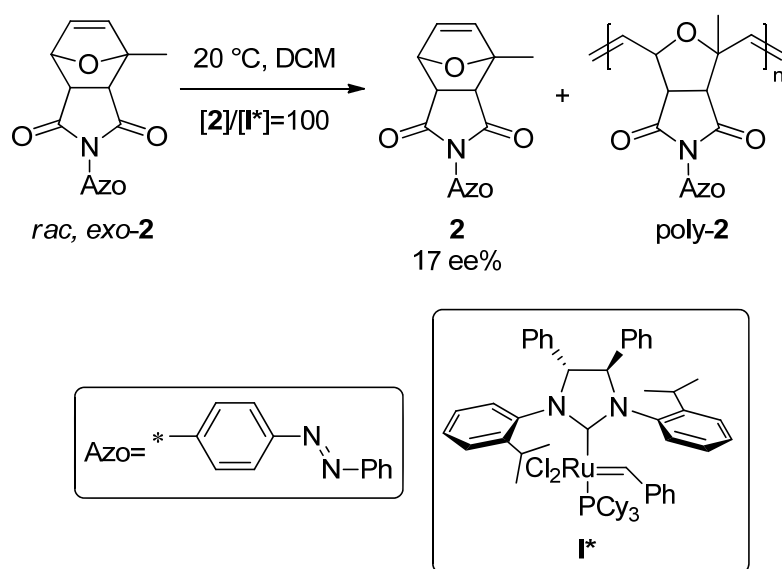
In a nitrogen-filled glovebox, a vial was charged with **2** (90 mg, 0.25 mmol) and dichloromethane (0.5 ml). In a separate vial, initiator **I*** (2.5 mg, 2.5 μmol, [**2**]$_0$/[**I***]=100) was dissolved in dichloromethane (0.5 ml). The initiator solution was added in one portion to the monomer solution. The reaction vial was sealed and removed from the glovebox. The polymerization was allowed to react for 40 minutes and was quenched with ethyl vinyl ether (100 μl) for 5 minutes. The reaction mixture was precipitated into methanol (10 ml) in a scintillation vial. The polymer suspensions were carefully filtered through folded filter paper in a funnel into a second scintillation vial.

The filtered methanol solution contained enantioenriched **2** and ruthenium residue. The ratio of enantiomers was determined by analysis of this solution by SFC (20% isopropanol; depleted enantiomer=8.83 minutes and enriched enantiomer=8.44 minutes). The polymer was recovered by elution with dichloromethane from the filter paper into a third, pre-weighed scintillation vial. The volatiles were removed first by rotary evaporation then *in vacuo* overnight to yield a polymer film (10 mg).

poly-**1**, ^{1}H NMR (500 MHz, CDCl$_3$)

poly-**1**, ^{1}H NMR (125 MHz, CDCl$_3$)

poly-**2**, ^{1}H NMR (500 MHz, CDCl$_3$)

poly-**2**, ^{1}H NMR (125 MHz, CDCl$_3$)
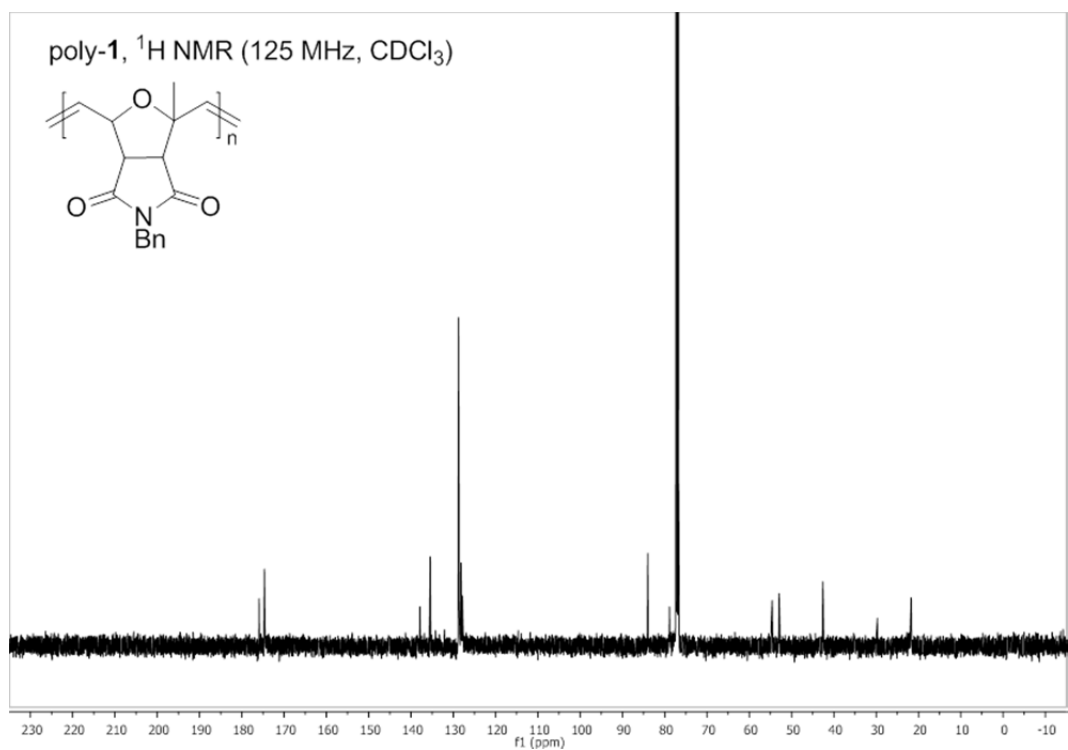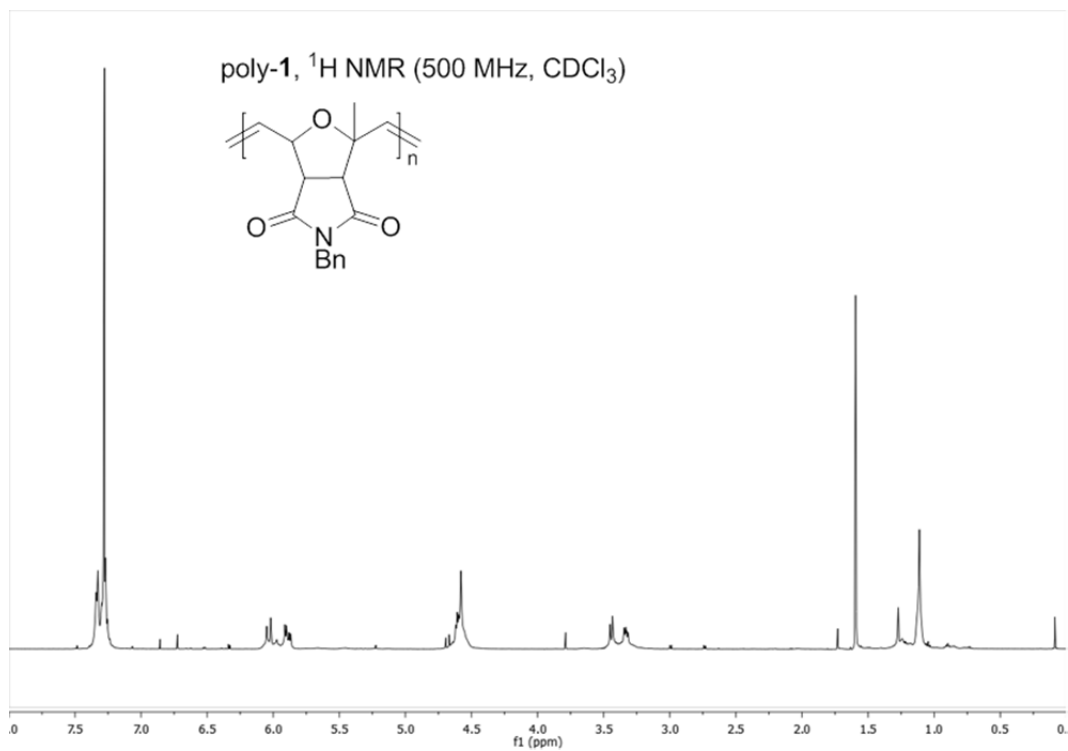
Circular dichroism spectra of poly-**1**

The enantiomeric excess is determined from the unreacted monomer. The isolated, unreacted monomer has no circular dichroic response.

UV-Vis spectra of **2** and poly-**2**

All spectra were obtained in methylene chloride.

Normalized Absorbance of **2** and poly-**2**

Extinction Coefficient of **2** and poly-**2**
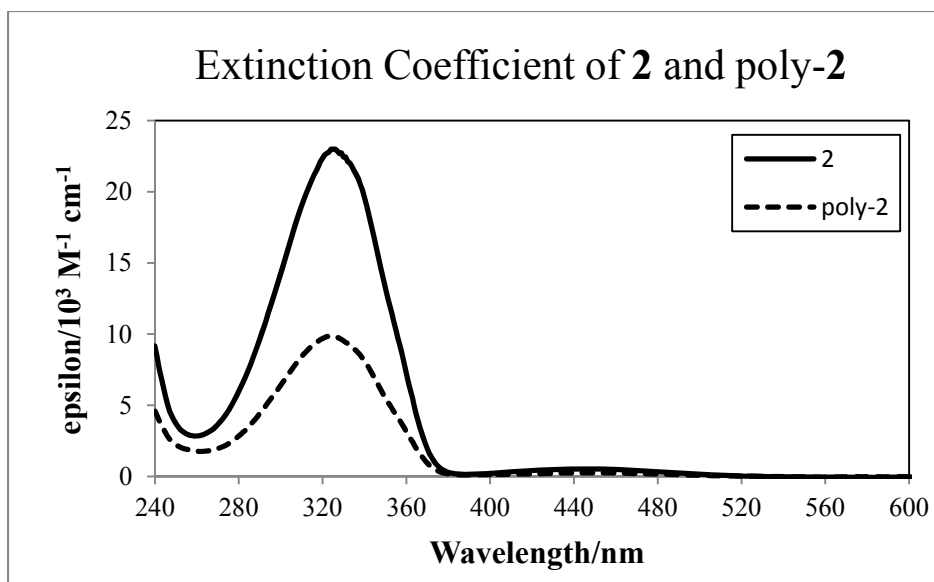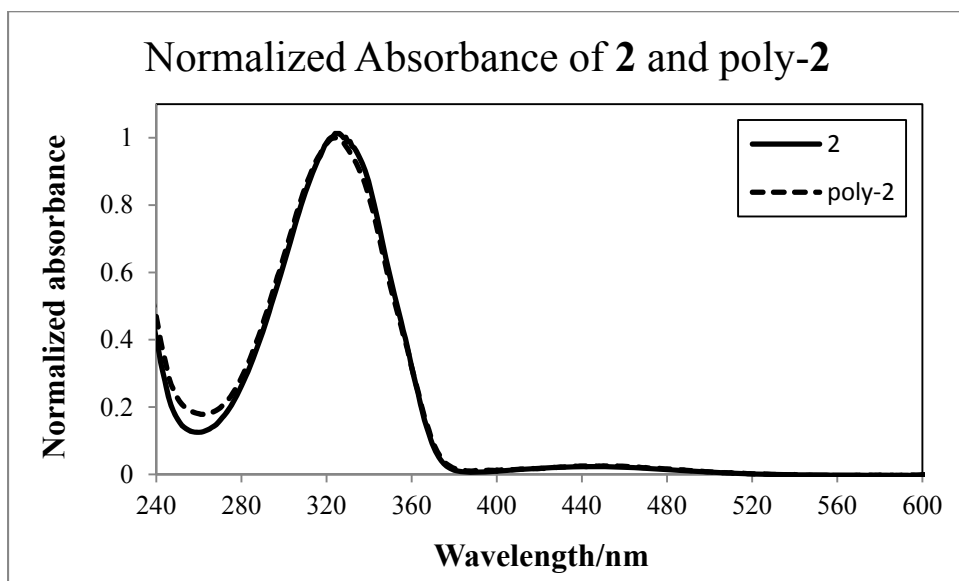
[1] (a) Hirahata, W.; Thomas, R. M.; Lobkovsky, E. B.; Coates, G. W. *J. Am. Chem. Soc.* **2008**, *130*, 17658–17659. (b) Thomas, R. M.; Widger, P. C. B.; Ahmed, S. M.; Jeske, R. C. ; Hirahata, W.; Lobkovsky, E. B.; Coates, G. W. *J. Am. Chem. Soc.* **2010**, *132*, 16520–16525.

[2] Miyake, G. M.; Chen, E. Y.-X. *Macromolecules*, **2011**, *44*, 4116–4124.

[3] Miyake, G.; Caporaso, L.; Cavallo, L.; Chen, E. Y.-X. *Macromolecules*, **2009**, *42*, 1462–1471.

[4] (a) Baar, C. R.; Levy, C. J.; Min, E. Y.-J.; Henling, L. M.; Day, M. W.; Bercaw, J. E. *J. Am. Chem. Soc.* **2004**, *126*, 8216–8231. (b) Byers, J. A.; Bercaw, J. E. *P. Natl. Acad. Sci. USA*, **2006**, *103*, 15303–15308. (c) Min, E. Y.-J.; Byers, J. A.; Bercaw, J. E. *Organometallics*, **2008**, *27*, 2179–2188.

[5] Fujimura, O.; Grubbs, R. H. *J. Am. Chem. Soc.* **1996**, *118*, 2499–2500.

[6] (a) Alexander, J. B.; La, D. S.; Cefalo, D. R.; Hoveyda, A. H.; Schrock, R. R. *J. Am. Chem. Soc.* **1998**, *120*, 4041–4042. (b) Dolman, S. J.; Sattely, E. S.; Hoveyda, A. H.; Schrock, R. R. *J. Am. Chem. Soc.* **2002**, *124*, 6991–6997

[7] (a) Ogasawara, M.; Watanabe, S.; Fan, L.; Nakajima, K.; Takahashi, T. *Organometallics*, **2006**, *25*, 5201–5203. (b) Ogasawara, M.; Watanabe, S.; Nakajima, K.; Takahashi, T. *J. Am. Chem. Soc.* **2010**, *132*, 2136–2137. (c) Ogasawara, M.; Wu, W.-Y.; Arae, S.; Watanabe, S.; Morita, T.; Takahashi, T.; Kamikawa, K. *Angew. Chem. Int. Ed.* **2012**, *51*, 2951–2955.

[8] (a) Seiders, T. J.; Ward, D. W.; Grubbs, R. H. *Org. Lett.*, **2001**, *3*, 3225–3228. (b) Funk, T. W.; Berlin, J. M.; Grubbs, R. H. *J. Am. Chem. Soc.* **2006**, *128*, 1840–1846. (c) Berlin, J. M.; Goldberg, S. D.; Grubbs, R. H. *Angew. Chem. Int. Ed.* **2006**, *45*, 7591–7595.

[9] (a) Zhang, J.; Lawrance, G. A.; Chau, N.; Robinson, P. J.; McCluskey, A. *New J. Chem.,* **2008**, *32*, 28–36. (b) Chen, Y. C.; Chang, S. C.; Wu, M. H.; Chuang, K. A.; Wu, J. Y.; Tsai, W. J.; Kuo, Y. C. *Life Sciences*, **2009**, *84*, 218–226. (c) Aghajan, M.; Jonai, N.; Flick, K.; Fu, F.; Luo, M.; Cai, X.; Ouni, I.; Pierce, N.; Tang, X.; Lomenick, B.; Damoiseaux, R.; Hao, R.; del Moral, P. M.; Verma, R.; Li, Y.; Li, C.; Houk, K. N.; Jung, M. E.; Zheng, N.; Huang, L.; Deshaies, R. J.; Kaiser, P.; Huang, J. *Nat. Biotechnol.*, **2010**, *28*, 738–744.

[10] (a) Yashima, E.; Maeda, K.; Iida, H.; Furusho, Y.; Nagai, K. *Chem. Rev.* **2009**, *109*, 6102–6211. (b) Miyake, G. M.; Iida, H.; Hu, H.-Y.; Tang, Z.; Chen, E. Y.-X.; Yashima, E. *J. Polym. Sci. Part A: Polym. Chem.* **2011**, *49*, 5192–5198.

[11] Pangborn, A. B.; Giardello, M. A.; Grubbs, R. H.; Rosen, R. K.; Timmers, F. J. *Organometallics* **1996**, *15*, 1518–1520.

[12] Lu, Z.; Weber, R.; Twieg, R. J. *Tetrahedron Lett.* **2006**, *47*, 7213–7217.

Chapter 4

Radical-Mediated Hydrophosphonation of Olefins

Abstract

The radical-mediated addition of triphenylphosphonium tetrafluoroborate to olefins (hydrophosphonation) is reported. Both standard radical initiators and photochemical conditions are effective, up to the gram scale. The phosphonium salts are shown to serve as *Z*-selective Wittig olefination reagents, even without purification.

Introduction

Phosphines are a diverse and valuable class of compounds employed in a range of applications from organometallic ligands to organocatalysts to olefination reagents. One common way to synthesize phosphines is the addition of the P-H bond to a carbon-carbon multiple bond, called hydrophosphination. Modern hydrophosphination methods include transition metal catalysis and radical-mediated additions to multiple bonds.[1,2] One application of phosphorus-based radical reactions is the synthesis of structurally complex Horner-Wadsworth-Emmons (HWE) phosphonate esters, which are precursors to *E*-olefins.[3] HWE reagents may also be subjected to conditions that preferentially provide *Z*-olefins, but this requires specialized phosphonate esters.[4] An alternative synthesis for *Z*-olefins uses alkyltriphenylphosphonium salts, known as Wittig reagents.[5] To our knowledge, there are no radical-based analogous methods to generate Wittig

phosphonium salts from olefins. Herein we describe a method to functionalize olefins by the radical-mediated addition of phosphonium salts.

Results and Discussion

In order to produce the desired phosphonium salts, the reaction conditions need to generate a triphenylphosphoniumyl radical cation ($PPh_3^{+\bullet}$) from a triphenylphosphonium salt, $[HPPh_3][X]$ (Figure 4.1). Triphenylphosphonium salts have been studied in the context of their acidity, not P-H bond homolysis, so we decided to investigate their reactivity under radical conditions.[6] We first attempted to hydrophosphonate a model substrate, 4-allylanisole, with a common radical initiator, azobisisobutyronitrile (AIBN), and a variety of $[HPPh_3][X]$. We found that a monoatomic anion, bromide, did not give the desired product **1[Br]**, but the noncoordinating anions BF_4^- and PF_6^- gave 50% and 13% conversion to **1[BF$_4$]** and **1[PF$_6$]**, respectively (Scheme 4.1). Encouraged by the initial results, we embarked on a screen of conditions, seeking to improve the efficiency of the hydrophosphonation reaction with $[HPPh_3][BF_4]$ and to gain a more complete understanding for the triphenylphosphoniumyl radical cation.
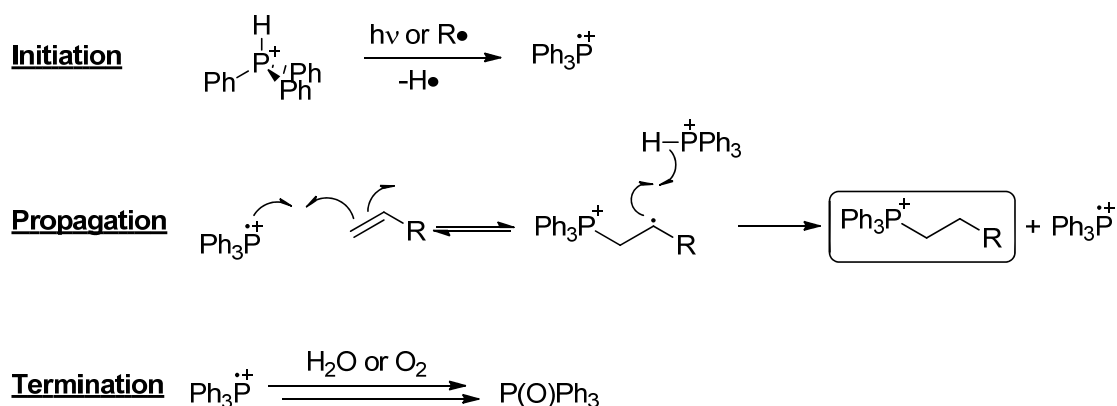
Figure 4.1. Proposed hydrophosphonation mechanism
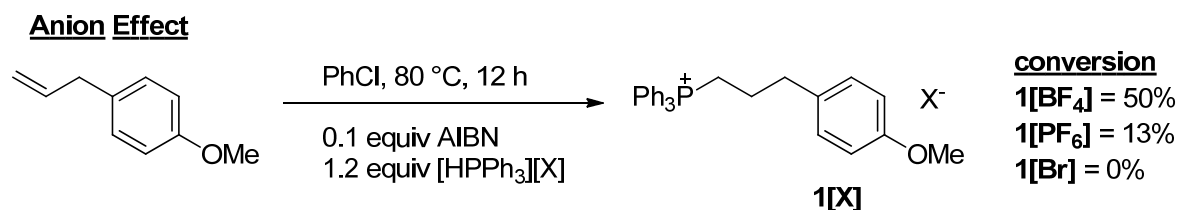
Scheme 4.1. Anion effect

We sought to optimize the hydrophosphonation conditions by examining the effects of initiator, temperature, and triphenylphosphine (PPh$_3$) additive (Table 4.1). The initiator 1,1'-azobis(cyclohexanecarbonitrile) (ACN), activated at 110 °C appears to be the most effective. Dibenzoyl peroxide (DBP) is the least effective, likely due to its oxidative ability. Triphenylphophine is an useful additive to the reaction mixture, increasing the yield slightly from 81% to 86% (entries 3 and 4). If the amount of PPh$_3$ is increased further, from 0.1 equiv to 0.5 equiv to 1 equiv, the conversion actually drops to 76% and 65%, respectively (entries 5 and 6). We believe that in small amounts, PPh$_3$ acts to prevent termination. Previous work has shown that PPh$_3$$^{+\bullet}$, generated by laser flash photolysis from PPh$_3$, will react with water and oxygen, with further PPh$_3$

participating to preserve the radical chain.[7] Under hydrophosphonation conditions, PPh_3 may play a similar role as the sacrificial link in the radical chain.

A Lewis acid-base pair of $PPh_3^{+\bullet}$-PPh_3 may be responsible for the deleterious effect of high PPh_3 concentration. When bound to PPh_3, $PPh_3^{+\bullet}$ would not be able to react with an olefin in the desired manner. This interaction would be favored at high concentration, leading to reduced conversions. Pulsed addition of both ACN and PPh_3 halfway through the reaction time provides the best conversions (entry 12).

Table 4.1. Hydrophosphonation optimization

Reaction scheme: allyl-anisole + PhCl, temp, 12 h; x equiv initiator; y equiv [HPPh$_3$][BF$_4$]; z equiv PPh$_3$ → Ph$_3$P$^+$–CH$_2$CH$_2$CH$_2$–(C$_6$H$_4$)–OMe BF$_4^-$ **1[BF$_4$]**

entry	initiator[a]	x[b]	y	z[b]	conv (%)[c]
1	ACN	0.01	2.4	0	78
2	ACN	0.02	2.4	0	72
3	ACN	0.02	2.4	0	81
4	ACN	0.02	2.4	0.1	86
5	ACN	0.02	2.4	0.5	76
6	ACN	0.02	2.4	1	65
7	ACN	0.1	1.2	0	50
8	ACN	0.2	1.5	0	57
9	ACN	0.2	1.5	0.1	67
10	ACN	2x(0.1)	1.5	0.1	72
11	ACN	2x(0.1)	2	0	81
12	ACN	2x(0.1)	2.4	2x(0.1)	94
13	AIBN	0.02	2.4	0	34
14	AIBN	0.2	1.2	0	36
15	AIBN	0.5	2	0	52
16	DBP	0.2	2.4	0	35
17	DBP	2x(0.1)	2.4	0	17

(a) ACN and DBP were activated at 110 °C. AIBN was activated at 80 °C. (b) 2x(0.1) indicates that 0.1 equiv of initiator was added at the beginning and halfway through the reaction. (c) Conversion measured by ^{1}H NMR and based on recovered starting material

Although standard radical conditions give **1[BF$_4$]** in high conversion (94%), we surmised that a complementary photochemical method could be developed.[8] The aforementioned photolysis gave us a clue that this might be possible. To test this hypothesis, 1-hexene was subjected to photochemical conditions, with the reaction monitored by NMR (Scheme 4.2). Phosphonium salt **2[BF$_4$]** was produced quantitatively in approximately two hours.[9] The effect of PPh$_3$ was also investigated. While there appears to be a general trend, as increasing amounts of PPh$_3$ gave higher conversions

(Figure 4.2), the mechanistic underpinnings for the this phenomenom are unknown. The photochemical hydrophosphonation method is scalable: one gram batches of **1[BF$_4$]** are easily prepared with 77% isolated yield by simple trituration of the crude reaction mixture with EtOAc.[10]

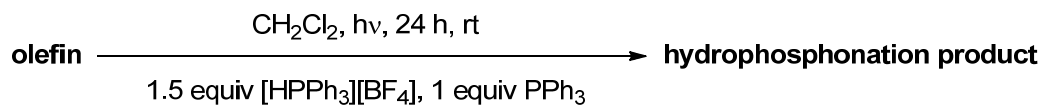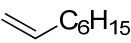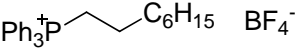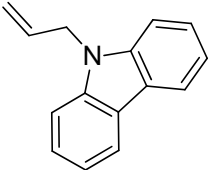**Scheme 4.2**. Photochemical hydrophosphonation of 1-hexene

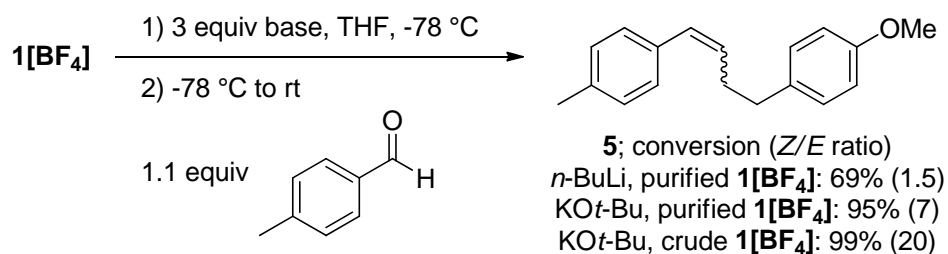| equiv PPh$_3$	conv (%)
0.00	0
0.10	31
0.25	65
0.50	61
1.00	72

Figure 4.2. Effect of PPh$_3$ in photochemical hydrophosphonation

With two hydrophosphonation methods in hand, the reaction was expanded to incorporate an array of functional groups and olefin substitution patterns (Table 4.2). Hydrophosphonation conditions were shown to tolerate ethers and a nitrogenous heterocycle. The PPh$_3^{+\bullet}$ species will add to monosubstituted olefins with preference over 1,2-disubstituted olefins.   Radical 5-*exo*- trig ring closures are also possible, simultaneously adding complexity and functionality to these substrates.

Importantly, the phosphonium salts should be viable Wittig reagents. To examine its efficacy, **1[BF$_4$]** was treated with *n*-BuLi or KO*t*-Bu at -78 °C. The phosphorus ylide intermediate was reacted with *p*-tolualdehyde and allowed to warm to room temperature. As expected, dissociating KO*t*-Bu conditions possess a better *Z:E* selectivity than *n*-BuLi for the production of 1,2-disubstituted styrene product **3** (*Z/E*=1.5 versus 7, Scheme 4.3). Furthermore, crude **1[BF$_4$]** can be used in the Wittig reaction with comparable yield and selectivity of **5** when compared to the reaction with purified **1[BF$_4$]**.[11] This obviates the need for a purification step.

Table 4.2. Substrate scope

$$\text{olefin} \xrightarrow[\text{1.5 equiv [HPPh}_3\text{][BF}_4\text{], 1 equiv PPh}_3]{\text{CH}_2\text{Cl}_2,\ h\nu,\ 24\ h,\ rt} \text{hydrophosphonation product}$$

Entry	Olefin	Product	Yield (%)
1	C₆H₁₅ **3a**	Ph₃⁺P C₆H₁₅ BF₄⁻ **4a**	95
2	**3b**	**4b**	93
3	**3c**	**4c**	41
4	**3d**	**4d**	93
5	**3e**	**4e**	52

Scheme 4.3. Wittig reaction with hydrophosphonation-derived phosphonium salts

Conclusions

We have developed a reliable method for the radical-mediated P-H bond addition of [HPPh$_3$][BF$_4$] to unactivated olefins. This reaction, called hydrophosphonation, may be performed using either standard radical initiators or photochemical conditions and was applied to a range of olefins. The alkyltriphenylphosphonium tetrafluoroborate products are shown to be *Z*-selective Wittig reagents. Future work in this area will pursue mechanistic studies and generalization to other classes of olefins.

Supporting Information
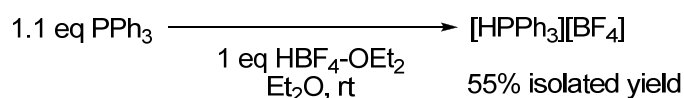
General Information

NMR spectra were recorded in CDCl$_3$ on Varian Mercury 300 MHz or INOVA 500 MHz spectrometers in the High-Resolution Nuclear Magnetic Resonance Facility at the California Institute of Technology (Caltech), unless otherwise noted. ^{1}H and ^{13}C chemical shifts are referenced relative to CDCl$_3$ (δ=7.27 for ^{1}H and δ=77.23 for ^{13}C). ^{19}F and ^{31}P chemical shift are referenced automatically by the VnmrJ software program. Spectral analysis was performed on MestReNova software. High-resolution mass spectra were provided by Caltech's Mass Spectrometry Facility.

Photoreactions were performed using a 450 W medium-pressure mercury arc lamp (Ace Glass) equipped with a water-cooled quartz jacket. The reaction vessels were Pyrex tubes sealed with PTFE closures. Pyrex glass has 90% transmittance at 350 nm.
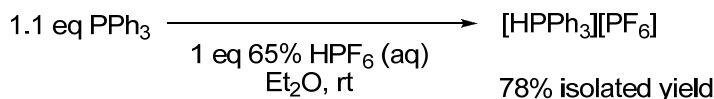
Materials

CH_2Cl_2 and THF were purified by passage through solvent purification columns by the method of Grubbs et al.[12] PhCl was purified by distillation from P_2O_5 under nitrogen atmosphere. Triphenylphosphine (PPh_3) was purified recrystallization from EtOH. 1-hexene was vacuum-transferred from CaH_2 before use. 1,1'-azobisisobutyronitrile (AIBN) was purified by recrystallization from Et_2O. 1,1′-azobis(cyclohexanenitrile) (ACN) was purified by recrystallization from MeOH. All other commercially available materials were obtained from Aldrich Chemical Company and used as received unless otherwise noted.
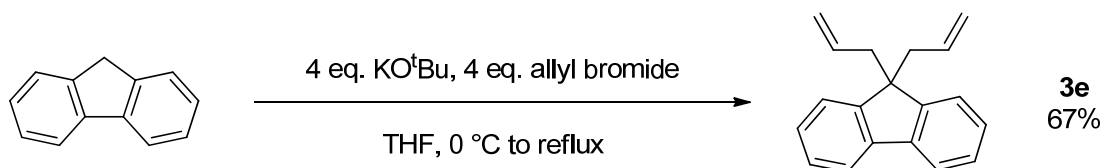
Triphenylphosphonium tetrafluoroborate, [HPPh$_3$][BF$_4$]

$$\text{1.1 eq } PPh_3 \xrightarrow[\substack{Et_2O, \text{ rt}}]{\text{1 eq } HBF_4\text{-}OEt_2}} [HPPh_3][BF_4]$$

[HPPh$_3$][BF$_4$]

55% isolated yield

To a 300 ml Erlenmeyer flask equipped with a stirbar was added PPh_3 (29.5 g, 112 mmol, 1.1 eq). The PPh_3 was dissolved in Et_2O (150 ml). Upon addition of HBF_4 in Et_2O (54 wt%, 14 ml, 100 mmol, 1 eq), a white solid precipitated. The white solid was collected by filtration and washed with Et_2O. Recrystallization of the solid from $CHCl_3$ (60 ml) gives [HPPh$_3$][BF$_4$] as colorless prisms in 55% yield (21.4 g, 55 mmol). A discussion of synthesis, characterization and acidity of [HPR$_3$][BF$_4$] salts is presented in Li et al. [13, 14]

Triphenylphosphonium hexafluorophosphate, [HPPh$_3$][BF$_4$]

1.1 eq PPh$_3$ $\xrightarrow{\text{1 eq 65\% HPF}_6\text{ (aq)}}$ [HPPh$_3$][PF$_6$]

Et$_2$O, rt   78% isolated yield

A 50 ml roundbottom flask was equipped with a stirbar and dried under vacuum. Under Ar flow, the flask was charged with PPh$_3$ (2 g, 7.6 mmol, 1.1 eq.), which was dissolved in Et$_2$O (10 ml). A 65% aqueous solution of HPF$_6$ (0.9 ml, 6.6 mmol, 1 eq) was added to the ethereal solution and a white solid precipitated. The white solid, [HPPh$_3$][PF$_6$], was collected by filtration in 78% yield (2 g, 5.1 mmol) and used without further purification.

9,9-diallylfluorene (**3b**)

4 eq. KO^{t}Bu, 4 eq. allyl bromide

THF, 0 °C to reflux

3e
67%

A flame-dried 250 ml Schlenk flask with a stirbar was charged with KO^{t}Bu (1.2 g, 20 mmol, 2 eq.), then evacuated and backfilled with Ar. The flask was cooled to 0 °C in an ice water bath. THF (100 ml) was transferred to the cooled flask *via* cannula. Fluorene (1.7 g, 10 mmol, 1 eq.) was added in one portion. The solution was stirred at 0 °C for 20 minutes, during which time the solution changed from colorless to orange. Allyl bromide (850 μl, 20 mmol, 2 eq) was added dropwise and the solution turned from orange to bright green. The solution was allowed to warm overnight to room temperature. Additional KO^{t}Bu (2 eq.) and allyl bromide (2 eq.) were added to the reaction and it was refluxed for 4 hours. When the reaction was complete, it was cooled to room temperature and quenched with MeOH, then water. The remaining water was removed by MgSO$_4$,

and all solids were filtered off. Excess solvent was removed by rotary evaporation to yield viscous oil. The oil was further purified by silica gel chromatography (hexanes, R_f=0.22) to yield 9,9-diallylfluorene (1.7 g, 6.7 mmol, 67%). ^{1}H NMR (500 MHz, CDCl$_3$): δ 7.73 (2H, d, J = 8 Hz), 7.44 (2H, d, J = 7 Hz), 7.36–7.31 (4H, m), 5.33–5.24 (2H, m), 4.86 (2H, dd, J = 17 Hz, 1 Hz), 4.77 (2H, d, J = 10 Hz), 2.74 (4H, d, J = 7 Hz). ^{13}C NMR (126 MHz, CDCl$_3$) δ 149.29, 140.71, 133.73, 127.08, 126.91, 123.62, 119.76, 117.48, 54.16, 43.49. HRMS (EI+): calculated = 246.1408, found = 246.1408.

Allyl *trans*-2-hexenyl ether (**3d**)

A 2-neck 250 ml roundbottom flask was fitted with a PTFE valve inlet and a septum. The flask was flame-dried. THF (100 ml) was transferred to the flask *via* cannula. The flask was then cooled to 0 °C in an ice bath and NaH (60% in mineral oil, 1.1 g, 27.5 mmol, 1.1 eq) was added. Dropwise, *trans*-2-hexen-1-ol (2.9 ml, 25 mmol, 1 eq) was added to the suspension. The reaction was allowed to stir for 90 minutes at 0 °C. Allyl bromide (2.3 ml, 27.5 mmol, 1.1 eq) was added dropwise to the cooled reaction. The mixture was allowed to warm overnight to room temperature. The reaction was quenched with water (50 ml). The aqueous layer was extracted with hexanes (2x25 ml), then the combined organic layers were washed with brine (50 ml). The organic layer was dried over MgSO$_4$, filtered, and the solvent was removed by rotary evaporation. The crude oil was purified by silica gel chromatography (9:1 hexanes:ethyl acetate) to yield

allyl *trans*-2-hexenyl ether (2.3 g, 16 mmol, 67%). ^{1}H NMR (500 MHz, CDCl$_3$) δ 5.94

(1H, m), 5.70 (1H, m), 5.59 (1H, m), 5.29 (1H, d, *J* = 17.2), 5.19 (1H, d, *J* = 9.9), 3.98

(2H, dd, *J* = 5.7, 1.2), 3.95 (2H, d, *J* = 6.2) 2.04 (2H, dd, *J* = 14.5, 6.9), 1.43 (dq, *J* = 14.8,

7.4, 2H), 0.92 (t, *J* = 7.4, 2H). ^{13}C NMR (126 MHz, CDCl$_3$) δ 134.81, 126.23, 116.98,

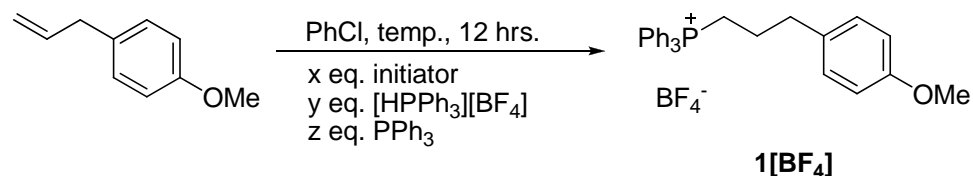70.92, 34.38, 29.69, 22.22, 21.14, 13.69. HRMS (EI+): calculated = 140.1201, found =

140.1215.

Allyl carbazole (**3b**)

Carbazole (3.3 g, 20 mmol, 1 equiv.), KOH (1.6g, 30 mmol, 1.5 equiv.), and NaI (160

mg, 1 mmol, 0.1 eq) were dissolved in DMSO (20 ml) in a 100 ml roundbottom flask.

Once all solids were dissolved, allyl bromide (1.8 ml, 22 mmol, 1.1 equiv.) was added *via*

syringe. The flask was capped and stirred at room temperature overnight. Water (25 ml)

was added to the reaction and large amount of yellow solid crashed out. The solid was

filtered and recrystallized from hexanes to give yellowish-brown crystals (2.2 g, 10.4

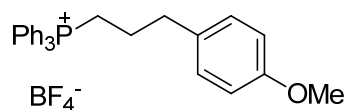mmol, 52% isolated yield). Characterization matches the previously published data.[15]

General setup for conditions screen with standard radical initiators
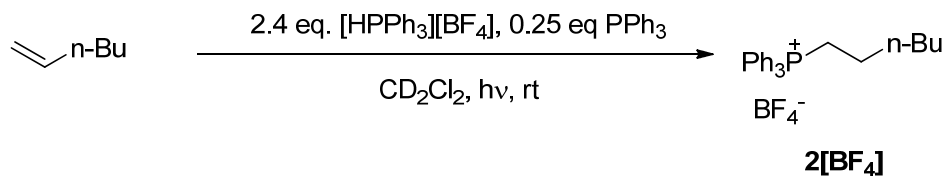

1[BF₄]

A Schlenk tube with a stirbar and PTFE closure was flame-dried under vacuum. The

tube was backfilled under Ar atmosphere. The appropriate amounts of initiator,

[HPPh₃][X], and PPh₃ were added to the tube. The tube was then charged with the

correct solvent (5 ml) and 4-allylanisole (24 μl, 0.15 mmol). The tube was sealed and

heated to the appropriate temperature in an oil bath (AIBN: 80 °C; ACN: 110 °C; DBP:

110 °C). After 12 hours, the tube was removed from the oil bath and cooled. The solvent

was removed by rotary evaporation and the conversion was measured by ^{1}H NMR. If the

reaction required a pulsed addition of initiator and/or [HPPh₃][BF₄], the tube was

removed from the oil bath after 6 hours, the additional reagents were added under Ar

flow, and the tube was resealed and heated for the final 6 hours. The products were

analyzed by ^{1}H NMR.
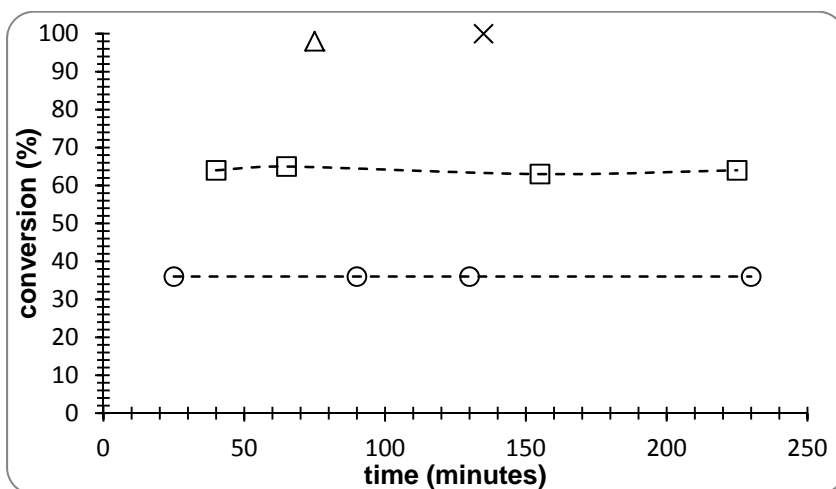
Characterization of **1[BF₄]**

^{1}H NMR (500 MHz, CDCl₃) δ 7.81–7.76 (3H, m), 7.72–7.56 (12H, m)), 7.10 (2H, d, $J =$

8.7), 6.82 (2H, d, J = 8.7), 3.79 (3H, s), 3.35–3.20 (2H, m), 2.86 (2H, t, J = 7.1), 1.89

(2H, d, J = 8.2). ^{13}C{^{1}H} NMR (126 MHz, CDCl₃) δ 158.21, 135.10 (d, J_{P-C} = 3.0),

133.38 (d, J_{P-C} = 9.9), 131.92, 129.90, 130.50 (d, J_{P-C} = 12.5), 118.05 (d, J_{P-C} = 86.1),

114.04, 55.28, 34.64 (d, J_{P-C} = 16.8), 24.71 (d, J = 4), 20.69 (d, J_{P-C} = 51.7).

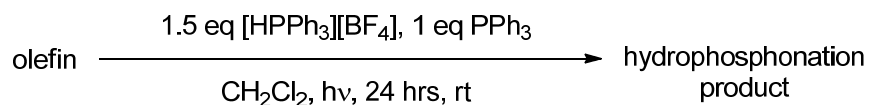NMR-scale kinetic analysis of photochemical hydrophosphonation

2.4 eq. [HPPh$_3$][BF$_4$], 0.25 eq PPh$_3$

CD$_2$Cl$_2$, hν, rt

Ph$_3$P$^+$ n-Bu

BF$_4^-$

2[BF$_4$]

In a nitrogen-filled glovebox, 1-hexene (38 µl, 0.3 mmol, 1 eq), [HPPh$_3$][BF$_4$] (268 mg, 0.75 mmol, 2.4 eq), PPh$_3$ (20 mg, 0.075 mmol, 0.25 eq), and 1,3,5-trimethoxybenzene (6.7 mg, 0.04 mmol, internal standard) were dissolved in CD$_2$Cl$_2$ (5 ml). The solution was divided into aliquots (5x1 ml) and placed in five screw-cap NMR tubes. The sealed tubes were removed from the glovebox. The NMR tubes were irradiated simultaneously in a photobox, and removed at the indicated intervals (O, 25 minutes; □, 40 minutes; Δ, 75 minutes; X, 135 minutes). Conversion was calculated from comparison to the 1,3,5-trimethoxybenzene internal standard. The spectral properties of **2[BF$_4$]** were similar to that of commercially available bromide analogue.

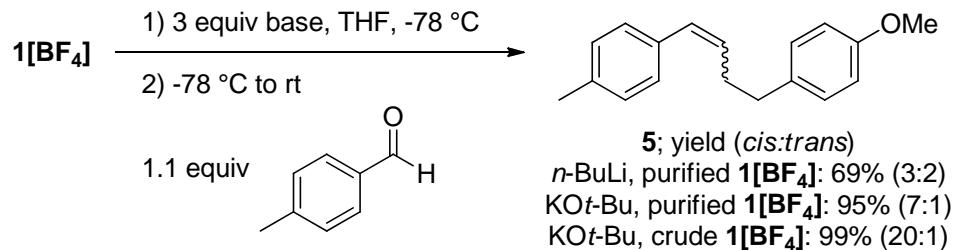General photochemical hydrophosphonation conditions

$$\text{olefin} \xrightarrow[\text{CH}_2\text{Cl}_2,\ h\nu,\ 24\ \text{hrs, rt}]{\text{1.5 eq [HPPh}_3][\text{BF}_4],\ 1\ \text{eq PPh}_3} \text{hydrophosphonation product}$$

A Pyrex Schlenk tube equipped with a stirbar and PTFE closure was flame-dried under vacuum. The tube was backfilled with Ar and charged with $[\text{HPPh}_3][\text{BF}_4]$ (525 mg, 1.5 mmol, 1.5 eq) and PPh_3 (262 mg, 1 mmol, 1 eq). The tube was evacuated and backfilled with Ar. The solids were dissolved in CH_2Cl_2 (10 ml). The substrate (1 mmol) was added in one portion. The Schlenk tube was sealed and placed in the photobox for 24 hours. The solvent was removed from the reaction mixture *via* rotary evaporation. The hydrophosphonation products were purified as outlined below.

Compound	Purification	Appearance
1[BF$_4$]	trituration with EtOac	powder
4a	*in vacuo*	amorphous
4b	trituration with EtOac	powder
4c	silica gel chromatography with acetone	amorphous
4d	silica gel chromatography with acetonitrile	amorphous
4e	trituration with EtOac then hexanes	powder

Wittig olefination with **1[BF₄]** for the synthesis of styrene 5

1) 3 equiv base, THF, -78 °C

1[BF₄]

2) -78 °C to rt

1.1 equiv

5; yield (*cis:trans*)
n-BuLi, purified **1[BF₄]**: 69% (3:2)
KO*t*-Bu, purified **1[BF₄]**: 95% (7:1)
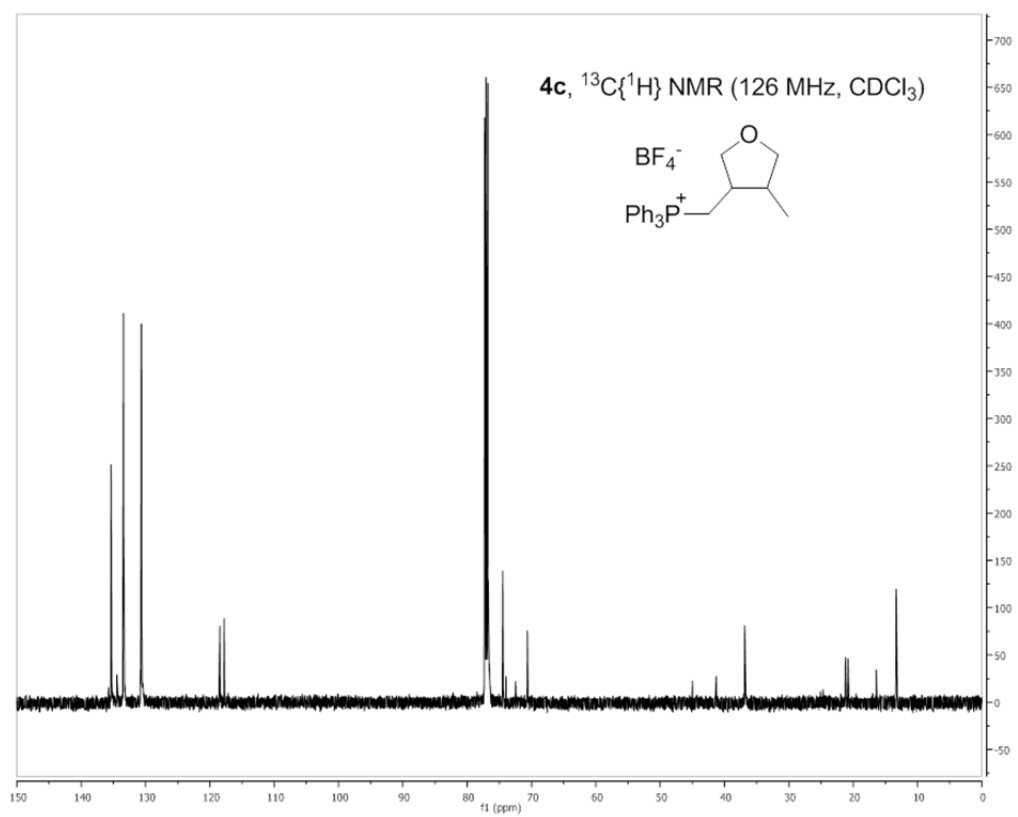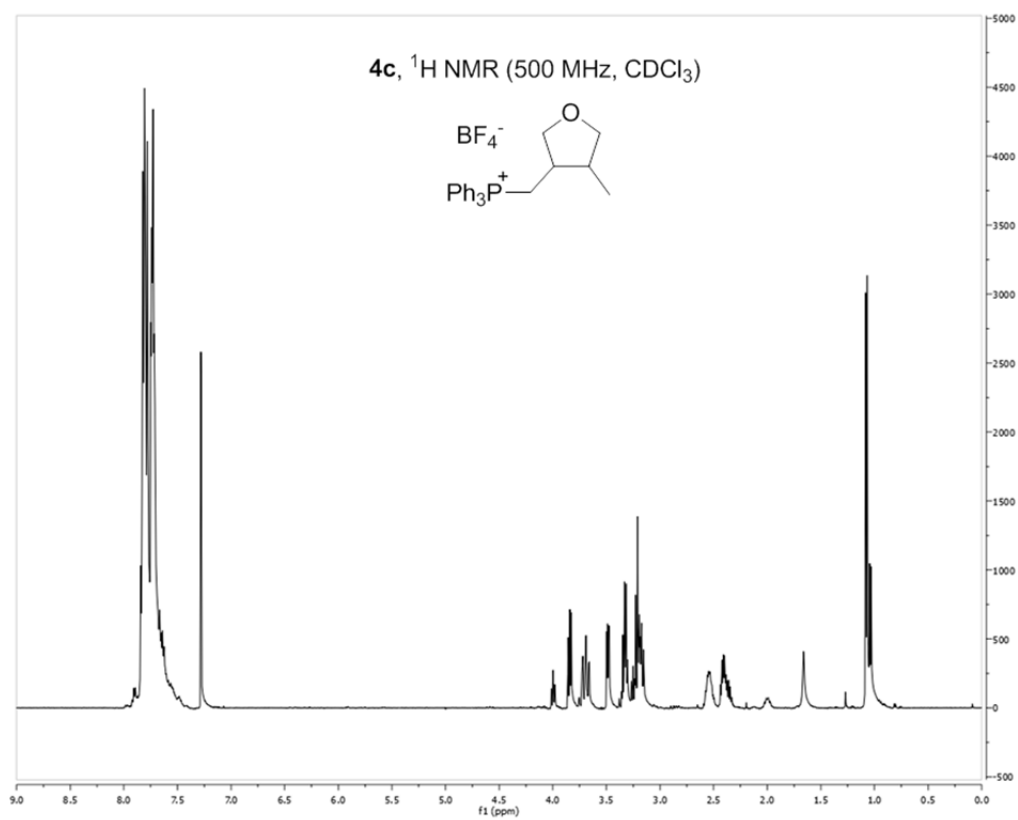KO*t*-Bu, crude **1[BF₄]**: 99% (20:1)

A 50 ml Schlenk flask equipped with a stirbar was flame-dried under vacuum. The flask was backfilled with Ar. Under Ar flow, the flask was charged with **1[BF₄]** (500 mg, 1 mmol, 1 eq.), then evacuated and backfilled. The flask was cooled to -78 °C in a CO_2(s)/acetone bath and charged with THF (12 ml). Potassium *t*-butoxide (340 mg, 3 mmol, 3 eq.) was added to the cooled suspension in one portion. The reaction mixture was allowed to stir for 30 minutes at -78 °C, becoming dark red. *Via* syringe, *p*-tolualdehyde (240 µl, 2 mmol, 2 eq.) was added to the solution. The reaction mixture was allowed to very slowly warm overnight. The reaction was quenched first with methanol (2 ml), then water (2 ml). The layers were separated. The aqueous layer was extracted with diethyl ether (2x20 ml). The combined organic layers were washed with brine (20 ml), dried over $MgSO_4$, and filtered. Excess solvent was removed by rotary evaporation. Characterization for Z-**5** ^{1}H NMR (500 MHz, CDCl₃) δ 7.17–7.12 (m, 6H), 6.85 (m, 2H), 6.42 (d, *J* = 11.7, 1H), 5.66 (dt, *J* = 11.6, 7.0, 1H), 3.81 (s, 3H), 2.73 (m, 2H), 2.64 (dd, *J* = 15.0, 7.9, 2H), 2.35 (2, 3H). ^{13}C NMR (126 MHz, CDCl₃) δ 157.82, 136.23, 134.71, 133.65, 131.21, 129.16, 128.69, 128.51, 128.45, 113.75, 55.26, 35.20, 30.71, 21.16. HRMS (EI+): calculated = 252.1514, found = 252.1515.
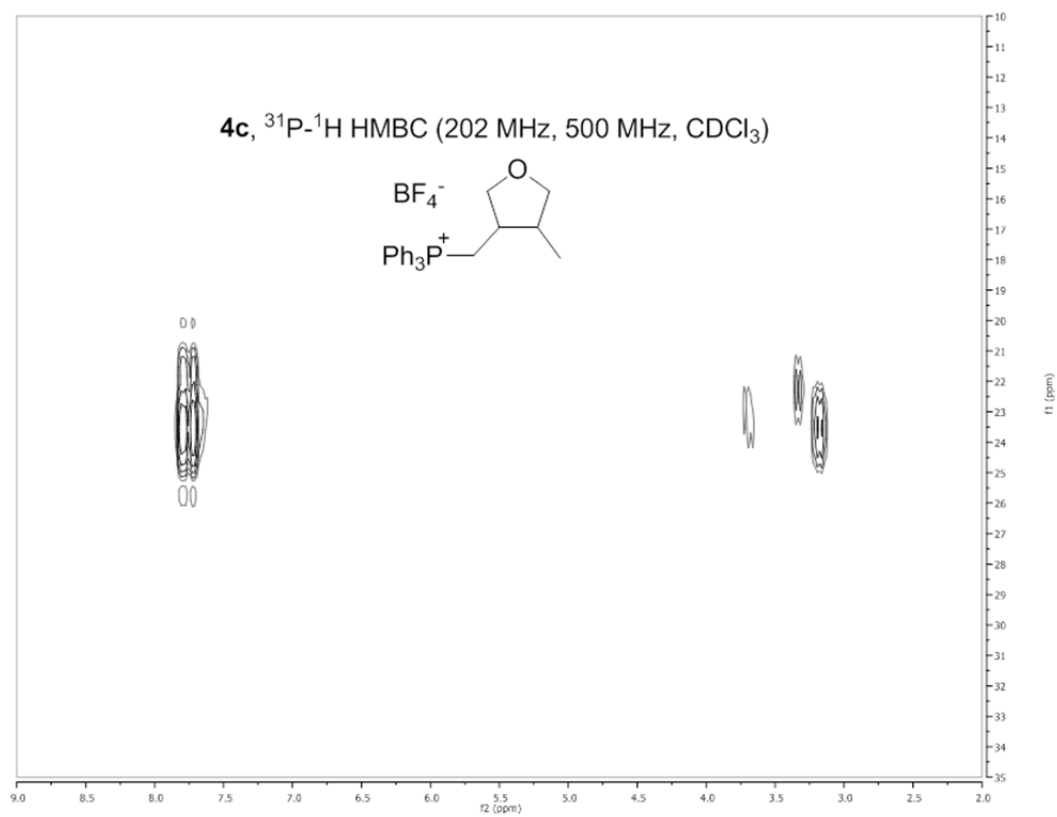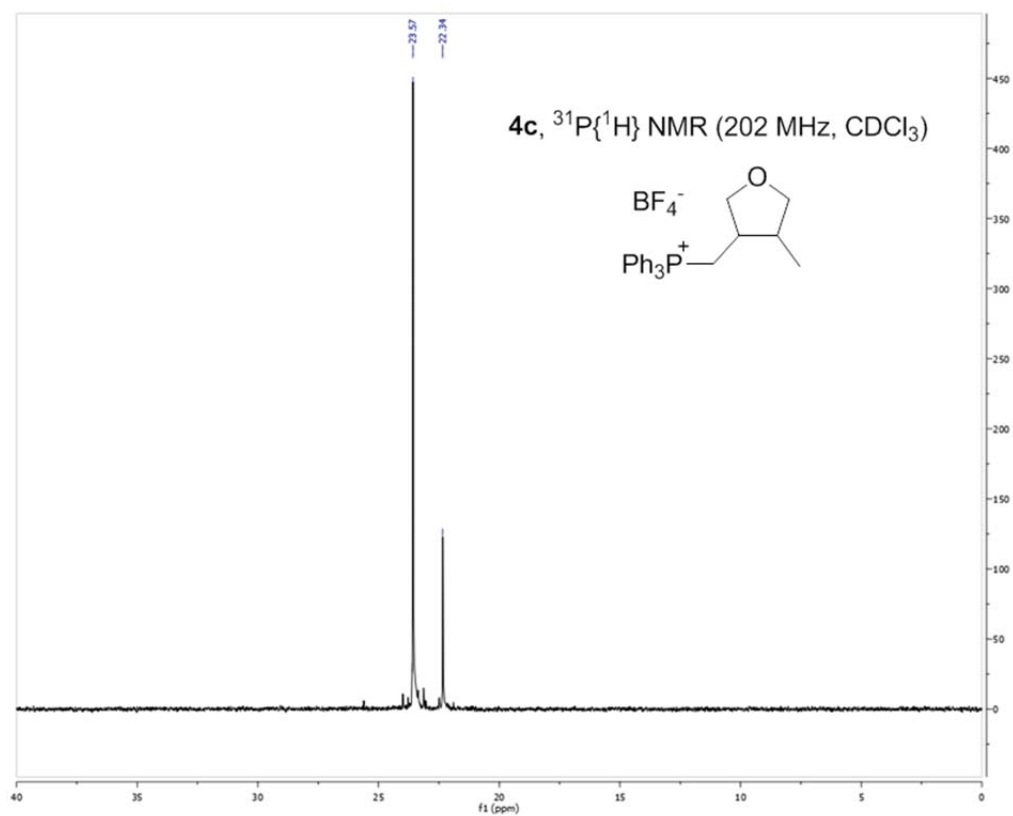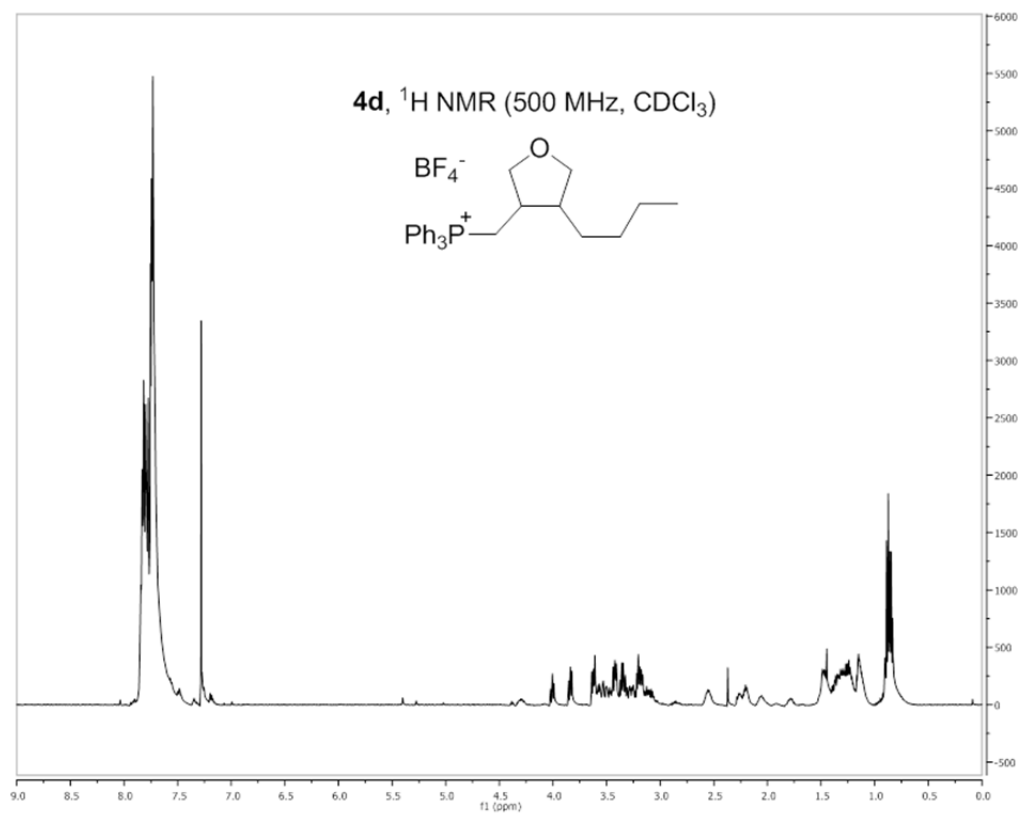
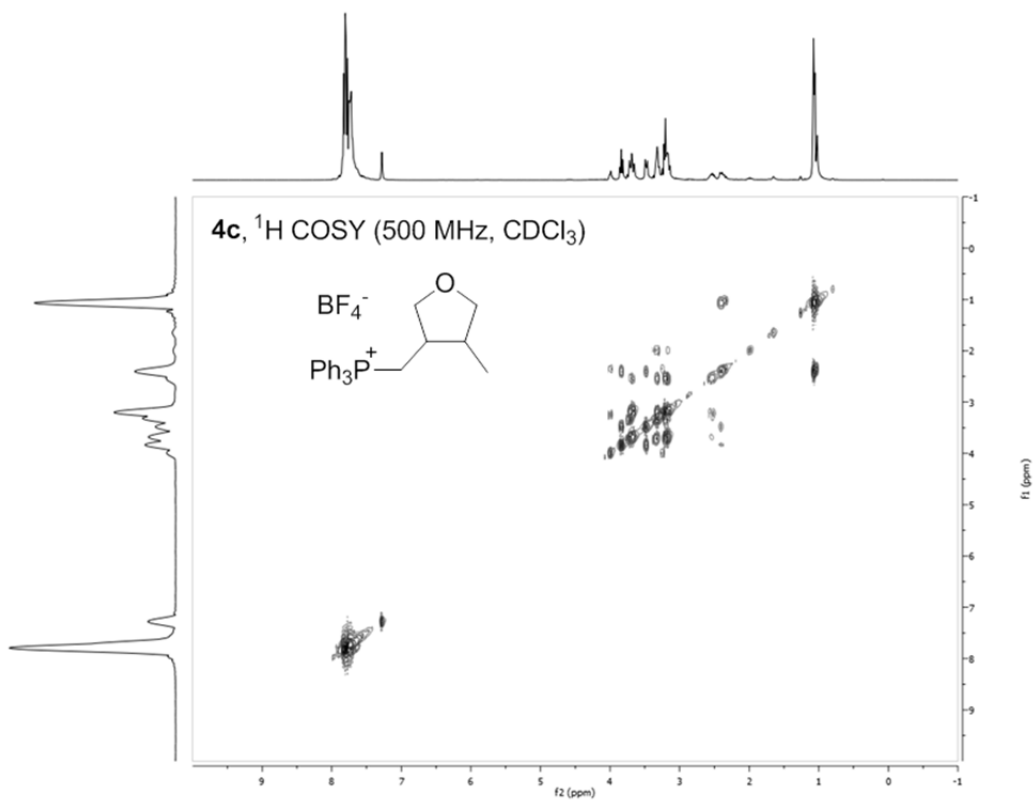Octyltriphenylphosphonium tetrafluoroborate (**4a**)

Ph_3^+P ~~~~ C_6H_{15} BF_4^-
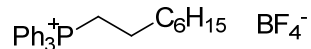
^{1}H NMR (500 MHz, CDCl$_3$) δ 7.80 (m, 3H), 7.72 (m, 12H), 3.24 (m, 2H), 1.58 (b, 4H), 1.20 (b, 8H), 0.84 (t, J = 7.0, 3H). ^{13}C{^{1}H} NMR (126 MHz, CDCl$_3$) δ 135.16 (d, J_{P-C} = 3.0), 133.39 (d, J_{P-C} = 9.9), 130.56 (d, J_{P-C} = 12.5), 118.13 (d, J_{P-C} = 86.0), 44.99, 31.63, 30.31 (d, J_{P-C} = 15.8), 28.96 (d, J_{P-C} = 1), 28.83, 22.54, 21.95 (d, J_{P-C} = 51.0), 14.04. HRMS (FAB+): calculated = 375.2242, found = 375.2250.
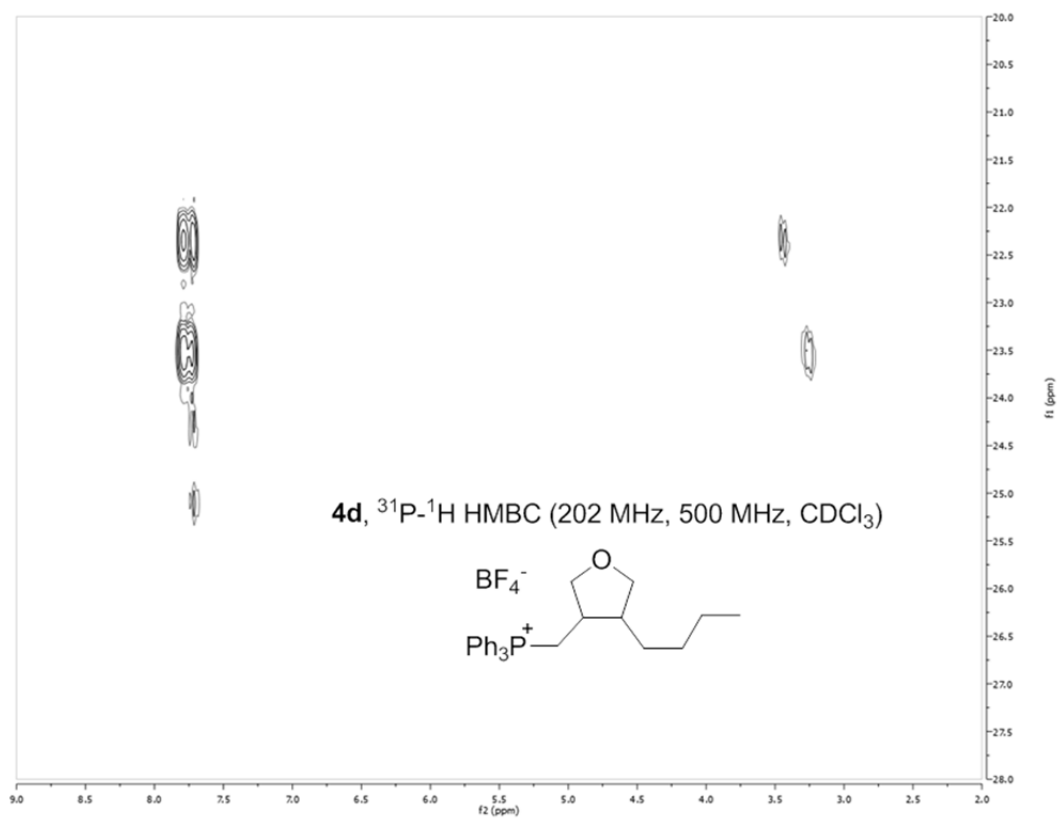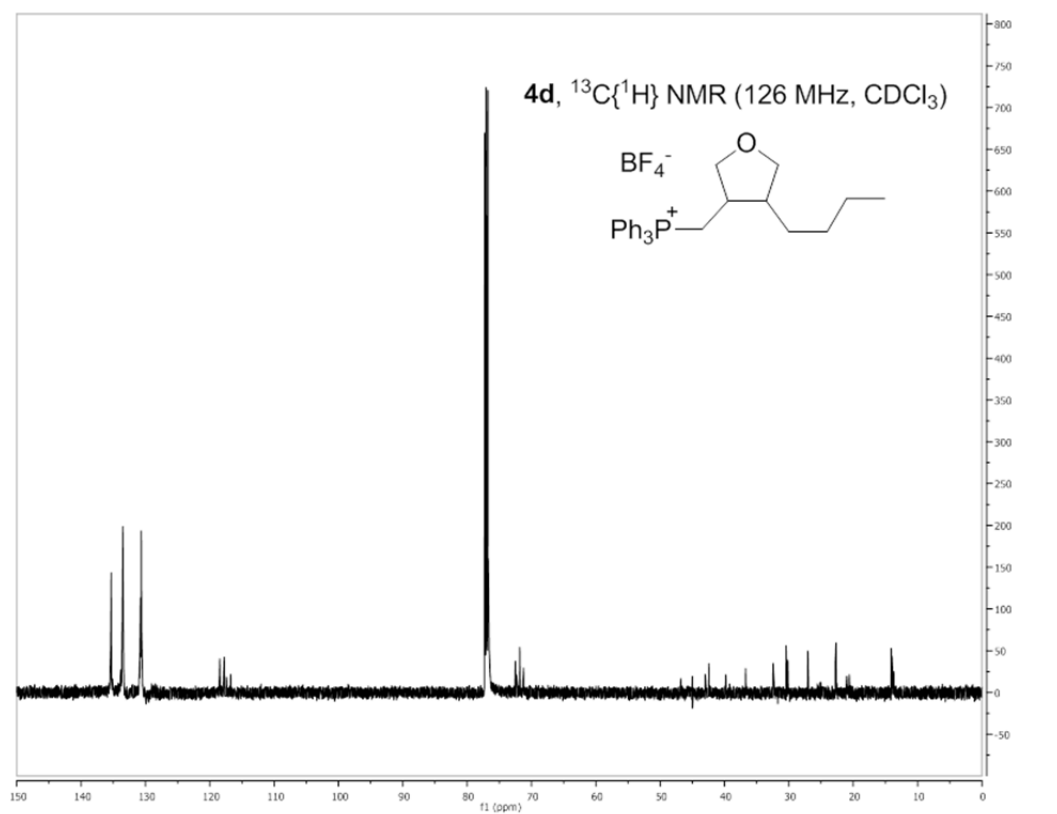
Hydrophosphonation product **4b**
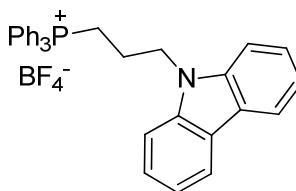
^{1}H NMR (500 MHz, CDCl$_3$) δ 8.08 (d, J = 7.7, 2H), 7.74 (m, 2H), 7.67 (m, 2H), 7.59 (m, 2H), 7.54–7.40 (m, 12H), 7.24 (t, J = 6.9, 3H), 4.66 (t, 2H, J = 6), 3.35 (m, 2H), 2.326 (m, 2H). ^{13}C{^{1}H} NMR (126 MHz, CDCl$_3$) δ 140.28, 134.97, 133.21 (d, J_{P-C} = 9.9), 130.36 (d, J_{P-C} = 12.6), 129.24 (d, J_{P-C} = 13.5), 126.25, 122.79, 120.19, 119.23, 117.65 (d, J_{P-C} = 86.4), 109.14, 42.03 (d, J_{P-C} = 19.1). HRMS (FAB+): calculated = 470.2038, found = 470.2054.

4c, ^{1}H NMR (500 MHz, CDCl$_3$)
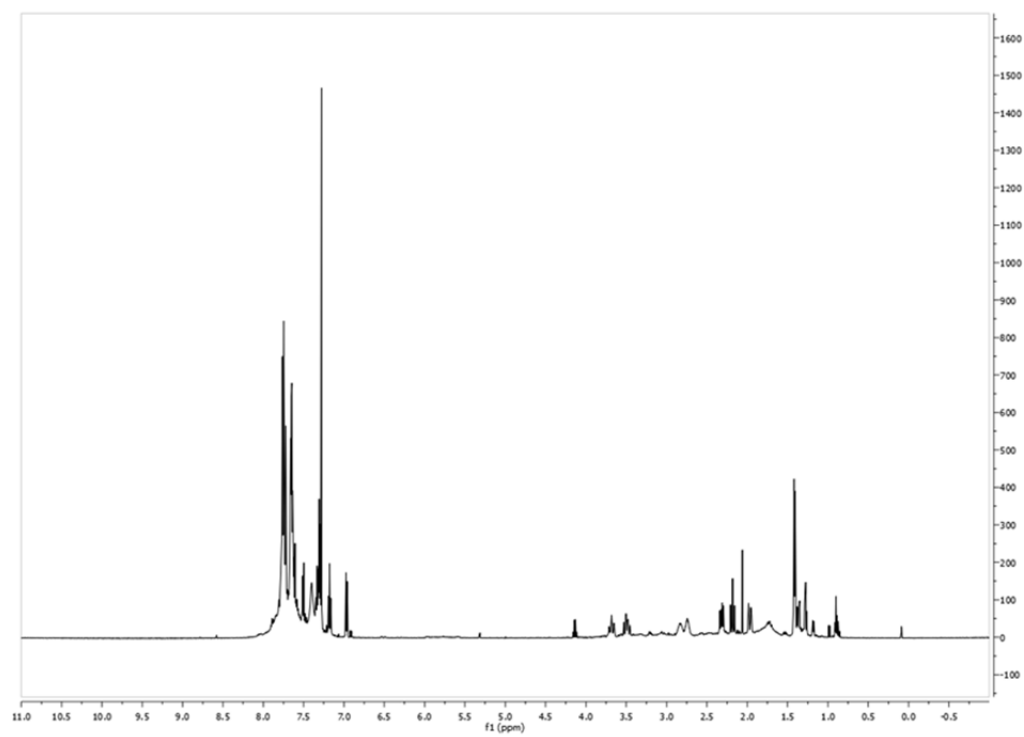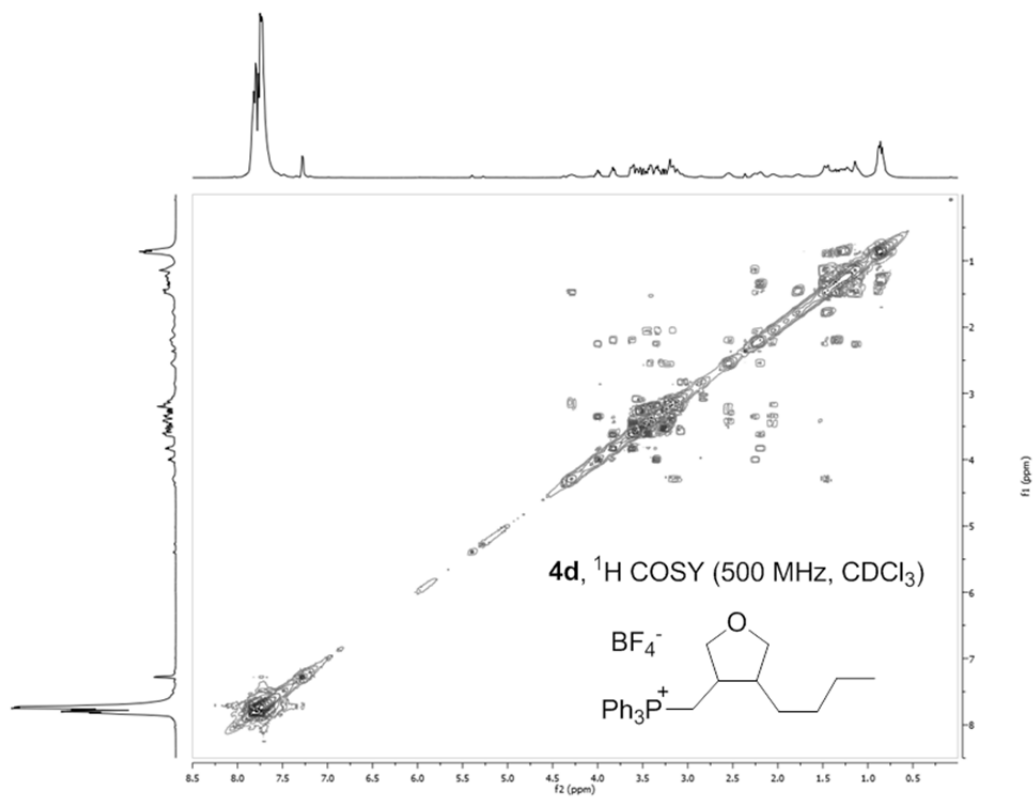
BF$_4^-$

Ph$_3$P$^+$

4c, ^{13}C{^{1}H} NMR (126 MHz, CDCl$_3$)

BF$_4^-$

Ph$_3$P$^+$

4c, ^{31}P{^{1}H} NMR (202 MHz, CDCl$_3$)

4c, ^{31}P-^{1}H HMBC (202 MHz, 500 MHz, CDCl$_3$)

4c, ¹H COSY (500 MHz, CDCl₃)

4d, ¹H NMR (500 MHz, CDCl₃)

4d, $^{13}C\{^1H\}$ NMR (126 MHz, CDCl$_3$)

4d, ^{31}P-^1H HMBC (202 MHz, 500 MHz, CDCl$_3$)

4d, ^{1}H COSY (500 MHz, CDCl$_3$)

4e, $^{13}C\{^1H\}$ NMR (126 MHz, CDCl$_3$)

4e, ^{31}P-^1H HMBC (202 MHz, 500 MHz, CDCl$_3$)

4e, ^{1}H COSY (500 MHz, CDCl$_3$)

Ph$_3$P$^+$

BF$_4^-$

f1 (ppm)

f2 (ppm)
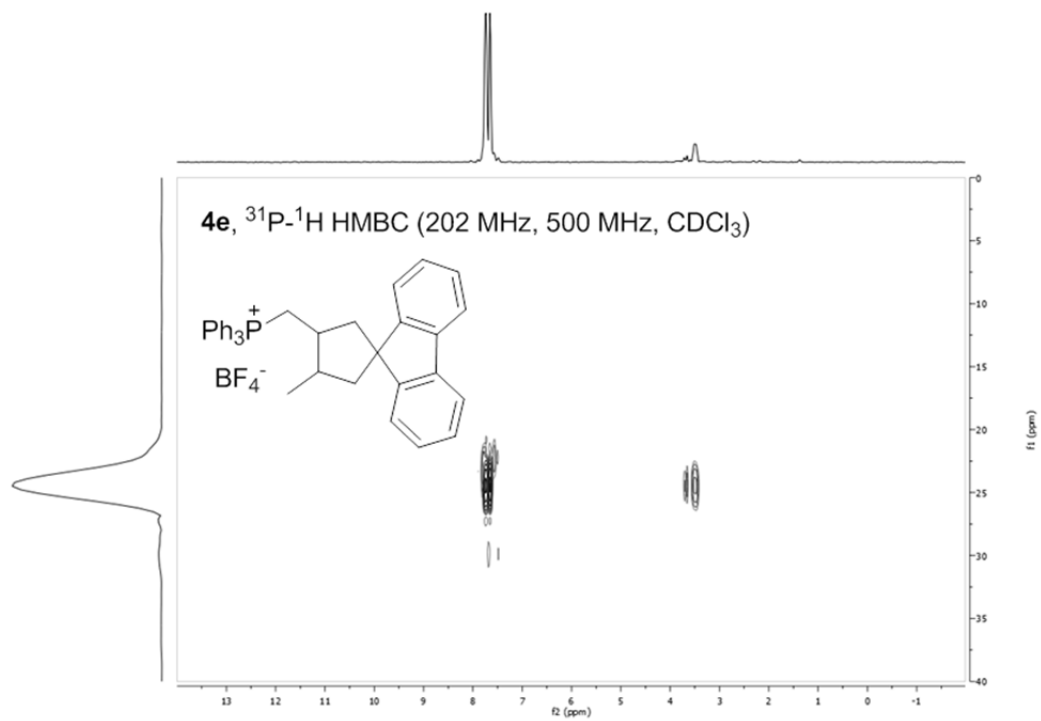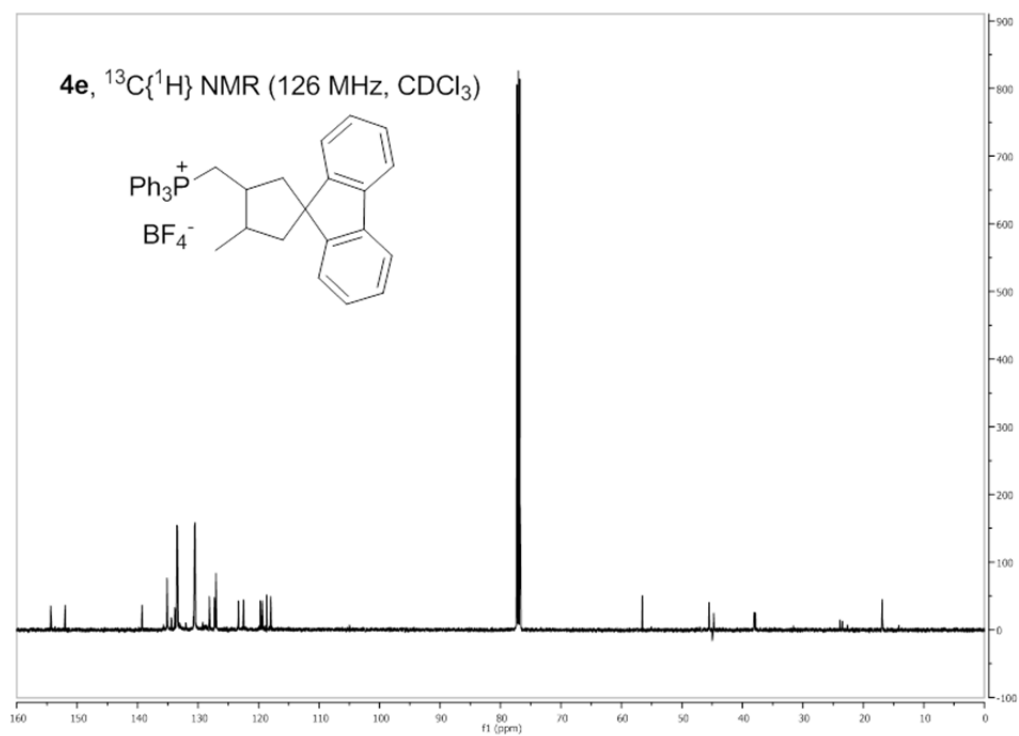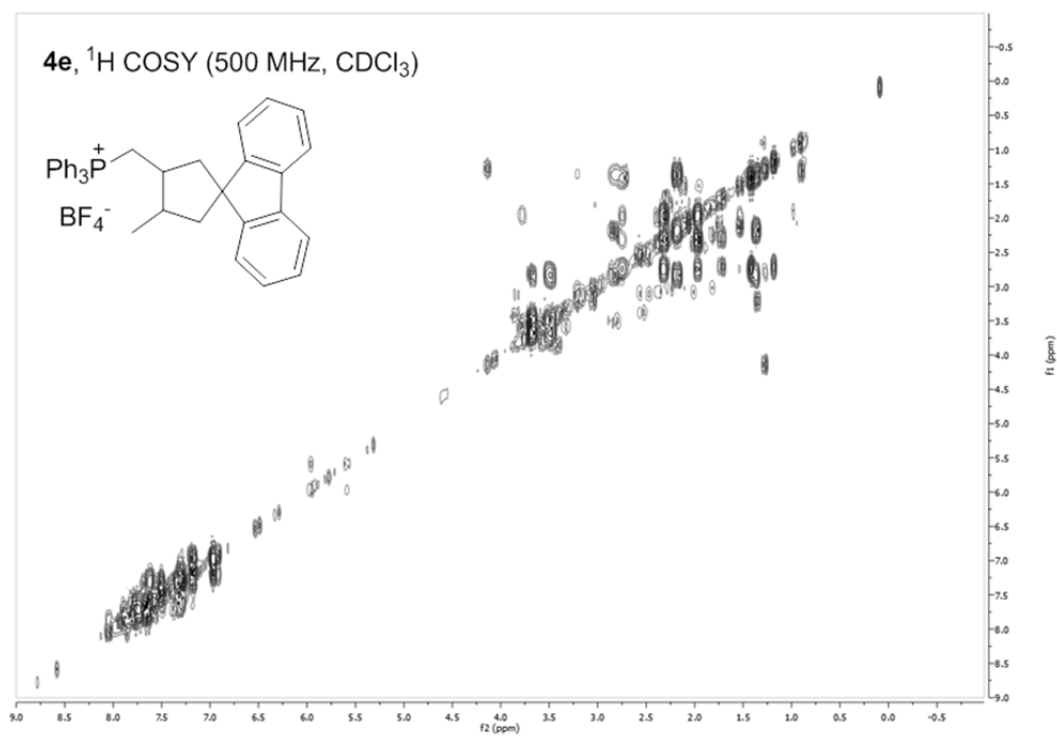
High-resolution Mass Spectrometry.

BF$_4^-$

Ph$_3$P$^+$
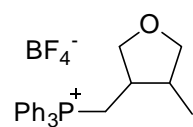
4c
calculated=361.1721
found=361.1706

Ph$_3$P$^+$

BF$_4^-$
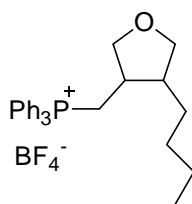
4d
calculated=403.2191
found=403.2200

Ph$_3$P$^+$

BF$_4^-$
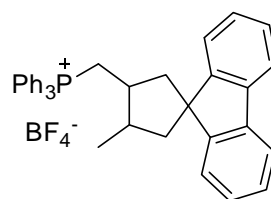
4e
calculated=509.2398
found=509.2394

(¹) Examples of transition-metal catalyzed hydrophosphination: (a) Wicht, D. K.; Kourkine, I. V.; Lew, B. M.; Nthenge, J. M.; Glueck, D. S. *J. Am. Chem. Soc.* **1997**, *119*, 5039. (b) Costa, E.; Pringe, P. G.; Worboys, K. *Chem. Commun.* **1998**, 49. (c) Wicht, D. K.; Kourkine, I. V. Kovacik, I. Glueck, D. S. *Organometallics*, **1999**, *18*, 5381. (d) Kovacik, I.; Wicht, D. K.; Grewal, N. S.; Glueck, D. S. *Organometallics* **2000,** *19*, 950.

(²) Examples of radical-mediated hydrophosphination: (a) Cho, D. H.; Jang, D. O. *Synlett* **2005**, *1,* 59. (b) Robertson, A.; Bradaric, C.; Frampton, C. S.; McNulty, J.; Capretta, A. *Tet. Lett.* **2001**, *42,* 2609. (c) Lopin, C.; Gouhier, G.; Gautier, A.; Piettre, S. R. *J. Org. Chem.* **2003**, *68,* 9916. (d) Beaufils, F.; Dénès, F.; Renaud, P. *Angew. Chem. Int. Ed.* **2005**, *44*, 5273. (e) Leca, D.; Fensterbank, L.; Laĉote, E.; Malacra, M. *Chem. Soc. Rev.* **2005**, *34*, 858. (f) Semezin, D.; Emetad-Moghadam, G.;Albouy, D.; Diallo, O.; Koenig, M. *J. Org. Chem.* **1997**, *62*, 2414.

(³)Healy, M. P.; Parsons, A. F.; Rawlinson, J. G. T. *Org. Lett.* **2005**, *7,* 1597.

(⁴) (a) Breuer, E.; Bannet, D. M. *Tetrahedron Lett.* **1977**, *18,* 1141. (b) Still, W. C.; Gennari, C. *Tetrahedron Lett.* **1983**, *24,* 4405.

(⁵)(a) Wittig, G.; Schollkopf, U. *Chem. Ber.* **1954**, *87,* 1318. (b) Wittig, G.; Haag, W. *Chem. Ber.* **1955**, *88,* 1654. (c) Maryanoff, B. E.; Reitz, A. B. *Chem. Rev.* **1989**, *89,* 863.

(⁶) (a) Abdur-Rashid, K.; Fing, T. P.; Greaves, B.; Gusev, D. G.; Hinman, J. G.; Landau, S. E.; Lough, A. J.; Morris, R. H. *J. Am. Chem. Soc.* **2000**, *122*, 9155. (b) Li, T.; Lough, A. J.; Zuccaccia, C.; Macchioni, A.; Morris, R. H. *Can. J. Chem.* **2006**, *84*, 164. (c) Li, T.; Lough, A. J.; Morris, R. H. *Chem. Eur. J.* **2007**, *13*, 3796.

([7]) (a) Nakamura, M.; Miki, M.; Majima, T. *J. Chem. Soc., Perkin Trans. 2*, **2000**, 1447. (b) Yasui, S.; Tojo, S.; Majima, T. *J. Org. Chem.* **2005**, *70*, 1276. (c) Yasui, S.; Tojo, S.; Majima, T. *Org. Biomol. Chem.* **2006**, *4*, 2969.

([8]) Additionally, standard radical conditions produce the $P(O)Ph_3$-BF_3 adduct as a side product that is difficult to separate from the crude reaction mixture.

([9]) $[HPPh_3][PF_6]$ and $[HPPh_3][Br]$ are not effective as hydrophosphonating reagents under photochemical conditions. Further experiments showed that the reaction would not continue without irradiation.

([10])All reactions were carried out in Pyrex glassware with a water-cooled, quartz-jacketed UV lamp. See Supporting Information for more details.

([11]) Crude **1[BF₄]** was obtained from photochemical hydrophosphonation conditions, where the mixture contains unreacted 4-allylanisole, $[HPPh_3][BF_4]$, and PPh_3.

[12] Pangborn, A. B.; Giardello, M. A.; Grubbs, R. H.; Rosen, R. K.; Timmers, F. J. *Organometallics* **1996**, *15*, 1518.

[13] Li, T.; Lough, A. J.; Zuccaccia, C.; Macchioni, A.; Morris, R. H. *Can. J. Chem.* **2006**, *84*, 164.

[14] Li, T.; Lough, A. J.; Morris, R. H. *Chem. Eur. J.* **2007**, *13*, 3796.

[15] Jordan-Hore, J. A.; Johansson, C. C. C.; Gulias, M.; Beck, E. M.; Gaunt, M. J. *J. Am. Chem. Soc.* **2008**, *130*, 16184.